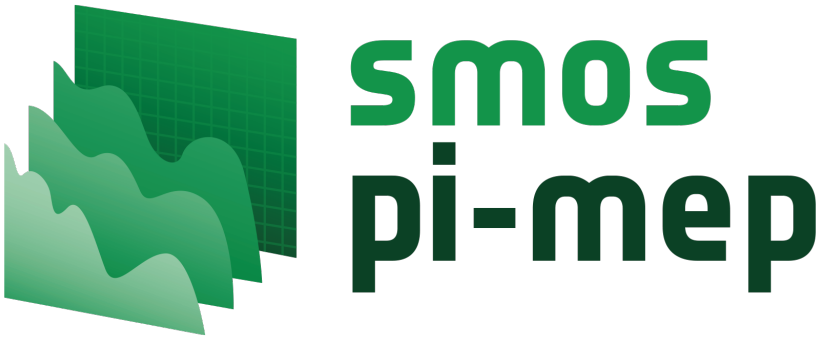

In Situ database Analyses Report

TSG

prepared by the Pi-MEP Consortium

December 15, 2022

Contents

Acronym

Aquarius	NASA/CONAE Salinity mission
ASCAT	Advanced Scatterometer
ATBD	Algorithm Theoretical Baseline Document
BLT	Barrier Layer Thickness
CMORPH	CPC MORPHing technique (precipitation analyses)
CPC	Climate Prediction Center
CTD	Instrument used to measure the conductivity, temperature, and pressure of seawater
DM	Delayed Mode
EO	Earth Observation
ESA	European Space Agency
FTP	File Transfer Protocol
GOSUD	Global Ocean Surface Underway Data
GTMBA	The Global Tropical Moored Buoy Array
Ifremer	Institut français de recherche pour l'exploitation de la mer
IPEV	Institut polaire français Paul-Émile Victor
IQR	Interquartile range
ISAS	*In Situ* Analysis System
Kurt	Kurtosis (fourth central moment divided by fourth power of the standard deviation)
L2	Level 2
LEGOS	Laboratoire d'Etudes en Géophysique et Océanographie Spatiales
LOCEAN	Laboratoire d'Océanographie et du Climat : Expérimentations et Approches Numériques
LOPS	Laboratoire d'Océanographie Physique et Spatiale
MDB	Match-up Data Base
MEOP	Marine Mammals Exploring the Oceans Pole to Pole
MLD	Mixed Layer Depth
NCEI	National Centers for Environmental Information
NRT	Near Real Time
NTAS	Northwest Tropical Atlantic Station
OI	Optimal interpolation
Pi-MEP	Pilot-Mission Exploitation Platform
PIRATA	Prediction and Researched Moored Array in the Atlantic
QC	Quality control
R_{sat}	Spatial resolution of the satellite SSS product
RAMA	Research Moored Array for African-Asian-Australian Monsoon Analysis and Prediction
r^2	Square of the Pearson correlation coefficient
RMS	Root mean square
RR	Rain rate
SAMOS	Shipboard Automated Meteorological and Oceanographic System
Skew	Skewness (third central moment divided by the cube of the standard deviation)
SMAP	Soil Moisture Active Passive (NASA mission)
SMOS	Soil Moisture and Ocean Salinity (ESA mission)
SPURS	Salinity Processes in the Upper Ocean Regional Study
SSS	Sea Surface Salinity
SSS_{insitu}	*In situ* SSS data considered for the match-up

SSS_{SAT}	Satellite SSS product considered for the match-up
ΔSSS	Difference between satellite and *in situ* SSS at colocalized point ($\Delta SSS = SSS_{SAT}$- SSS_{insitu})
SST	Sea Surface Temperature
Std	Standard deviation
Std*	Robust Standard deviation = median(abs(x-median (x)))/0.67 (less affected by outliers than Std)
Stratus	Surface buoy located in the eastern tropical Pacific
Survostral	SURVeillance de l'Océan AuSTRAL (Monitoring the Southern Ocean)
TAO	Tropical Atmosphere Ocean
TSG	ThermoSalinoGraph
WHOI	Woods Hole Oceanographic Institution
WHOTS	WHOI Hawaii Ocean Time-series Station
WOA	World Ocean Atlas

1 Overview

This report presents some characteristics of the TSG in situ dataset used by the Pi-MEP to validate SMOS, SMAP and Aquarius satellite SSS products. A series of plots is proposed showing:

- Number of SSS data as a function of time and distance to coast
- Histogram of shallowest salinity and pressure (if relevant)
- Temporal mean of shallowest salinity pressure measurements (if relevant)
- Spatial density of shallowest salinity
- Spatial Maps of the Time-mean and temporal Std of *in situ* and satellite SSS and of the ΔSSS
- Time series of the monthly median and Std of *in situ* and satellite SSS and of the ΔSSS
- Zonal mean and Std of *in situ* and satellite SSS and of the ΔSSS
- Scatterplots of ISAS vs *in situ* SSS by latitudinal bands
- Time series of the monthly median and Std of the ΔSSS sorted by latitudinal bands
- ΔSSS sorted as function of geophysical parameters
- ΔSSS maps and statistics for different geophysical conditions

1.1 TSG *In situ* datasets

The TSG dataset is subdivided into 8 subdatasets following TSG data providers subdivisions:

- LEGOS-DM:
  The TSG-LEGOS-DM dataset corresponds to sea surface salinity delayed mode data derived from voluntary observing ships collected, validated, archived, and made freely available by the French Sea Surface Salinity Observation Service (Alory et al. (2015)). Adjusted values when available and only collected TSG data that exhibit quality flags=1 and 2 were used.
- GOSUD-Research-vessel:
  The TSG (GOSUD-Research-vessel) dataset corresponds to French research vessels SSS data that have been collected since the early 2000 as a contribution to the Global Ocean Surface Underway Data (GOSUD) program. The set of homogeneous instruments is permanently monitored and regularly calibrated. Water samples are taken on a daily basis by the crew and later analysed in the laboratory. The careful calibration and instrument maintenance, complemented with a rigorous adjustment on water samples, lead to reach an accuracy of a few 10^{-2} PSS in salinity. This delayed mode dataset (Kolodziejczyk et al. (2021)) is updated annually and freely available here. Adjusted values when available and only collected TSG data that exhibit quality flags 1 or 2 were used.
- GOSUD-Sailing-ship: The TSG-GOSUD-Sailing-ship dataset corresponds to observations of sea surface salinity obtained from voluntary sailing ships using medium or small size sensors. They complement the networks installed on research vessels or commercial ships. This delayed mode dataset (Reynaud et al. (2021)) is updated annually as a contribution to GOSUD (`http://www.gosud.org`) and freely available here. Adjusted values when available and only collected TSG data that exhibit quality flags=1 and 2 were used.

- SAMOS: The TSG-SAMOS dataset corresponds to "Research" quality data from the US Shipboard Automated Meteorological and Oceanographic System (SAMOS) initiative (Smith et al. (2009)). Data are available at http://samos.coaps.fsu.edu/html/. Adjusted values when available and only collected TSG data that exhibit quality flags=1 and 2 were used. After visual inspection, data from the NANCY FOSTER (ID="WTER", IMO="008993227") with date 2011/03/21 and all data from the ATLANTIS (ID="KAQP", IMO="009105798") for year 2010 has been removed from this dataset.

- LEGOS-Survostral: The TSG-LEGOS-Survostral dataset corresponds to delayed mode regional data from TSG installed on the Astrolabe vessel (IPEV) during the round trips between Hobart (Tasmania) and the French Antarctic base at Dumont d'Urville (Morrow and Kestenare (2014)). It is provided by the Survostral project and available via ftp. Adjusted values when available and only collected TSG data that exhibit quality flags=1 and 2 were used.

- LEGOS-Survostral-Adélie: The TSG-LEGOS-Surv-Adel dataset corresponds to delayed mode regional dataset along the Adelie coast provided by the Survostral project and available via ftp. Adjusted values when available and only collected TSG data that exhibit quality flags=1 and 2 were used.

- Polarstern: The TSG-POLARSTERN dataset has been gathered through the https://www.pangaea.de/ data warehouse utility using the following criteria: basis:"Polarstern" , device:"Underway cruise track measurements (CT)" , time coverage form 2010/01/01 to present. The result of the query is a collection of 79 different datasets with the following identification numbers: 736345, 742729, 753224, 753225, 753226, 753227, 758080, 760120, 760121, 761277, 770034, 770035, 770828, 776596, 776597, 780004, 802809, 802810, 802811, 802812, 803431, 808835, 808836, 808838, 809727, 810678, 816055, 819831, 823259, 839406, 839407, 839408, 848615, 858879, 858880, 858881, 858882, 858883, 858884, 858885, 863228, 863229, 863230, 863231, 863232, 863234, 873145, 873147, 873151, 873153, 873155, 873156, 873158, 887767, 889444, 889513, 889515, 889516, 889517, 889535, 889542, 889548, 895578, 895579, 895581, 898225, 898233, 898266, 905555, 905562, 905608, 905610, 905734, 930022, 930023, 930024, 930026, 930027, 930028.

- NCEI-0170743: The TSG-NCEI-0170743 dataset (Aulicino et al. (2018)) contains sea surface temperature and salinity data collected from 2010 to 2017 in the South Atlantic Ocean and Southern Ocean from S.A. Agulhas and Agulhas-II research vessels, in the framework of South African National Antarctic Programme (SANAP), South African Department of Environmental Affairs (DEA) and Italian National Antarctic Research Programme (PNRA) scientific activities. Measurements have been obtained through thermosalinograph (TSG) during several cruises to both Antarctica and sub-Antarctic islands. On-board TSG devices have been regularly calibrated and continuously monitored in-between cruises; no appreciable sensor drift emerged. Independent water samples taken along the cruises have been used to validate the data; salinity measurement error was a few hundredths of a unit on the practical salinity scale. A careful quality control allowed to discard bad data for each single campaign.

1.2 Auxiliary geophysical datasets

Additional EO datasets are used to characterize the geophysical conditions at the *in situ* measurement locations and time, and 10 days prior to the measurements, to get an estimate of the

geophysical concomitant condition and history. As discussed in Boutin et al. (2016), the presence of vertical gradients in, and horizontal variability of, sea surface salinity indeed complicates comparison of satellite and *in situ* measurements. The additional EO data are used here to get a first estimates of conditions for which L-band satellite SSS measured in the first centimeters of the upper ocean within a 50-150 km diameter footprint might differ from pointwise *in situ* measurements performed in general between 10 and 5 m depth below the surface. The spatio-temporal variability of SSS within a satellite footprint (50-150 km) is a major issue for satellite SSS validation in the vicinity of river plumes, frontal zones, and significant precipitation areas, among others. Rainfall can in some cases produce vertical salinity gradients exceeding 1 pss m^{-1}; consequently, it is recommended that satellite and *in situ* SSS measurements less than 3–6 h after rain events should be considered with care when used in satellite calibration/validation analyses. To identify such situation, the Pi-MEP platform is first using CMORPH products to characterize the local value and history of rain rate and ASCAT gridded data are used to characterize the local surface wind speed and history. For validation purpose, the ISAS monthly SSS *in situ* analysed fields at 5 m depth are collocated and compared with the *in situ* SSS value. The use of ISAS is motivated by the fact that it is used in the SMOS L2 official validation protocol in which systematic comparisons of SMOS L2 retrieved SSS with ISAS are done. In complement to ISAS, annual std climatological field from the World Ocean Atlas (WOA13) at the *in situ* location are also used to have an a priori information of the local SSS variability.

1.2.1 CMORPH

Precipitation are estimated using the CMORPH 3-hourly products at 1/4° resolution (Joyce et al. (2004)). CMORPH (CPC MORPHing technique) produces global precipitation analyses at very high spatial and temporal resolution. This technique uses precipitation estimates that have been derived from low orbiter satellite microwave observations exclusively, and whose features are transported via spatial propagation information that is obtained entirely from geostationary satellite IR data. At present NOAA incorporate precipitation estimates derived from the passive microwaves aboard the DMSP 13, 14 and 15 (SSM/I), the NOAA-15, 16, 17 and 18 (AMSU-B), and AMSR-E and TMI aboard NASA's Aqua, TRMM and GPM spacecraft, respectively. These estimates are generated by algorithms of Ferraro (1997) for SSM/I, Ferraro et al. (2000) for AMSU-B and Kummerow et al. (2001) for TMI. Note that this technique is not a precipitation estimation algorithm but a means by which estimates from existing microwave rainfall algorithms can be combined. Therefore, this method is extremely flexible such that any precipitation estimates from any microwave satellite source can be incorporated.

With regard to spatial resolution, although the precipitation estimates are available on a grid with a spacing of 8 km (at the equator), the resolution of the individual satellite-derived estimates is coarser than that - more on the order of 12 x 15 km or so. The finer "resolution" is obtained via interpolation.

In effect, IR data are used as a means to transport the microwave-derived precipitation features during periods when microwave data are not available at a location. Propagation vector matrices are produced by computing spatial lag correlations on successive images of geostationary satellite IR which are then used to propagate the microwave derived precipitation estimates. This process governs the movement of the precipitation features only. At a given location, the shape and intensity of the precipitation features in the intervening half hour periods between microwave scans are determined by performing a time-weighting interpolation between microwave-derived features that have been propagated forward in time from the previous microwave observation and those that have been propagated backward in time from the following microwave scan. NOAA refer to this latter step as "morphing" of the features.

For the present Pi-MEP products, we only considered the 3-hourly products at 1/4 degree resolution. The entire CMORPH record (December 2002-present) for 3-hourly, 1/4 degree lat/lon resolution can be found at: ftp://ftp.cpc.ncep.noaa.gov/precip/CMORPH_V1.0/CRT/. CMORPH estimates cover a global belt (-180°W to 180°E) extending from 60°S to 60°N latitude and are available for the complete period of the Pi-MEP core datasets (Jan 2010-now).

1.2.2 ASCAT

Advanced SCATterometer (ASCAT) daily data produced and made available at Ifremer/CERSAT on a 0.25°x0.25° resolution grid (Bentamy and Fillon (2012)) since March 2007 are used to characterize the mean daily wind at the match-up pair location as well as the wind history during the 10-days period preceding the in situ measurement date. These wind fields are calculated based on a geostatistical method with external drift. Remotely sensed data from ASCAT are considered as observations while those from numerical model analysis (ECMWF) are associated with the external drift. The spatial and temporal structure functions for wind speed, zonal and meridional wind components are estimated from ASCAT retrievals. Furthermore, the new procedure includes a temporal interpolation of the retrievals based on the complex empirical orthogonal function (CEOF) approach, in order to enhance the sampling length of the scatterometer observations. The resulting daily wind fields involves the main known surface wind patterns as well as some variation modes associated with temporal and spatial moving features. The accuracy of the gridded winds was investigated through comparisons with moored buoy data in Bentamy et al. (2012) and resulted in rms differences for wind speed and direction are about 1.50 $m.s^{-1}$ and 20°.

1.2.3 ISAS

The In Situ Analysis System (ISAS), as described in Gaillard et al. (2016) is a data based reanalysis of temperature and salinity fields over the global ocean 70°N–70°S on a 1/2° grid. It was initially designed to synthesize the temperature and salinity profiles collected by the Argo program. It has been later extended to accommodate all type of vertical profile as well as time series. ISAS gridded fields are entirely based on *in situ* measurements. The methodology and configuration have been conceived to preserve as much as possible the data information content and resolution. ISAS is developed and run in a research laboratory (LOPS) in close collaboration with Coriolis, one of Argo Global Data Assembly Center and unique data provider for the Mercator operational oceanography system. In Pi-MEP, the products used are the INSITU_GLO_TS_OA_REP_OBSERVATIONS_013_002_b for the period 2010 to 2019 and the INSITU_GLO_TS_OA_NRT_OBSERVATIONS_013_002_a for the Near-Real Time (2020-2021) derived at the Coriolis data center and provided by the Copernicus Marine Environment Monitoring Service (CMEMS). The major contribution to the data set is from Argo array of profiling floats, reaching an approximate resolution of one profile every 10-days and every 3-degrees over the satellite SSS period (http://www.umr-lops.fr/SNO-Argo/Products/ISAS-T-S-fields/); in this version SSS from ship of opportunity thermosalinographs are not used, so that we can consider SMOS SSS validation using these measurements independent of ISAS. The ISAS optimal interpolation involves a structure function modeled as the sum of two Gaussian functions, each associated with specific time and space scales, resulting in a smoothing over typically 3 degrees. The smallest scale which can be retrieved with ISAS analysis is not smaller than 300–500 km (Kolodziejczyk et al. (2015)). For validation purpose, the ISAS monthly SSS fields at 5 m depth are collocated and compared with the satellite SSS products and included in the Pi-MEP Match-up files. In addition, the "percentage of variance" fields (PCTVAR) contained in the

ISAS analyses provide information on the local variability of *in situ* SSS measurements within 1/2°x1/2° boxes.

1.2.4 World Ocean Atlas Climatology

The World Ocean Atlas 2013 version 2 (WOA13 V2) is a set of objectively analyzed (1° grid) climatological fields of *in situ* temperature, salinity and other variables provided at standard depth levels for annual, seasonal, and monthly compositing periods for the World Ocean. It also includes associated statistical fields of observed oceanographic profile data interpolated to standard depth levels on 5°, 1°, and 0.25° grids. We use these fields in complement to ISAS to characterize the climatological fields (annual mean and std) at the match-up pairs location and date.

2 In Situ Dababase Analyses

2.1 TSG (LEGOS-DM)

2.1.1 Introduction

The TSG-LEGOS-DM dataset corresponds to sea surface salinity delayed mode data derived from voluntary observing ships collected, validated, archived, and made freely available by the French Sea Surface Salinity Observation Service (Alory et al. (2015)). Adjusted values when available and only collected TSG data that exhibit quality flags=1 and 2 were used.

2.1.2 Number of SSS data as a function of time and distance to coast

Figure 1 shows the time (a) and distance to coast (b) distributions of the TSG (LEGOS-DM) *in situ* dataset.

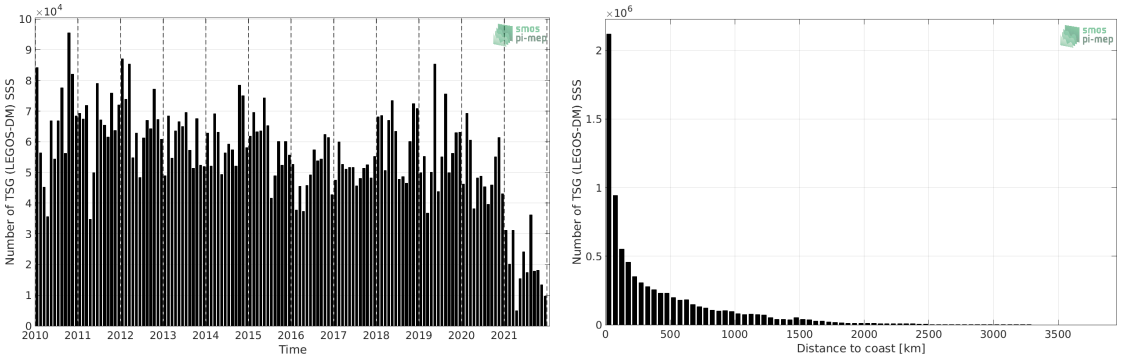

(a) (b)

Figure 1: Number of SSS from TSG (LEGOS-DM) as a function of time (a) and distance to coast (b).

2.1.3 Histograms of SSS

Figure 2 shows the SSS distribution of the TSG (LEGOS-DM) (a) and colocalized ISAS (b) dataset.

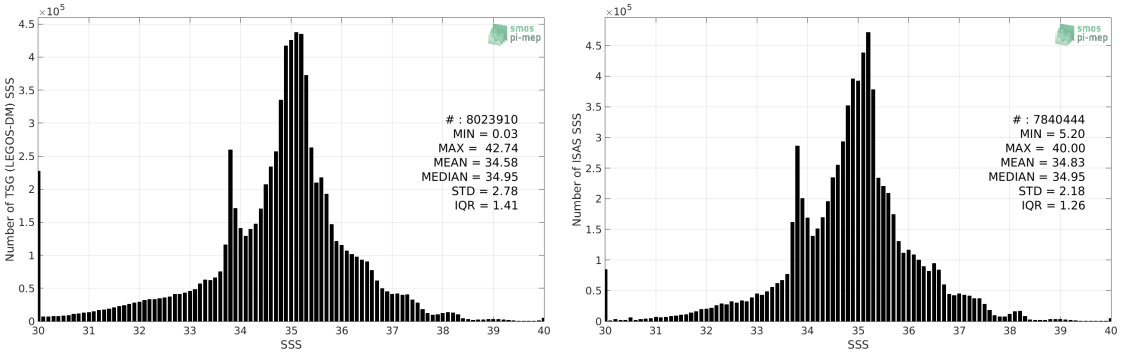

(a) (b)

Figure 2: Histograms of SSS from TSG (LEGOS-DM) (a) and ISAS (b) per bins of 0.1.

2.1.4 Distribution of *in situ* SSS depth measurements

In Figure 3, we show the depth distribution of the *in situ* salinity dataset (a) and the spatial distribution of the depth temporal mean in 1°x1° boxes and considering the full *in situ* dataset period (b).

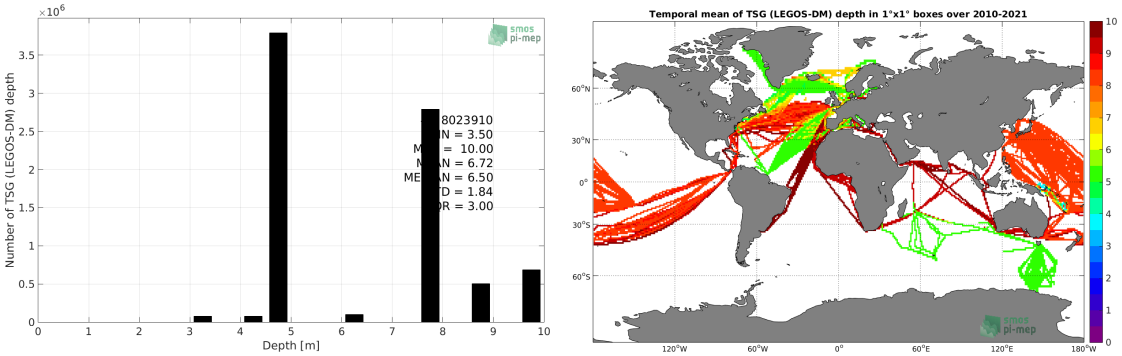

(a) (b)

Figure 3: Depth distribution of the upper level SSS measurements from TSG (LEGOS-DM) (a) and spatial distribution of the *in situ* SSS depth measurements showing the mean value in 1°x1° boxes and considering the full *in situ* dataset period (b).

2.1.5 Spatial distribution of SSS

In Figure 4, the number of TSG (LEGOS-DM) SSS measurements in 1°x1° boxes is shown.

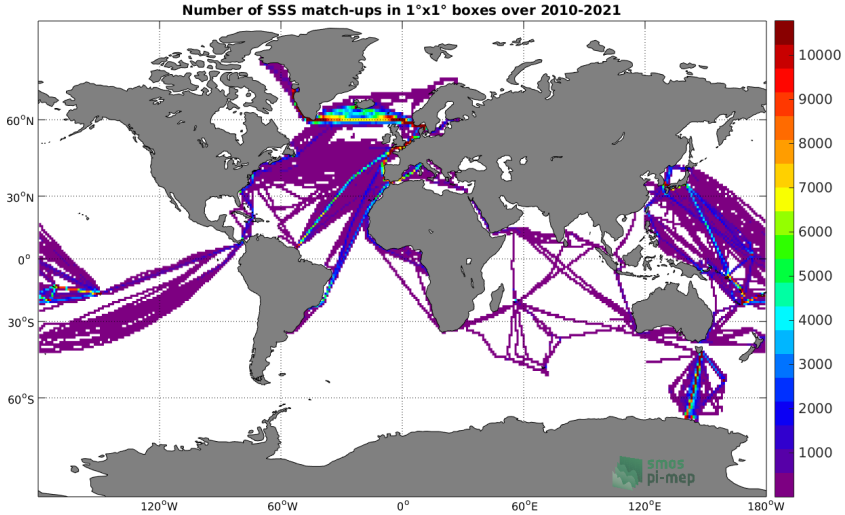

Figure 4: Number of SSS from TSG (LEGOS-DM) in 1°x1° boxes.

2.1.6 Spatial Maps of the Temporal mean and Std of *in situ* and ISAS SSS and of the difference (ΔSSS)

In Figure 5, maps of temporal mean (left) and standard deviation (right) of ISAS (top), TSG (LEGOS-DM) *in situ* dataset (middle) and the difference ΔSSS(ISAS -TSG (LEGOS-DM)) (bottom) are shown. The temporal mean and std are calculated using all match-up pairs falling in spatial boxes of size 1°x1° over the full TSG (LEGOS-DM) dataset period.

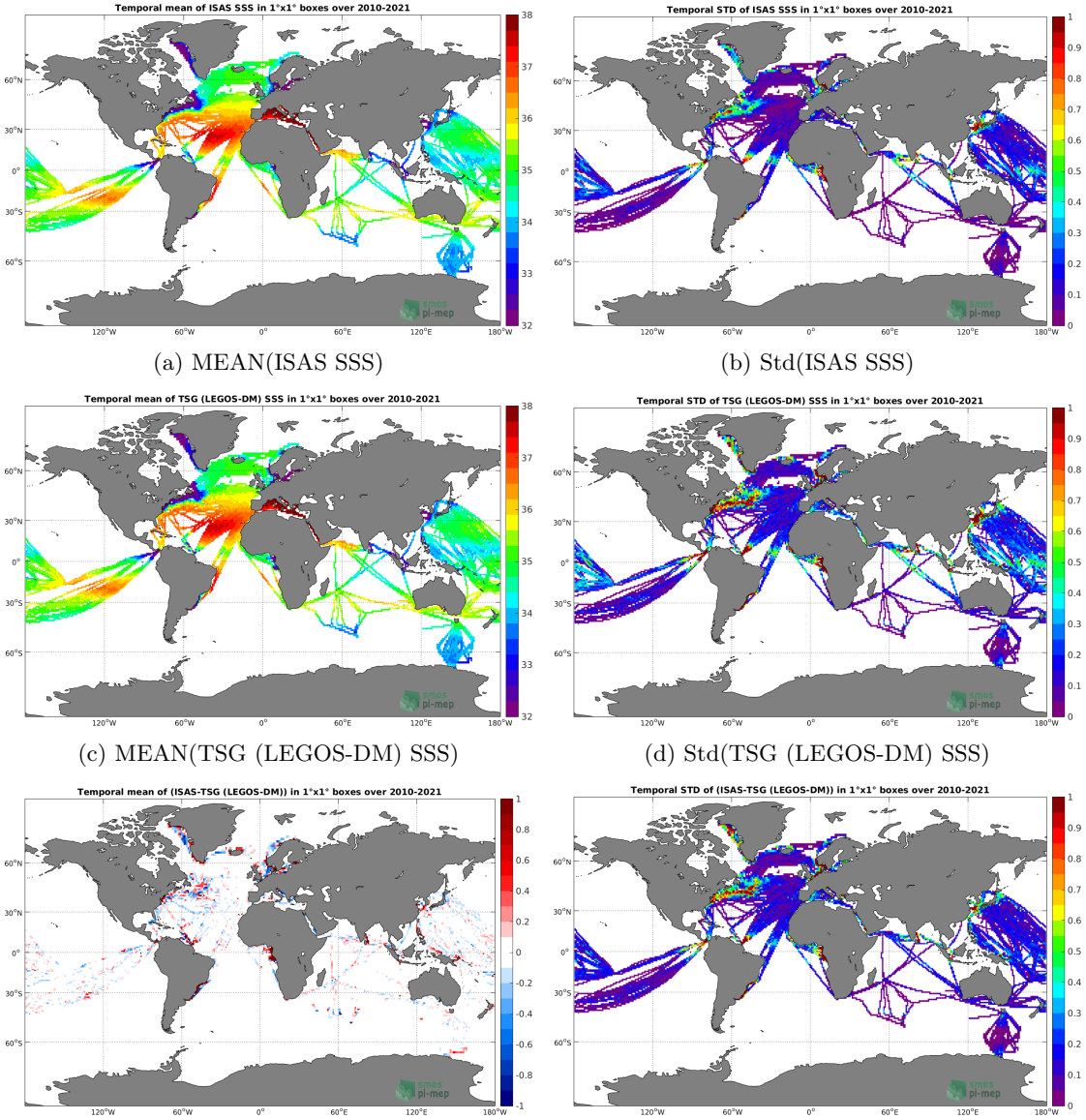

(a) MEAN(ISAS SSS)

(b) Std(ISAS SSS)

(c) MEAN(TSG (LEGOS-DM) SSS)

(d) Std(TSG (LEGOS-DM) SSS)

(e) MEAN(ΔSSS) (ISAS - TSG (LEGOS-DM))

(f) Std(ΔSSS) (ISAS - TSG (LEGOS-DM))

Figure 5: Temporal mean (left) and Std (right) of SSS from ISAS (top), TSG (LEGOS-DM) (middle), and of ΔSSS (ISAS - TSG (LEGOS-DM)). Only match-up pairs are used to generate these maps.

2.1.7 Time series of the monthly median and Std of *in situ* and ISAS SSS and of the difference (ΔSSS)

In the top panel of Figure 6, we show the time series of the monthly median SSS estimated for both ISAS SSS product (in black) and the TSG (LEGOS-DM) *in situ* dataset (in blue) at the collected Pi-MEP match-up pairs.

In the middle panel of Figure 6, we show the time series of the monthly median of ΔSSS (ISAS - TSG (LEGOS-DM)) for the collected Pi-MEP match-up pairs.

In the bottom panel of Figure 6, we show the time series of the monthly standard deviation of the ΔSSS (ISAS - TSG (LEGOS-DM)) for the collected Pi-MEP match-up pairs.

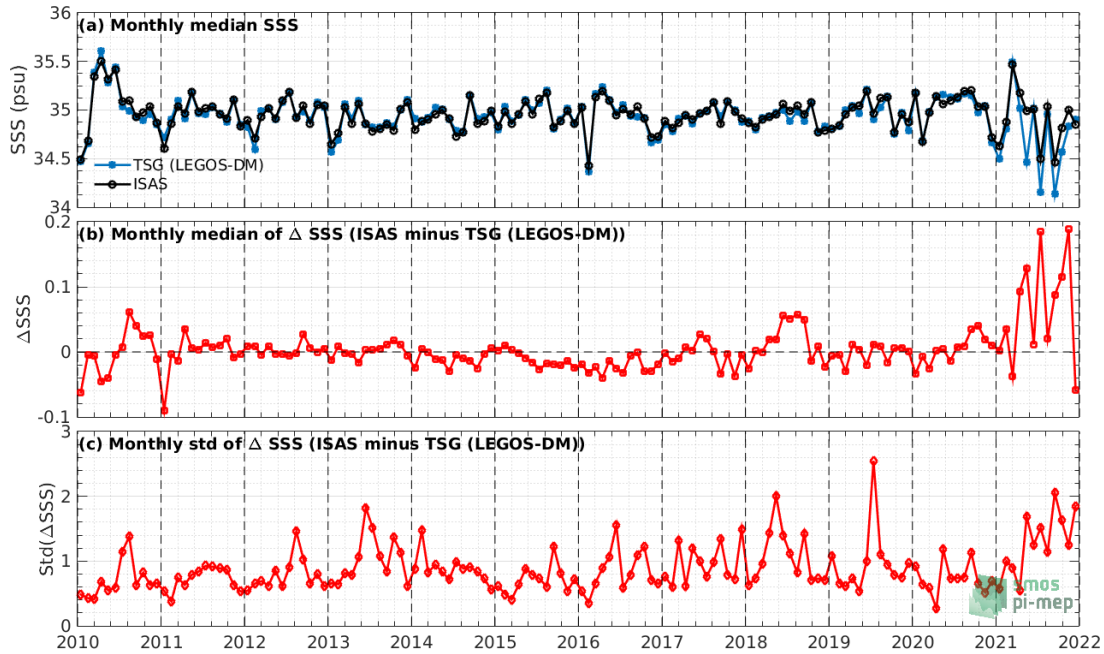

Figure 6: Time series of the monthly median SSS (top), median of ΔSSS (ISAS - TSG (LEGOS-DM)) and Std of ΔSSS (ISAS - TSG (LEGOS-DM)) considering all match-ups collected by the Pi-MEP.

2.1.8 Zonal mean and Std of *in situ* and ISAS SSS and of the difference ΔSSS

In Figure 7 left panel, we show the zonal mean SSS considering all Pi-MEP match-up pairs for both ISAS SSS product (in black) and the TSG (LEGOS-DM) *in situ* dataset (in blue). The full *in situ* dataset period is used to derive the mean.

In the right panel of Figure 7, we show the zonal mean of ΔSSS (ISAS - TSG (LEGOS-DM)) for all the collected Pi-MEP match-up pairs estimated over the full *in situ* dataset period.

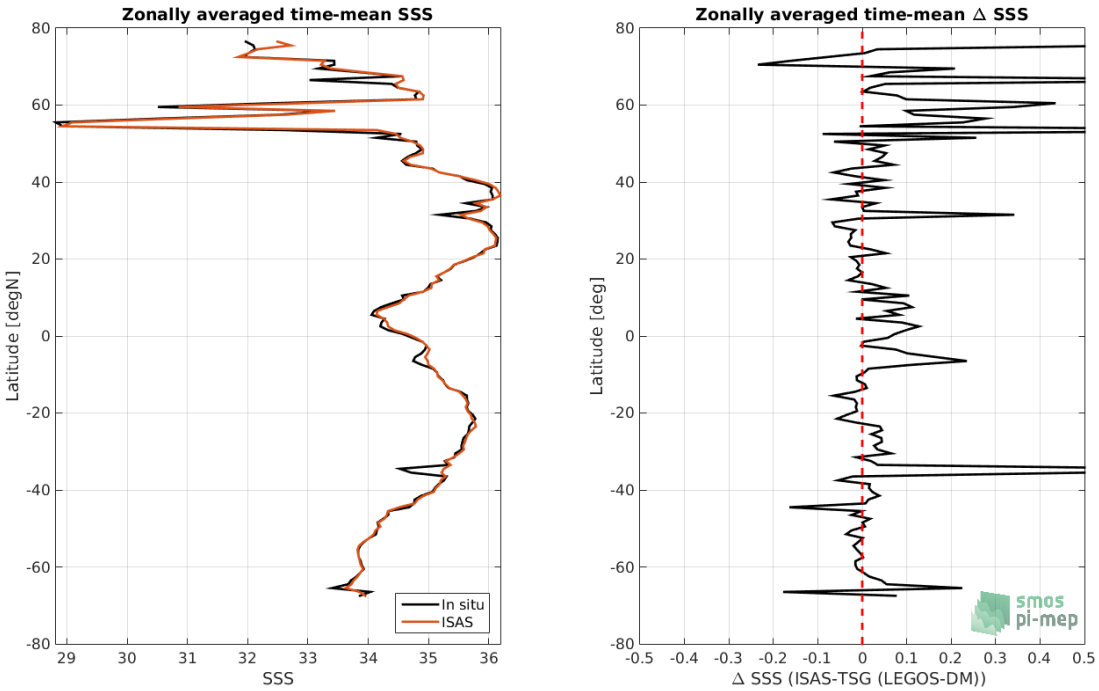

Figure 7: Left panel: Zonal mean SSS from ISAS product (black) and from TSG (LEGOS-DM) (blue). Right panel: Zonal mean of ΔSSS (ISAS - TSG (LEGOS-DM)) for all the collected Pi-MEP match-up pairs estimated over the full *in situ* dataset period.

2.1.9 Scatterplots of ISAS vs *in situ* SSS by latitudinal bands

In Figure 8, contour maps of the concentration of ISAS SSS (y-axis) versus TSG (LEGOS-DM) SSS (x-axis) at match-up pairs for different latitude bands: (a) 80°S-80°N, (b) 20°S-20°N, (c) 40°S-20°S and 20°N-40°N and (d) 60°S-40°S and 40°N-60°N. For each plot, the red line shows x=y. The black thin and dashed lines indicate a linear fit through the data cloud and the ±95% confidence levels, respectively. The number match-up pairs n, the slope and R^2 coefficient of the linear fit, the root mean square (RMS) and the mean bias between ISAS and *in situ* data are indicated for each latitude band in each plots.

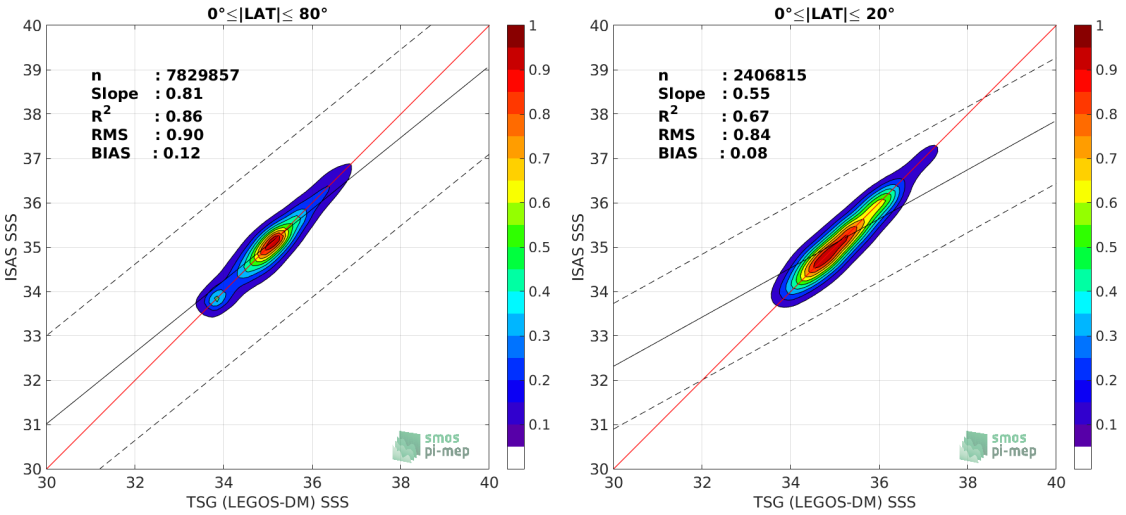

(a) $0° \leq |\text{LAT}| \leq 80°$ (b) $0° \leq |\text{LAT}| \leq 20°$

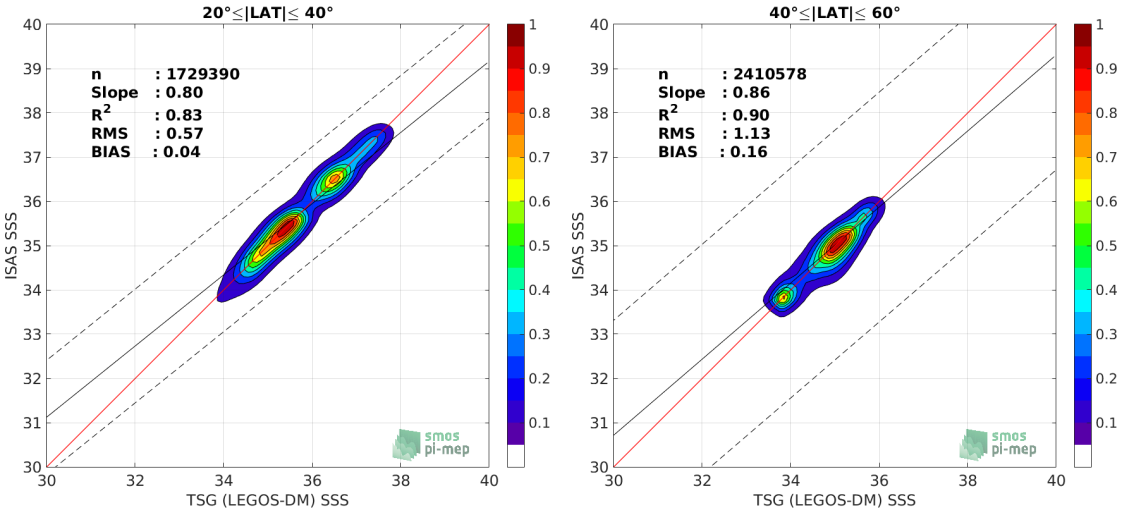

(c) $20° \leq |\text{LAT}| \leq 40°$ (d) $40° \leq |\text{LAT}| \leq 60°$

Figure 8: Contour maps of the concentration of ISAS SSS (y-axis) versus TSG (LEGOS-DM) SSS (x-axis) at match-up pairs for different latitude bands. For each plot, the red line shows x=y. The black thin and dashed lines indicate a linear fit through the data cloud and the ±95% confidence levels, respectively. The number match-up pairs n, the slope and R^2 coefficient of the linear fit, the root mean square (RMS) and the mean bias between ISAS and *in situ* data are indicated for each latitude band in each plots.

2.1.10 Time series of the monthly median and Std of the difference ΔSSS sorted by latitudinal bands

In Figure 9, time series of the monthly median (red curves) of ΔSSS (ISAS - TSG (LEGOS-DM)) and ±1 Std (black vertical thick bars) as function of time for all the collected Pi-MEP match-up pairs estimated for the full *in situ* dataset period are shown for different latitude bands: (a) 80°S-80°N, (b) 20°S-20°N, (c) 40°S-20°S and 20°N-40°N and (d) 60°S-40°S and 40°N-60°N.

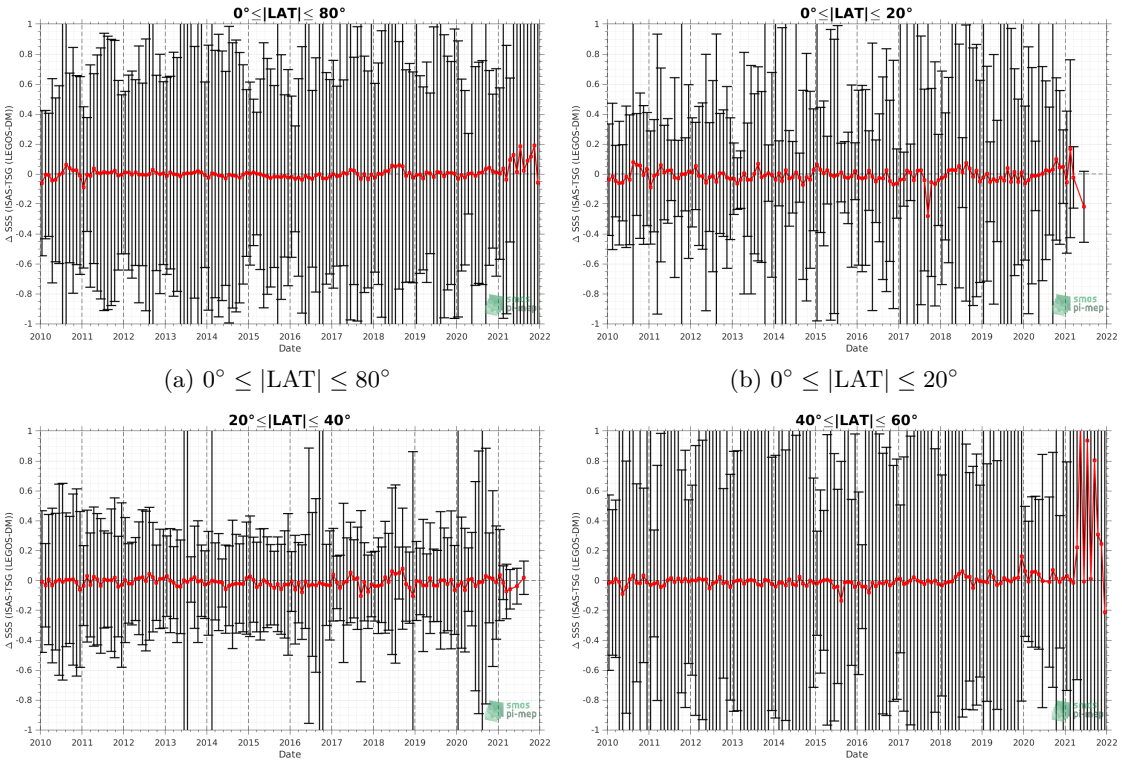

(a) $0° \leq |\text{LAT}| \leq 80°$

(b) $0° \leq |\text{LAT}| \leq 20°$

(c) $20° \leq |\text{LAT}| \leq 40°$

(d) $40° \leq |\text{LAT}| \leq 60°$

Figure 9: Monthly median (red curves) of ΔSSS (ISAS - TSG (LEGOS-DM)) and ±1 Std (black vertical thick bars) as function of time for all the collected Pi-MEP match-up pairs for the full *in situ* dataset period are shown for different latitude bands: (a) 80°S-80°N, (b) 20°S-20°N, (c) 40°S-20°S and 20°N-40°N and (d) 60°S-40°S and 40°N-60°N.

2.1.11 ΔSSS sorted as geophysical conditions

In Figure 10, we classify the match-up differences ΔSSS (ISAS - *in situ*) as function of the geophysical conditions at match-up points. The mean and std of ΔSSS (ISAS - TSG (LEGOS-DM)) is thus evaluated as function of the

- *in situ* SSS values per bins of width 0.2,
- *in situ* SST values per bins of width 1°C,
- ASCAT daily wind values per bins of width 1 m/s,
- CMORPH 3-hourly rain rates per bins of width 1 mm/h, and,
- distance to coasts per bins of width 50 km,
- *in situ* measurement depth (if relevant).

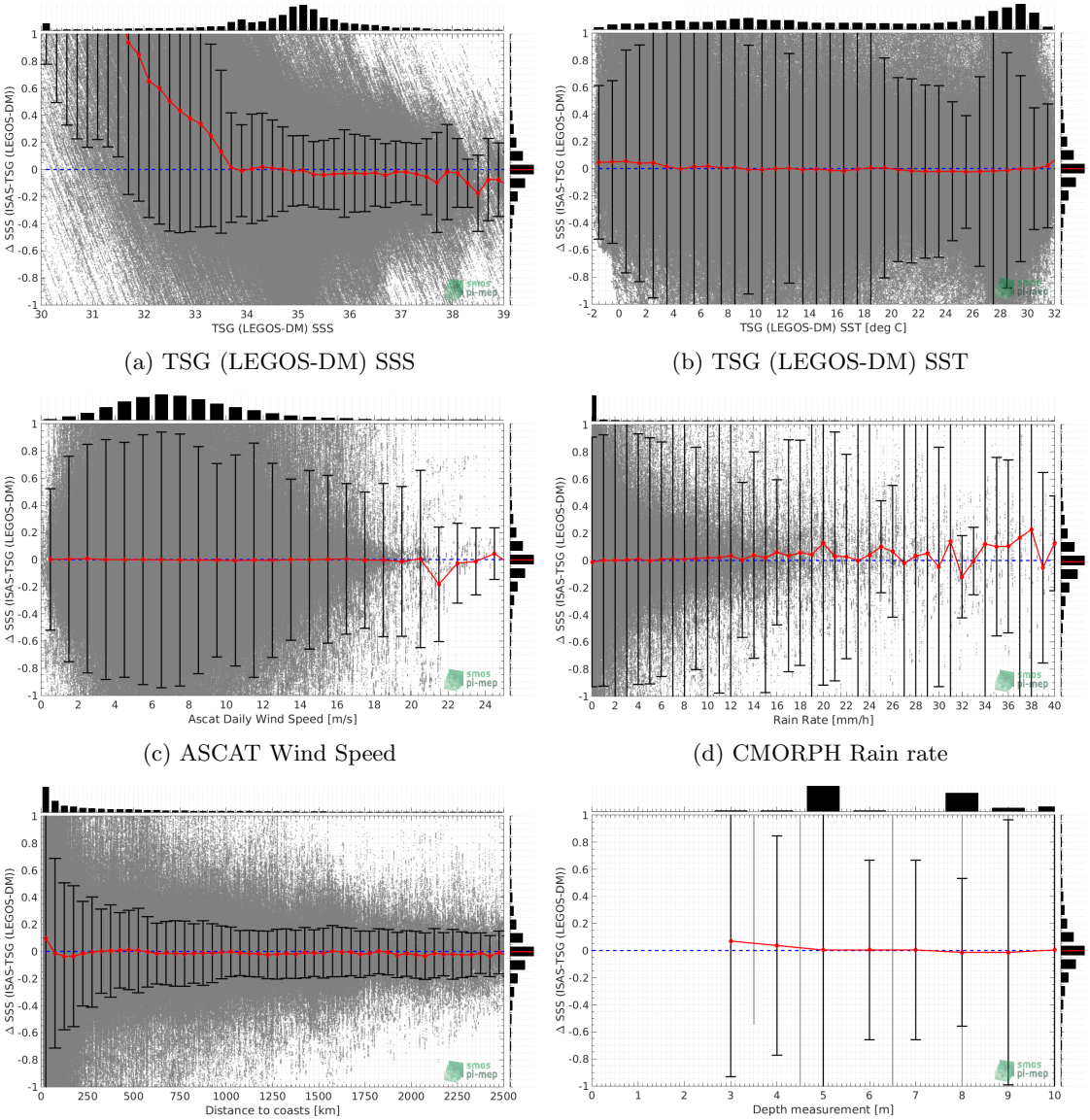

(a) TSG (LEGOS-DM) SSS

(b) TSG (LEGOS-DM) SST

(c) ASCAT Wind Speed

(d) CMORPH Rain rate

(e) Distance to coast

(f) Depth

Figure 10: Δ SSS (ISAS - TSG (LEGOS-DM)) sorted as geophysical conditions: TSG (LEGOS-DM) SSS a), TSG (LEGOS-DM) SST b), ASCAT Wind speed c), CMORPH rain rate d), distance to coast (e) and depth measurements (f).

2.1.12 ΔSSS maps and statistics for different geophysical conditions

In Figures 11 and 12, we focus on sub-datasets of the match-up differences ΔSSS (ISAS - *in situ*) for the following specific geophysical conditions:

- **C1**:if the local value at *in situ* location of estimated rain rate is zero, mean daily wind is in the range [3, 12] m/s, the SST is $> 5°$C and distance to coast is > 800 km.
- **C2**:if the local value at *in situ* location of estimated rain rate is zero, mean daily wind is

in the range [3, 12] m/s.

- **C3**:if the local value at *in situ* location of estimated rain rate is high (ie. > 1 mm/h) and mean daily wind is low (ie. < 4 m/s).
- **C5**:if the *in situ* data is located where the climatological SSS standard deviation is low (ie. above < 0.2).
- **C6**:if the *in situ* data is located where the climatological SSS standard deviation is high (ie. above > 0.2).

For each of these conditions, the temporal mean (gridded over spatial boxes of size 1°x1°) and the histogram of the difference ΔSSS (ISAS - *in situ*) are presented.

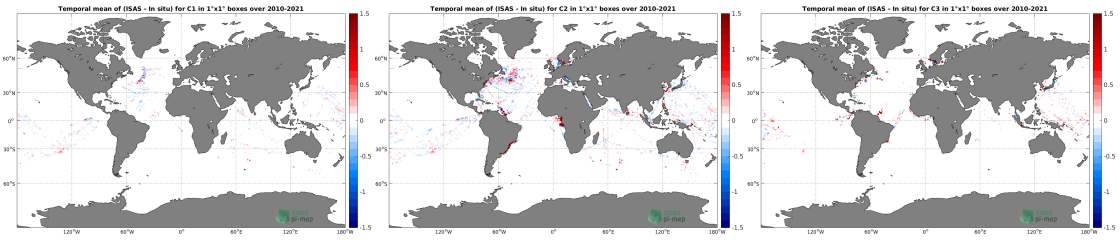

(a) RR=0 mm/h, 3< U_{10} <12 m/s, SST>5°C, distance to coast > 800 km (b) RR=0 mm/h, 3< U_{10} <12 m/s (c) RR>1mm/h and U_{10} <4m/s

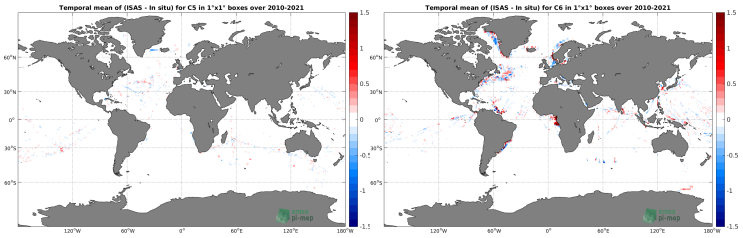

(d) WOA2013 SSS Std<0.2 (e) WOA2013 SSS Std>0.2

Figure 11: Temporal mean gridded over spatial boxes of size 1°x1° of ΔSSS (ISAS - TSG (LEGOS-DM)) for 5 different subdatasets corresponding to:RR=0 mm/h, 3< U_{10} <12 m/s, SST>5°C, distance to coast > 800 km (a), RR=0 mm/h, 3< U_{10} <12 m/s (b), RR>1mm/h and U_{10} <4m/s (c),WOA2013 SSS Std<0.2 (d),WOA2013 SSS Std>0.2 (e).

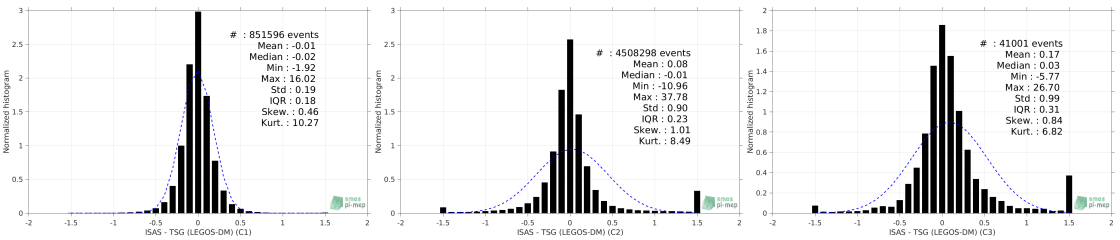

(a) RR=0 mm/h, 3< U_{10} <12 m/s, SST>5°C, distance to coast > 800 km (b) RR=0 mm/h, 3< U_{10} <12 m/s (c) RR>1mm/h and U_{10} <4m/s

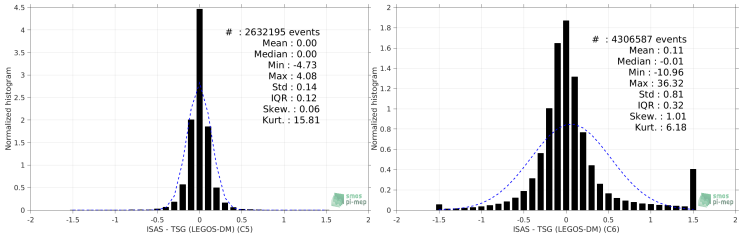

(d) WOA2013 SSS Std<0.2 (e) WOA2013 SSS Std>0.2

Figure 12: Normalized histogram of ΔSSS (ISAS - TSG (LEGOS-DM)) for 5 different subdatasets corresponding to:RR=0 mm/h, 3< U_{10} <12 m/s, SST>5°C, distance to coast > 800 km (a), RR=0 mm/h, 3< U_{10} <12 m/s (b), RR>1mm/h and U_{10} <4m/s (c),WOA2013 SSS Std<0.2 (d),WOA2013 SSS Std>0.2 (e).

2.1.13 Summary

Table 1 shows the mean, median, standard deviation (Std), root mean square (RMS), interquartile range (IQR), correlation coefficient (r^2) and robust standard deviation (Std*) of the match-up differences ΔSSS (ISAS - TSG (LEGOS-DM)) for the following conditions:

- all: All the match-up pairs satellite/in situ SSS values are used to derive the statistics
- C1: only pairs where RR=0 mm/h, 3< U_{10} <12 m/s, SST>5°C, distance to coast > 800 km
- C2: only pairs where RR=0 mm/h, 3< U_{10} <12 m/s
- C3: only pairs where RR>1mm/h and U_{10} <4m/s
- C5: only pairs where WOA2013 SSS Std<0.2
- C6: only pairs where WOA2013 SSS Std>0.2
- C7a: only pairs with a distance to coast < 150 km.
- C7b: only pairs with a distance to coast in the range [150, 800] km.
- C7c: only pairs with a distance to coast > 800 km.
- C8a: only pairs where SST is < 5°C.
- C8b: only pairs where SST is in the range [5, 15]°C.
- C8c: only pairs where SST is > 15°C.

- C9a: only pairs where SSS is < 33.
- C9b: only pairs where SSS is in the range [33, 37].
- C9c: only pairs where SSS is > 37.

Table 1: Statistics of ΔSSS (ISAS - TSG (LEGOS-DM))

Condition	#	Median	Mean	Std	RMS	IQR	r^2	Std*
all	7840444	0.00	0.13	0.94	0.94	0.24	0.866	0.18
C1	851596	-0.02	-0.01	0.19	0.19	0.18	0.962	0.14
C2	4508298	-0.01	0.08	0.90	0.90	0.23	0.873	0.17
C3	41001	0.03	0.17	0.99	1.00	0.31	0.806	0.23
C5	2632195	0.00	0.00	0.14	0.14	0.12	0.977	0.09
C6	4306587	-0.01	0.11	0.81	0.81	0.32	0.868	0.23
C7a	3432897	0.02	0.30	1.35	1.38	0.46	0.858	0.32
C7b	3078101	-0.01	0.00	0.35	0.35	0.16	0.858	0.12
C7c	1323778	-0.01	-0.01	0.19	0.19	0.17	0.967	0.12
C8a	1030267	0.02	0.34	0.94	1.00	0.51	0.774	0.24
C8b	2270903	0.00	0.13	1.11	1.12	0.18	0.880	0.14
C8c	4539273	-0.01	0.08	0.83	0.83	0.25	0.845	0.19
C9a	768016	1.04	1.52	2.41	2.85	1.98	0.813	1.41
C9b	6735512	-0.01	-0.02	0.33	0.33	0.20	0.848	0.15
C9c	336916	-0.05	-0.08	0.28	0.29	0.22	0.821	0.17

Table 1 numerical values can be downloaded as a csv file here.

2.2 TSG (GOSUD-Research-vessel)

2.2.1 Introduction

The TSG (GOSUD-Research-vessel) dataset corresponds to French research vessels SSS data that have been collected since the early 2000 as a contribution to the Global Ocean Surface Underway Data (GOSUD) program. The set of homogeneous instruments is permanently monitored and regularly calibrated. Water samples are taken on a daily basis by the crew and later analysed in the laboratory. The careful calibration and instrument maintenance, complemented with a rigorous adjustment on water samples, lead to reach an accuracy of a few 10^{-2} PSS in salinity. This delayed mode dataset (Kolodziejczyk et al. (2021)) is updated annually and freely available here. Adjusted values when available and only collected TSG data that exhibit quality flags 1 or 2 were used.

2.2.2 Number of SSS data as a function of time and distance to coast

Figure 13 shows the time (a) and distance to coast (b) distributions of the TSG (GOSUD-Research-vessel) *in situ* dataset.

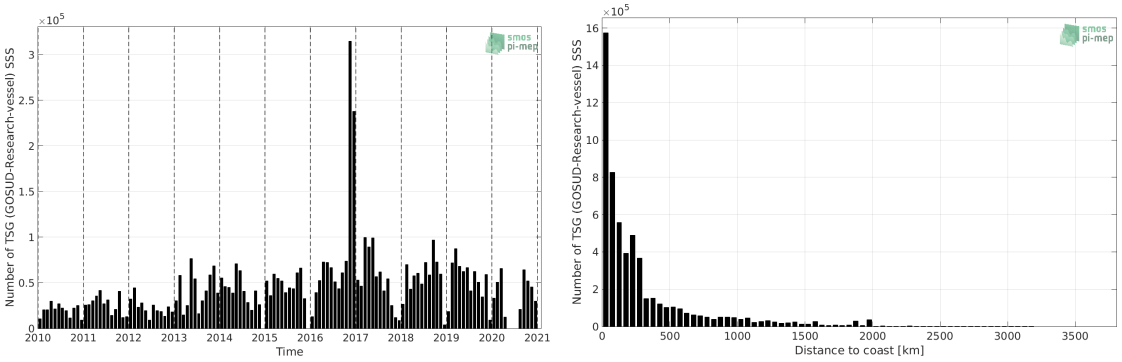

(a) (b)

Figure 13: Number of SSS from TSG (GOSUD-Research-vessel) as a function of time (a) and distance to coast (b).

2.2.3 Histograms of SSS

Figure 14 shows the SSS distribution of the TSG (GOSUD-Research-vessel) (a) and colocalized ISAS (b) dataset.

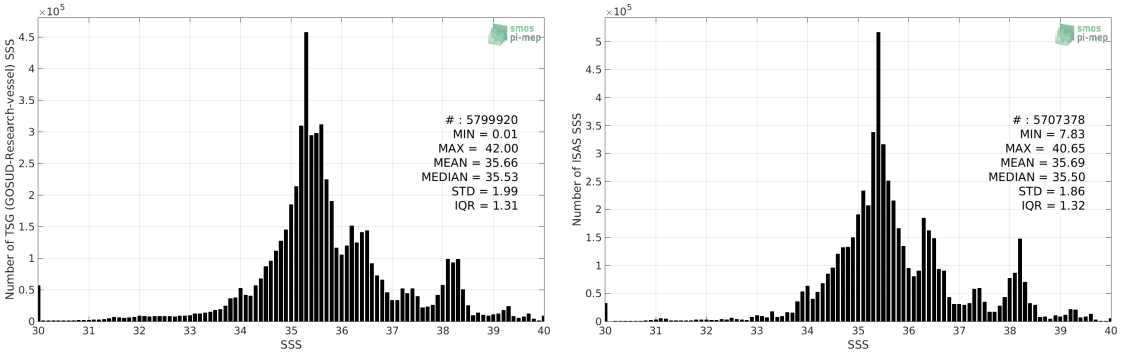

(a) (b)

Figure 14: Histograms of SSS from TSG (GOSUD-Research-vessel) (a) and ISAS (b) per bins of 0.1.

2.2.4 Distribution of *in situ* SSS depth measurements

In Figure 15, we show the depth distribution of the *in situ* salinity dataset (a) and the spatial distribution of the depth temporal mean in 1°x1° boxes and considering the full *in situ* dataset period (b).

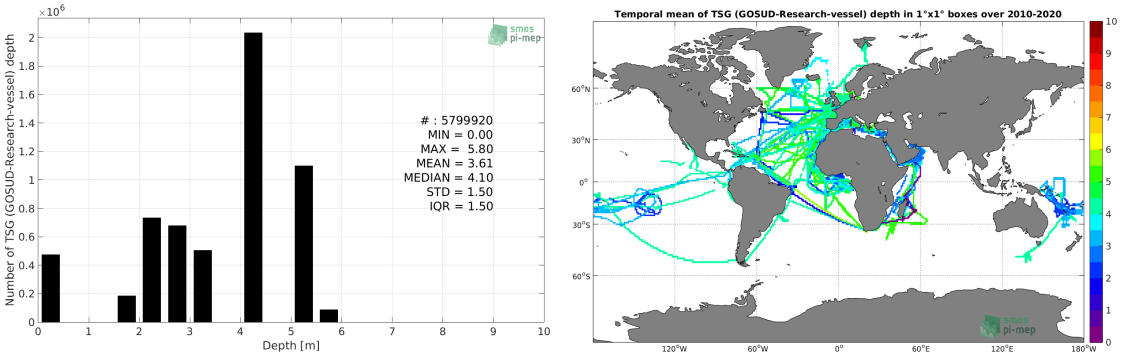

(a) (b)

Figure 15: Depth distribution of the upper level SSS measurements from TSG (GOSUD-Research-vessel) (a) and spatial distribution of the *in situ* SSS depth measurements showing the mean value in 1°x1° boxes and considering the full *in situ* dataset period (b).

2.2.5 Spatial distribution of SSS

In Figure 16, the number of TSG (GOSUD-Research-vessel) SSS measurements in 1°x1° boxes is shown.

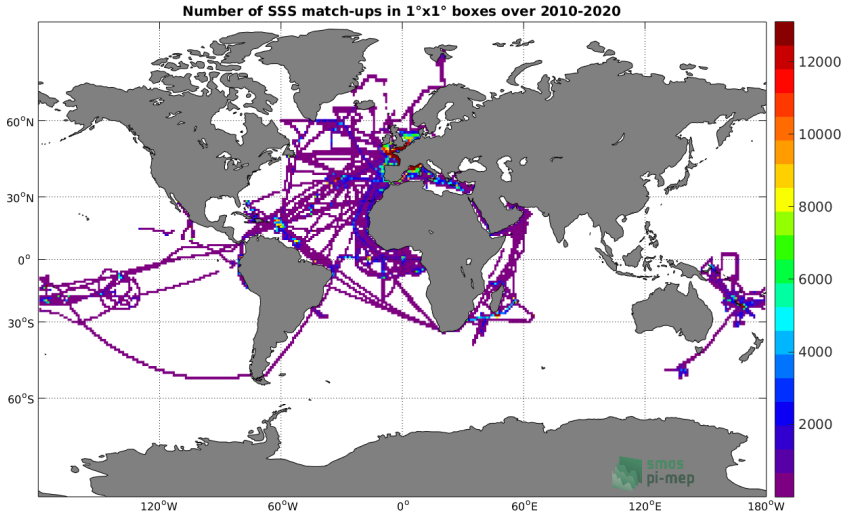

Figure 16: Number of SSS from TSG (GOSUD-Research-vessel) in 1°x1° boxes.

2.2.6 Spatial Maps of the Temporal mean and Std of *in situ* and ISAS SSS and of the difference (ΔSSS)

In Figure 17, maps of temporal mean (left) and standard deviation (right) of ISAS (top), TSG (GOSUD-Research-vessel) *in situ* dataset (middle) and the difference ΔSSS(ISAS -TSG (GOSUD-Research-vessel)) (bottom) are shown. The temporal mean and std are calculated using all match-up pairs falling in spatial boxes of size 1°x1° over the full TSG (GOSUD-Research-vessel) dataset period.

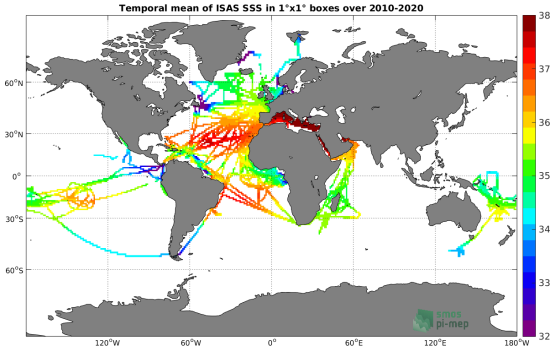

(a) MEAN(ISAS SSS)

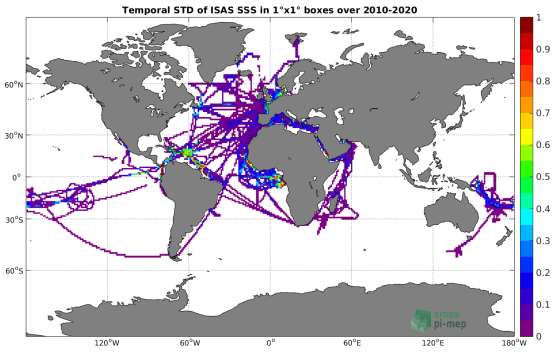

(b) Std(ISAS SSS)

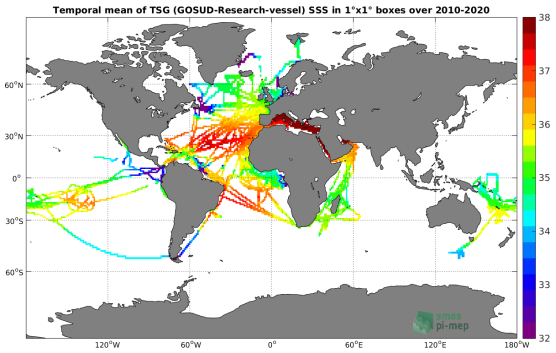

(c) MEAN(TSG (GOSUD-Research-vessel) SSS)

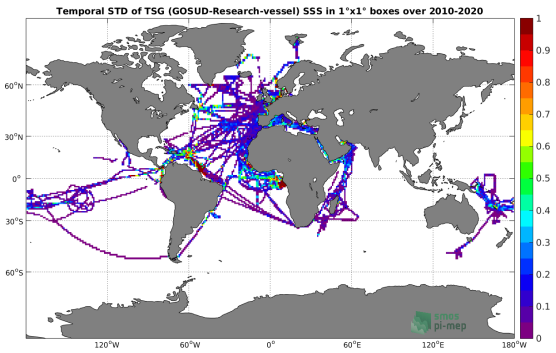

(d) Std(TSG (GOSUD-Research-vessel) SSS)

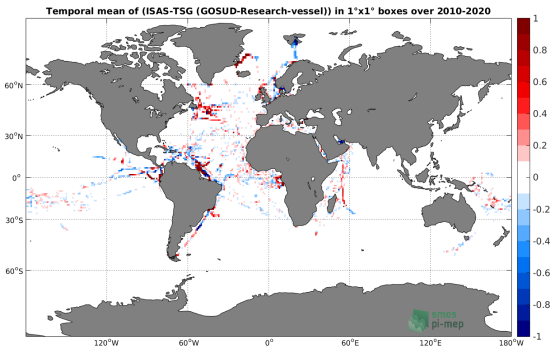

(e) MEAN(ΔSSS) (ISAS - TSG (GOSUD-Research-vessel))

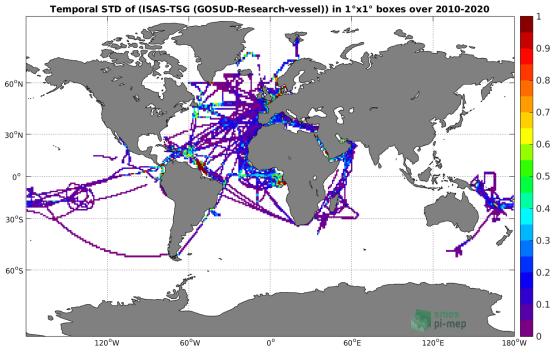

(f) Std(ΔSSS) (ISAS - TSG (GOSUD-Research-vessel))

Figure 17: Temporal mean (left) and Std (right) of SSS from ISAS (top), TSG (GOSUD-Research-vessel) (middle), and of ΔSSS (ISAS - TSG (GOSUD-Research-vessel)). Only match-up pairs are used to generate these maps.

2.2.7 Time series of the monthly median and Std of *in situ* and ISAS SSS and of the difference (ΔSSS)

In the top panel of Figure 18, we show the time series of the monthly median SSS estimated for both ISAS SSS product (in black) and the TSG (GOSUD-Research-vessel) *in situ* dataset (in blue) at the collected Pi-MEP match-up pairs.

In the middle panel of Figure 18, we show the time series of the monthly median of ΔSSS

(ISAS - TSG (GOSUD-Research-vessel)) for the collected Pi-MEP match-up pairs.

In the bottom panel of Figure 18, we show the time series of the monthly standard deviation of the ΔSSS (ISAS - TSG (GOSUD-Research-vessel)) for the collected Pi-MEP match-up pairs.

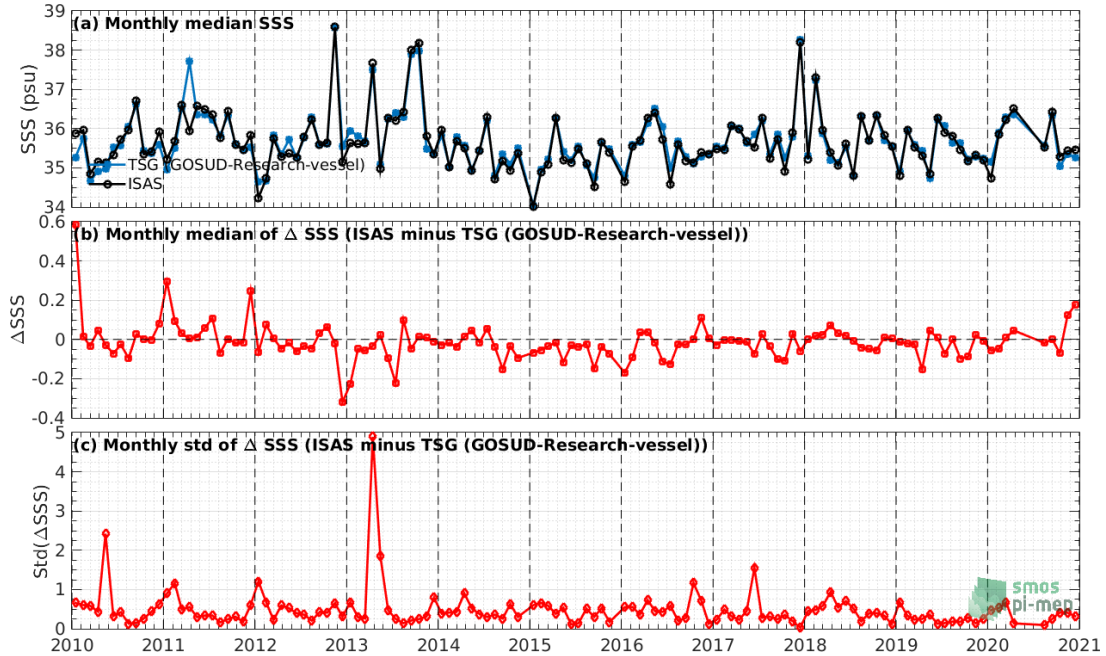

Figure 18: Time series of the monthly median SSS (top), median of ΔSSS (ISAS - TSG (GOSUD-Research-vessel)) and Std of ΔSSS (ISAS - TSG (GOSUD-Research-vessel)) considering all match-ups collected by the Pi-MEP.

2.2.8 Zonal mean and Std of *in situ* and ISAS SSS and of the difference ΔSSS

In Figure 19 left panel, we show the zonal mean SSS considering all Pi-MEP match-up pairs for both ISAS SSS product (in black) and the TSG (GOSUD-Research-vessel) *in situ* dataset (in blue). The full *in situ* dataset period is used to derive the mean.

In the right panel of Figure 19, we show the zonal mean of ΔSSS (ISAS - TSG (GOSUD-Research-vessel)) for all the collected Pi-MEP match-up pairs estimated over the full *in situ* dataset period.

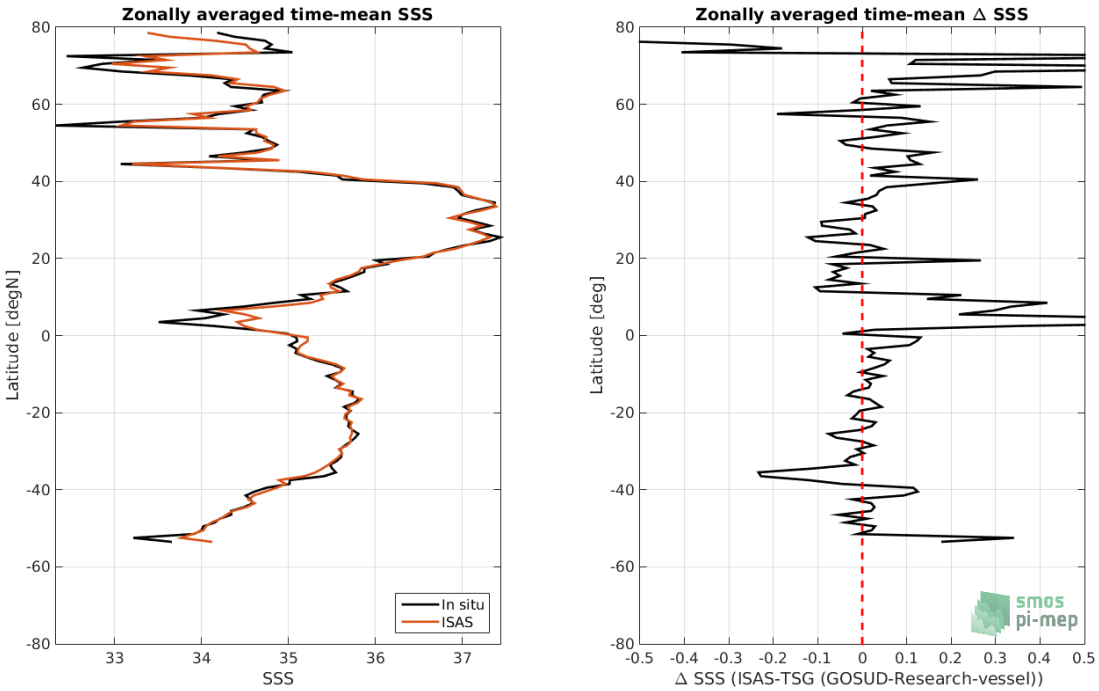

Figure 19: Left panel: Zonal mean SSS from ISAS product (black) and from TSG (GOSUD-Research-vessel) (blue). Right panel: Zonal mean of ΔSSS (ISAS - TSG (GOSUD-Research-vessel)) for all the collected Pi-MEP match-up pairs estimated over the full *in situ* dataset period.

2.2.9 Scatterplots of ISAS vs *in situ* SSS by latitudinal bands

In Figure 20, contour maps of the concentration of ISAS SSS (y-axis) versus TSG (GOSUD-Research-vessel) SSS (x-axis) at match-up pairs for different latitude bands: (a) 80°S-80°N, (b) 20°S-20°N, (c) 40°S-20°S and 20°N-40°N and (d) 60°S-40°S and 40°N-60°N. For each plot, the red line shows x=y. The black thin and dashed lines indicate a linear fit through the data cloud and the ±95% confidence levels, respectively. The number match-up pairs n, the slope and R^2 coefficient of the linear fit, the root mean square (RMS) and the mean bias between ISAS and *in situ* data are indicated for each latitude band in each plots.

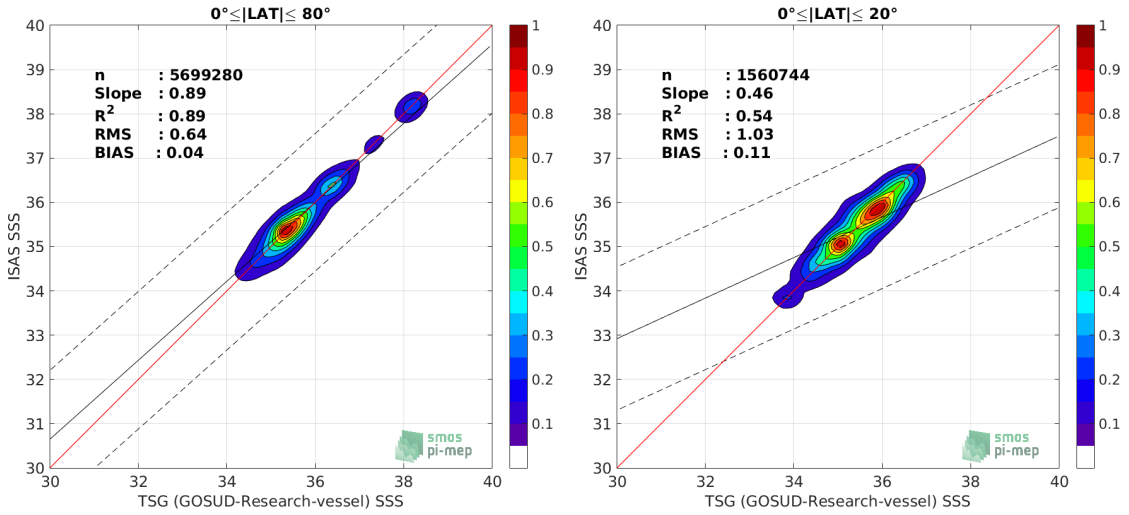

(a) $0° \leq |\text{LAT}| \leq 80°$

(b) $0° \leq |\text{LAT}| \leq 20°$

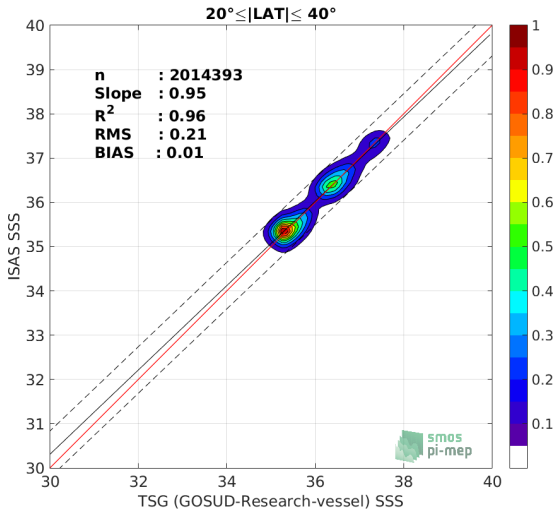

(c) $20° \leq |\text{LAT}| \leq 40°$

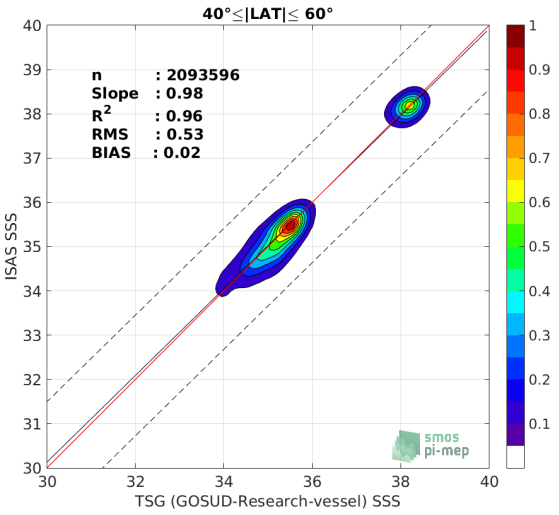

(d) $40° \leq |\text{LAT}| \leq 60°$

Figure 20: Contour maps of the concentration of ISAS SSS (y-axis) versus TSG (GOSUD-Research-vessel) SSS (x-axis) at match-up pairs for different latitude bands. For each plot, the red line shows x=y. The black thin and dashed lines indicate a linear fit through the data cloud and the ±95% confidence levels, respectively. The number match-up pairs n, the slope and R^2 coefficient of the linear fit, the root mean square (RMS) and the mean bias between ISAS and *in situ* data are indicated for each latitude band in each plots.

2.2.10 Time series of the monthly median and Std of the difference ΔSSS sorted by latitudinal bands

In Figure 21, time series of the monthly median (red curves) of ΔSSS (ISAS - TSG (GOSUD-Research-vessel)) and ±1 Std (black vertical thick bars) as function of time for all the collected Pi-MEP match-up pairs estimated for the full *in situ* dataset period are shown for different latitude bands: (a) 80°S-80°N, (b) 20°S-20°N, (c) 40°S-20°S and 20°N-40°N and (d) 60°S-40°S

and 40°N-60°N.

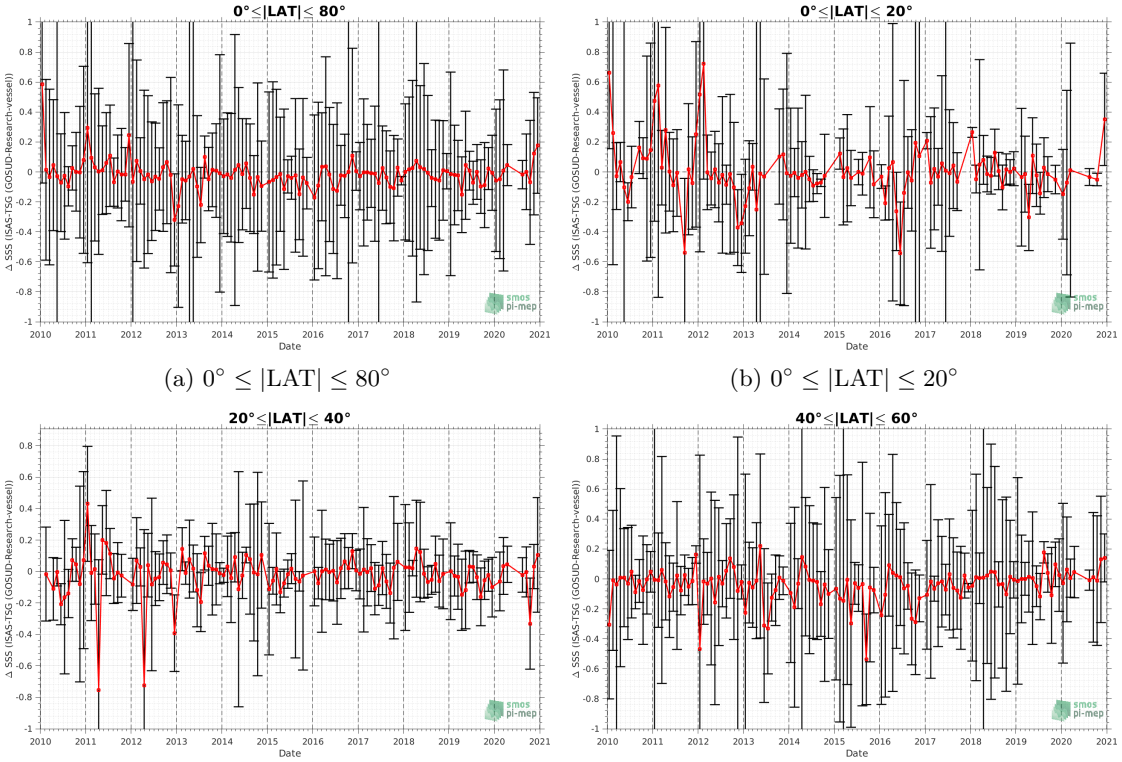

(a) $0° \leq |\text{LAT}| \leq 80°$

(b) $0° \leq |\text{LAT}| \leq 20°$

(c) $20° \leq |\text{LAT}| \leq 40°$

(d) $40° \leq |\text{LAT}| \leq 60°$

Figure 21: Monthly median (red curves) of ΔSSS (ISAS - TSG (GOSUD-Research-vessel)) and ±1 Std (black vertical thick bars) as function of time for all the collected Pi-MEP match-up pairs for the full *in situ* dataset period are shown for different latitude bands: (a) 80°S-80°N, (b) 20°S-20°N, (c) 40°S-20°S and 20°N-40°N and (d) 60°S-40°S and 40°N-60°N.

2.2.11 ΔSSS sorted as geophysical conditions

In Figure 22, we classify the match-up differences ΔSSS (ISAS - *in situ*) as function of the geophysical conditions at match-up points. The mean and std of ΔSSS (ISAS - TSG (GOSUD-Research-vessel)) is thus evaluated as function of the

- *in situ* SSS values per bins of width 0.2,
- *in situ* SST values per bins of width 1°C,
- ASCAT daily wind values per bins of width 1 m/s,
- CMORPH 3-hourly rain rates per bins of width 1 mm/h, and,
- distance to coasts per bins of width 50 km,
- *in situ* measurement depth (if relevant).

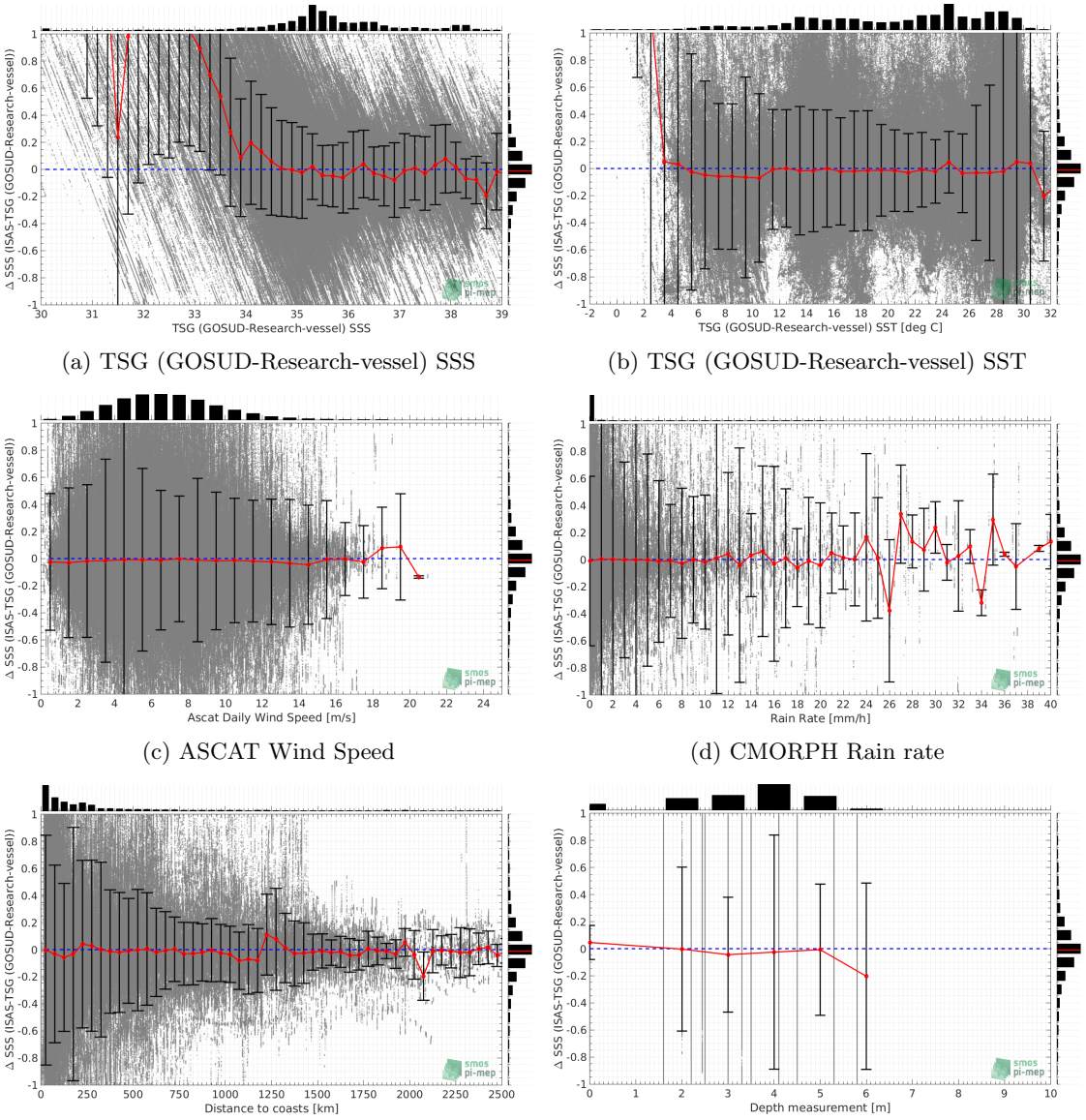

(a) TSG (GOSUD-Research-vessel) SSS

(b) TSG (GOSUD-Research-vessel) SST

(c) ASCAT Wind Speed

(d) CMORPH Rain rate

(e) Distance to coast

(f) Depth

Figure 22: Δ SSS (ISAS - TSG (GOSUD-Research-vessel)) sorted as geophysical conditions: TSG (GOSUD-Research-vessel) SSS a), TSG (GOSUD-Research-vessel) SST b), ASCAT Wind speed c), CMORPH rain rate d), distance to coast (e) and depth measurements (f).

2.2.12 ΔSSS maps and statistics for different geophysical conditions

In Figures 23 and 24, we focus on sub-datasets of the match-up differences ΔSSS (ISAS - *in situ*) for the following specific geophysical conditions:

- **C1**:if the local value at *in situ* location of estimated rain rate is zero, mean daily wind is in the range [3, 12] m/s, the SST is $> 5°$C and distance to coast is > 800 km.
- **C2**:if the local value at *in situ* location of estimated rain rate is zero, mean daily wind is

in the range [3, 12] m/s.

- **C3**:if the local value at *in situ* location of estimated rain rate is high (ie. $>$ 1 mm/h) and mean daily wind is low (ie. $<$ 4 m/s).
- **C5**:if the *in situ* data is located where the climatological SSS standard deviation is low (ie. above $<$ 0.2).
- **C6**:if the *in situ* data is located where the climatological SSS standard deviation is high (ie. above $>$ 0.2).

For each of these conditions, the temporal mean (gridded over spatial boxes of size 1°x1°) and the histogram of the difference ΔSSS (ISAS - *in situ*) are presented.

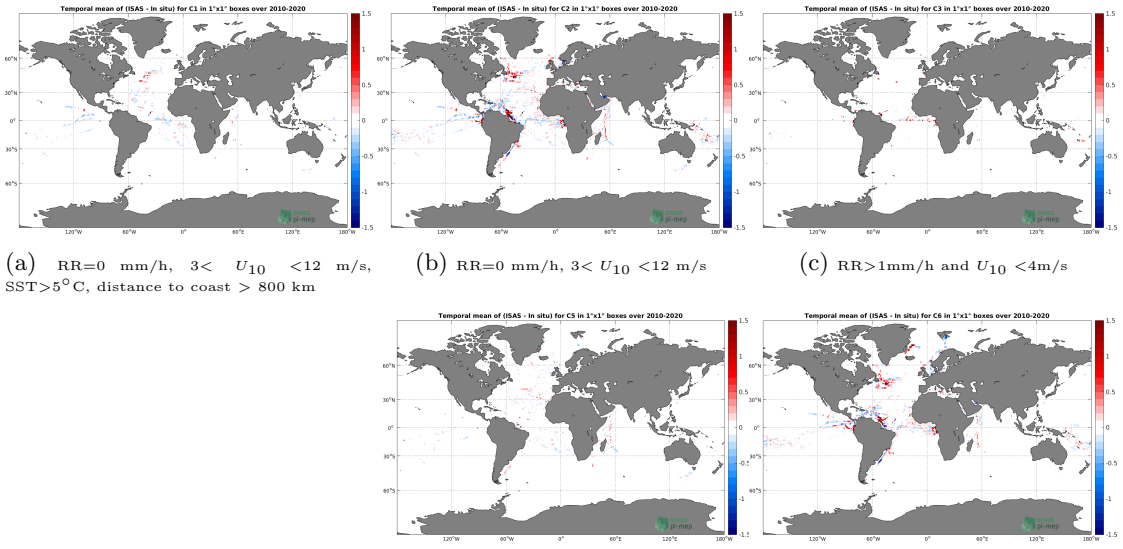

(a) RR=0 mm/h, 3< U_{10} <12 m/s, SST>5°C, distance to coast > 800 km (b) RR=0 mm/h, 3< U_{10} <12 m/s (c) RR>1mm/h and U_{10} <4m/s

(d) WOA2013 SSS Std<0.2 (e) WOA2013 SSS Std>0.2

Figure 23: Temporal mean gridded over spatial boxes of size 1°x1° of ΔSSS (ISAS - TSG (GOSUD-Research-vessel)) for 5 different subdatasets corresponding to:RR=0 mm/h, 3< U_{10} <12 m/s, SST>5°C, distance to coast > 800 km (a), RR=0 mm/h, 3< U_{10} <12 m/s (b), RR>1mm/h and U_{10} <4m/s (c),WOA2013 SSS Std<0.2 (d),WOA2013 SSS Std>0.2 (e).

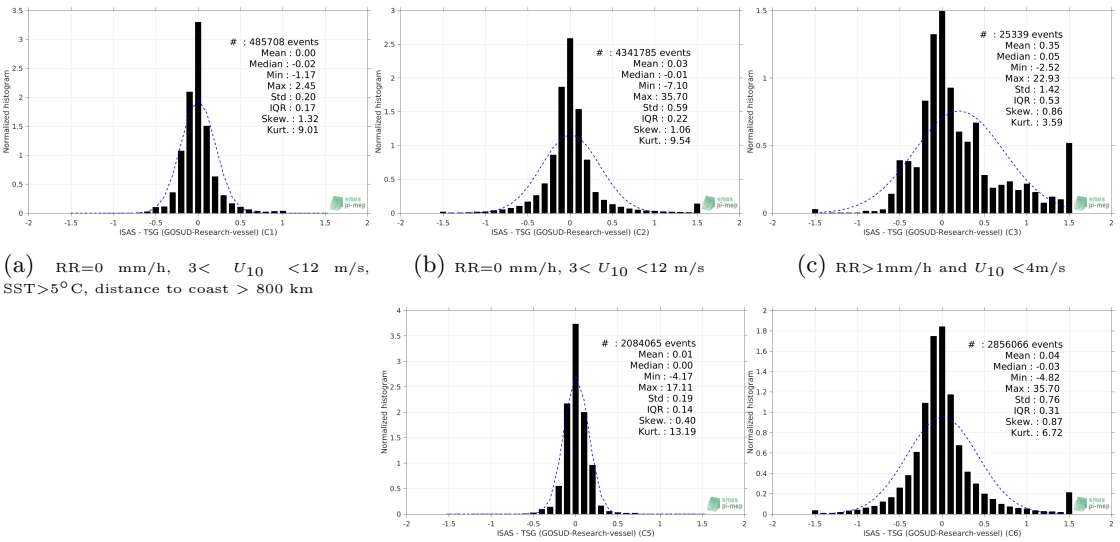

(a) RR=0 mm/h, 3< U_{10} <12 m/s, SST>5°C, distance to coast > 800 km (b) RR=0 mm/h, 3< U_{10} <12 m/s (c) RR>1mm/h and U_{10} <4m/s

(d) WOA2013 SSS Std<0.2 (e) WOA2013 SSS Std>0.2

Figure 24: Normalized histogram of ΔSSS (ISAS - TSG (GOSUD-Research-vessel)) for 5 different subdatasets corresponding to:RR=0 mm/h, 3< U_{10} <12 m/s, SST>5°C, distance to coast > 800 km (a), RR=0 mm/h, 3< U_{10} <12 m/s (b), RR>1mm/h and U_{10} <4m/s (c),WOA2013 SSS Std<0.2 (d),WOA2013 SSS Std>0.2 (e).

2.2.13 Summary

Table 1 shows the mean, median, standard deviation (Std), root mean square (RMS), interquartile range (IQR), correlation coefficient (r^2) and robust standard deviation (Std*) of the match-up differences ΔSSS (ISAS - TSG (GOSUD-Research-vessel)) for the following conditions:

- all: All the match-up pairs satellite/in situ SSS values are used to derive the statistics
- C1: only pairs where RR=0 mm/h, 3< U_{10} <12 m/s, SST>5°C, distance to coast > 800 km
- C2: only pairs where RR=0 mm/h, 3< U_{10} <12 m/s
- C3: only pairs where RR>1mm/h and U_{10} <4m/s
- C5: only pairs where WOA2013 SSS Std<0.2
- C6: only pairs where WOA2013 SSS Std>0.2
- C7a: only pairs with a distance to coast < 150 km.
- C7b: only pairs with a distance to coast in the range [150, 800] km.
- C7c: only pairs with a distance to coast > 800 km.
- C8a: only pairs where SST is < 5°C.
- C8b: only pairs where SST is in the range [5, 15]°C.
- C8c: only pairs where SST is > 15°C.

- C9a: only pairs where SSS is < 33.
- C9b: only pairs where SSS is in the range [33, 37].
- C9c: only pairs where SSS is > 37.

Table 1: Statistics of ΔSSS (ISAS - TSG (GOSUD-Research-vessel))

Condition	#	Median	Mean	Std	RMS	IQR	r^2	Std*
all	5707378	-0.01	0.04	0.66	0.66	0.23	0.888	0.17
C1	485708	-0.02	0.00	0.20	0.20	0.17	0.959	0.13
C2	4341785	-0.01	0.03	0.59	0.59	0.22	0.908	0.17
C3	25339	0.05	0.35	1.42	1.47	0.53	0.655	0.36
C5	2084065	0.00	0.01	0.19	0.19	0.14	0.960	0.11
C6	2856066	-0.03	0.04	0.76	0.76	0.31	0.893	0.23
C7a	2869194	-0.03	0.04	0.75	0.75	0.28	0.909	0.21
C7b	2214243	0.01	0.05	0.63	0.63	0.20	0.774	0.15
C7c	623089	-0.02	0.00	0.22	0.22	0.18	0.953	0.13
C8a	27431	0.13	0.51	1.47	1.56	1.54	0.918	1.17
C8b	1135698	-0.02	0.01	0.53	0.53	0.22	0.850	0.16
C8c	4267025	-0.01	0.04	0.69	0.70	0.23	0.890	0.17
C9a	183963	1.06	1.55	2.89	3.28	2.39	0.773	1.78
C9b	4615639	-0.01	0.00	0.32	0.32	0.23	0.813	0.17
C9c	907776	-0.03	-0.04	0.25	0.25	0.19	0.859	0.14

Table 1 numerical values can be downloaded as a csv file here.

2.3 TSG (GOSUD-Sailing-ship)

2.3.1 Introduction

The TSG-GOSUD-Sailing-ship dataset corresponds to observations of sea surface salinity obtained from voluntary sailing ships using medium or small size sensors. They complement the networks installed on research vessels or commercial ships. This delayed mode dataset (Reynaud et al. (2021)) is updated annually as a contribution to GOSUD (`http://www.gosud.org`) and freely available here. Adjusted values when available and only collected TSG data that exhibit quality flags=1 and 2 were used.

2.3.2 Number of SSS data as a function of time and distance to coast

Figure 25 shows the time (a) and distance to coast (b) distributions of the TSG (GOSUD-Sailing-ship) *in situ* dataset.

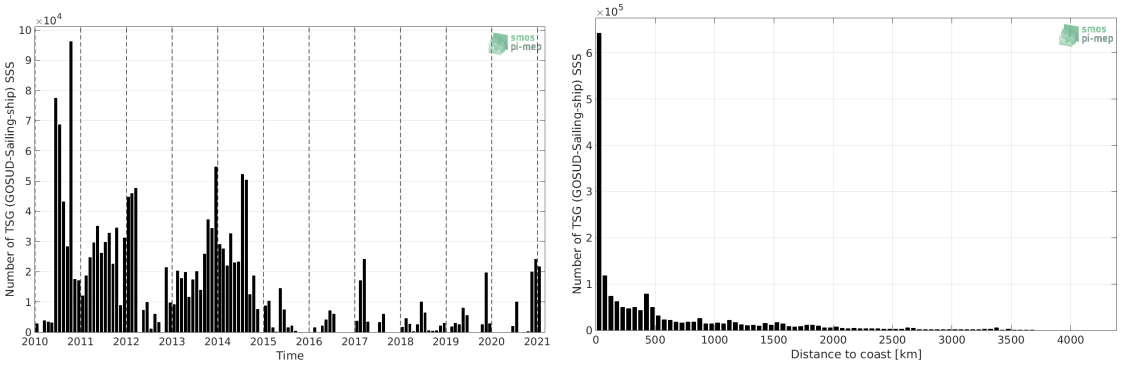

(a) (b)

Figure 25: Number of SSS from TSG (GOSUD-Sailing-ship) as a function of time (a) and distance to coast (b).

2.3.3 Histograms of SSS

Figure 26 shows the SSS distribution of the TSG (GOSUD-Sailing-ship) (a) and colocalized ISAS (b) dataset.

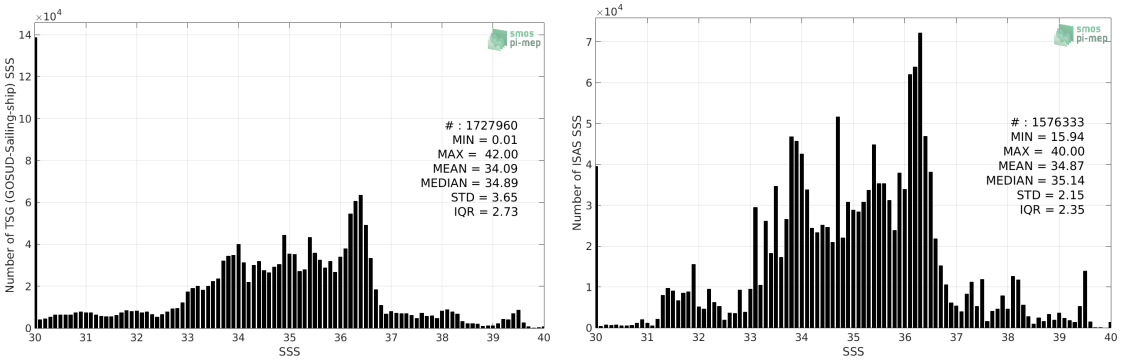

(a) (b)

Figure 26: Histograms of SSS from TSG (GOSUD-Sailing-ship) (a) and ISAS (b) per bins of 0.1.

2.3.4 Distribution of *in situ* SSS depth measurements

In Figure 27, we show the depth distribution of the *in situ* salinity dataset (a) and the spatial distribution of the depth temporal mean in 1°x1° boxes and considering the full *in situ* dataset period (b).

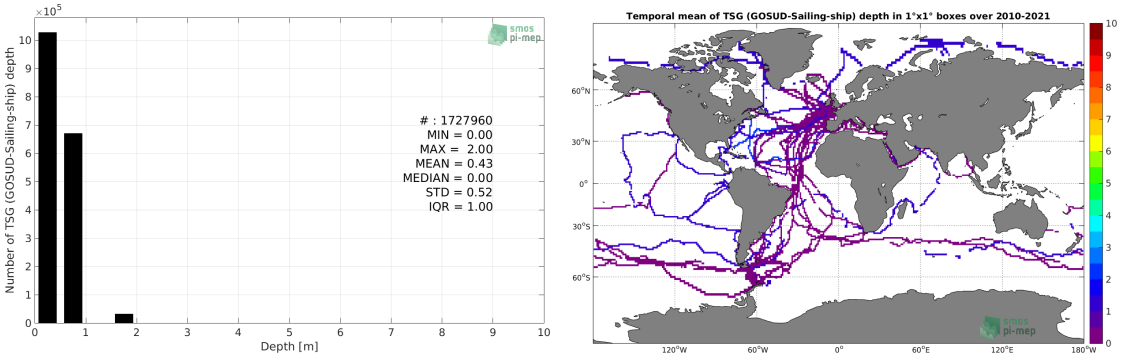

(a) (b)

Figure 27: Depth distribution of the upper level SSS measurements from TSG (GOSUD-Sailing-ship) (a) and spatial distribution of the *in situ* SSS depth measurements showing the mean value in 1°x1° boxes and considering the full *in situ* dataset period (b).

2.3.5 Spatial distribution of SSS

In Figure 28, the number of TSG (GOSUD-Sailing-ship) SSS measurements in 1°x1° boxes is shown.

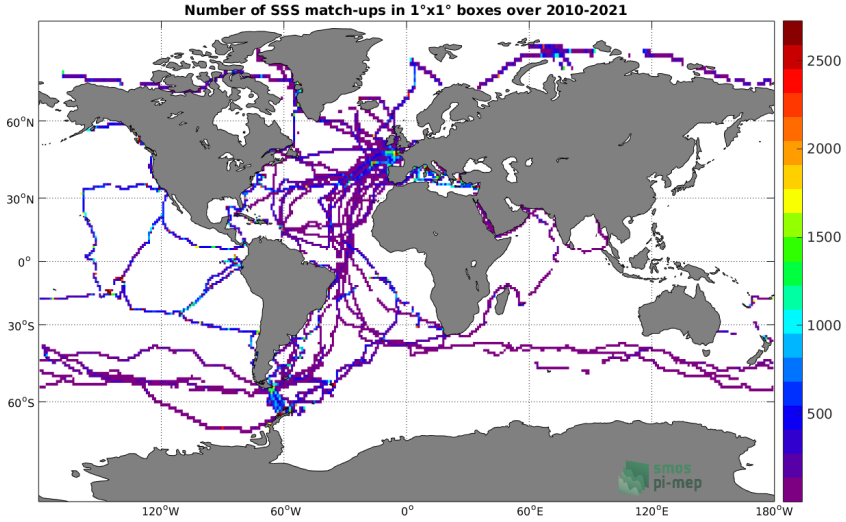

Figure 28: Number of SSS from TSG (GOSUD-Sailing-ship) in 1°x1° boxes.

2.3.6 Spatial Maps of the Temporal mean and Std of *in situ* and ISAS SSS and of the difference (ΔSSS)

In Figure 29, maps of temporal mean (left) and standard deviation (right) of ISAS (top), TSG (GOSUD-Sailing-ship) *in situ* dataset (middle) and the difference ΔSSS(ISAS -TSG (GOSUD-Sailing-ship)) (bottom) are shown. The temporal mean and std are calculated using all match-up pairs falling in spatial boxes of size 1°x1° over the full TSG (GOSUD-Sailing-ship) dataset period.

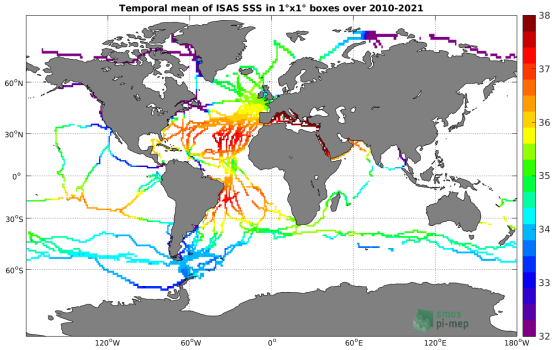

(a) MEAN(ISAS SSS)

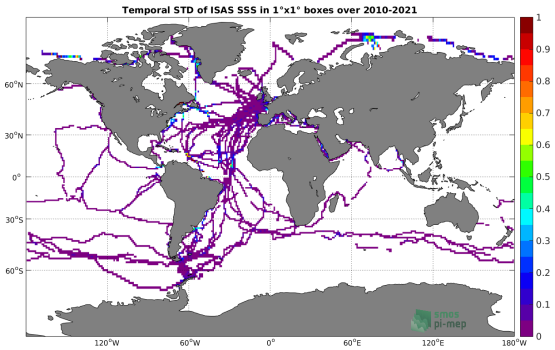

(b) Std(ISAS SSS)

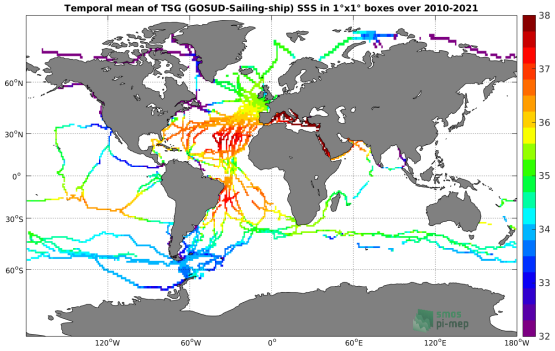

(c) MEAN(TSG (GOSUD-Sailing-ship) SSS)

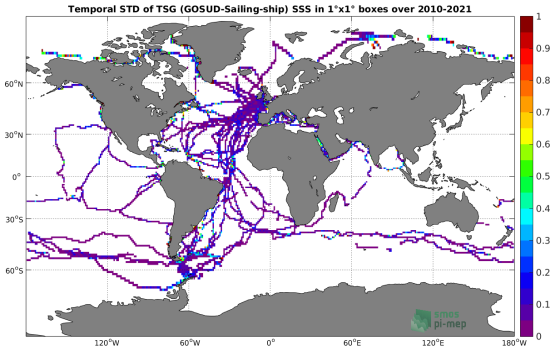

(d) Std(TSG (GOSUD-Sailing-ship) SSS)

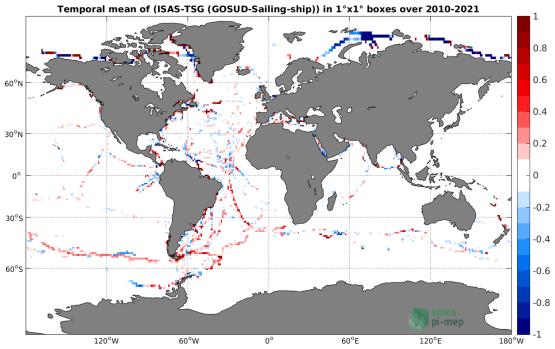

(e) MEAN(ΔSSS) (ISAS - TSG (GOSUD-Sailing-ship))

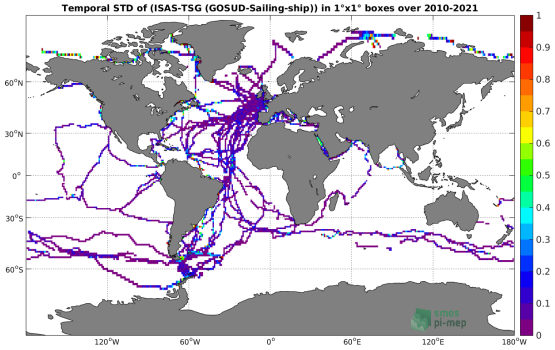

(f) Std(ΔSSS) (ISAS - TSG (GOSUD-Sailing-ship))

Figure 29: Temporal mean (left) and Std (right) of SSS from ISAS (top), TSG (GOSUD-Sailing-ship) (middle), and of ΔSSS (ISAS - TSG (GOSUD-Sailing-ship)). Only match-up pairs are used to generate these maps.

2.3.7 Time series of the monthly median and Std of *in situ* and ISAS SSS and of the difference (ΔSSS)

In the top panel of Figure 30, we show the time series of the monthly median SSS estimated for both ISAS SSS product (in black) and the TSG (GOSUD-Sailing-ship) *in situ* dataset (in blue) at the collected Pi-MEP match-up pairs.

In the middle panel of Figure 30, we show the time series of the monthly median of ΔSSS

(ISAS - TSG (GOSUD-Sailing-ship)) for the collected Pi-MEP match-up pairs.

In the bottom panel of Figure 30, we show the time series of the monthly standard deviation of the ΔSSS (ISAS - TSG (GOSUD-Sailing-ship)) for the collected Pi-MEP match-up pairs.

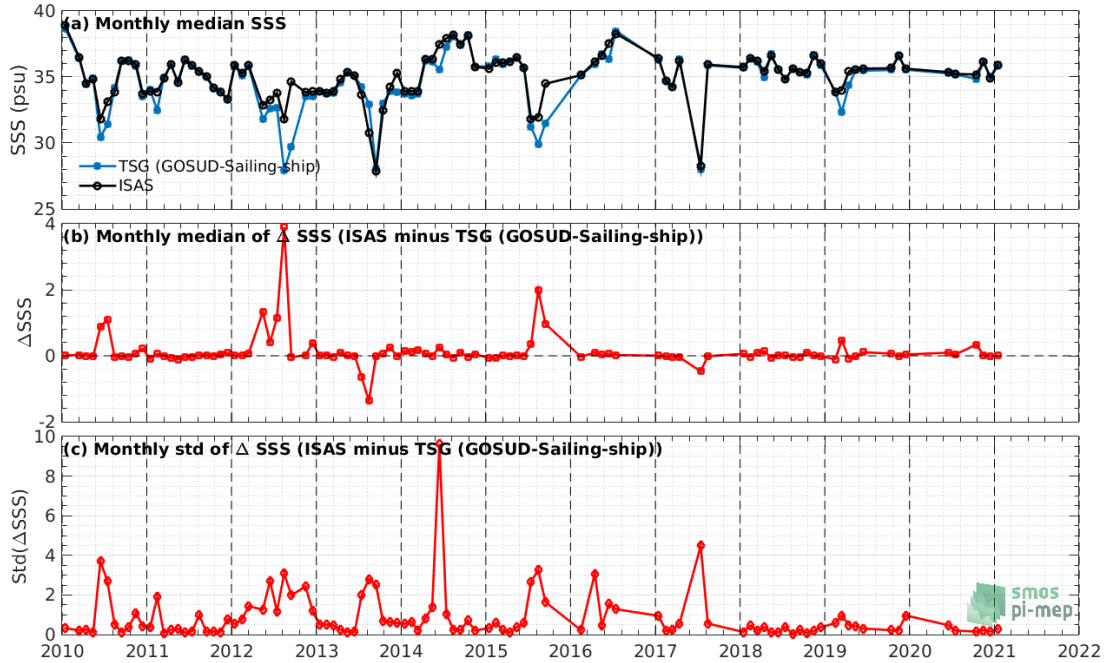

Figure 30: Time series of the monthly median SSS (top), median of ΔSSS (ISAS - TSG (GOSUD-Sailing-ship)) and Std of ΔSSS (ISAS - TSG (GOSUD-Sailing-ship)) considering all match-ups collected by the Pi-MEP.

2.3.8 Zonal mean and Std of *in situ* and ISAS SSS and of the difference ΔSSS

In Figure 31 left panel, we show the zonal mean SSS considering all Pi-MEP match-up pairs for both ISAS SSS product (in black) and the TSG (GOSUD-Sailing-ship) *in situ* dataset (in blue). The full *in situ* dataset period is used to derive the mean.

In the right panel of Figure 31, we show the zonal mean of ΔSSS (ISAS - TSG (GOSUD-Sailing-ship)) for all the collected Pi-MEP match-up pairs estimated over the full *in situ* dataset period.

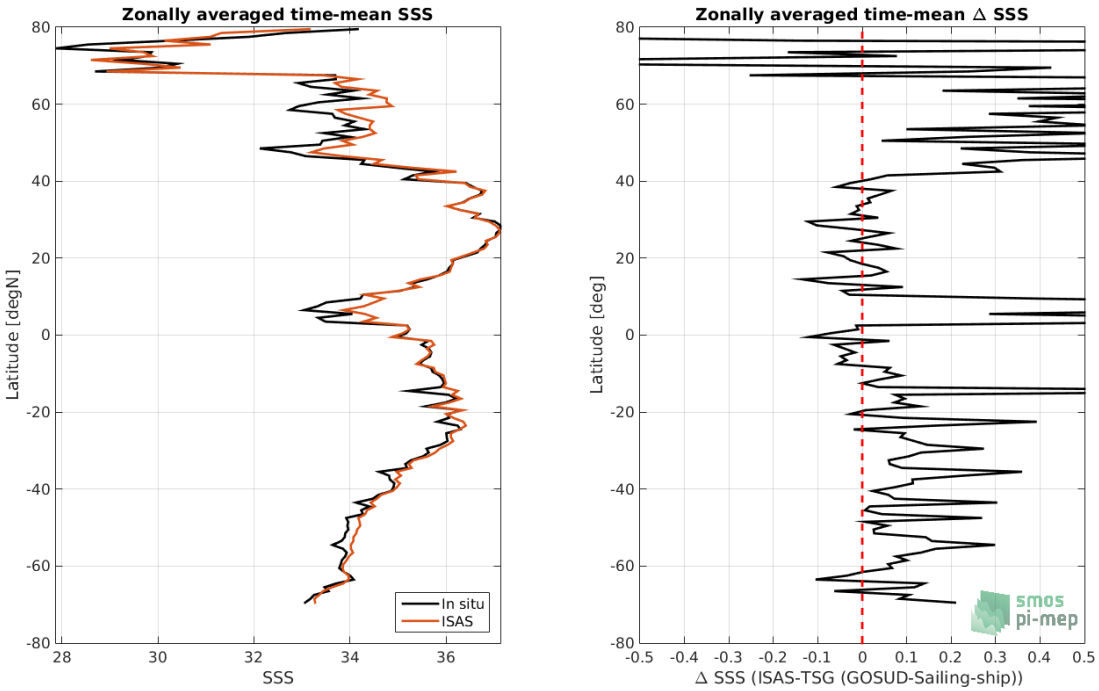

Figure 31: Left panel: Zonal mean SSS from ISAS product (black) and from TSG (GOSUD-Sailing-ship) (blue). Right panel: Zonal mean of ΔSSS (ISAS - TSG (GOSUD-Sailing-ship)) for all the collected Pi-MEP match-up pairs estimated over the full *in situ* dataset period.

2.3.9 Scatterplots of ISAS vs *in situ* SSS by latitudinal bands

In Figure 32, contour maps of the concentration of ISAS SSS (y-axis) versus TSG (GOSUD-Sailing-ship) SSS (x-axis) at match-up pairs for different latitude bands: (a) 80°S-80°N, (b) 20°S-20°N, (c) 40°S-20°S and 20°N-40°N and (d) 60°S-40°S and 40°N-60°N. For each plot, the red line shows x=y. The black thin and dashed lines indicate a linear fit through the data cloud and the ±95% confidence levels, respectively. The number match-up pairs n, the slope and R^2 coefficient of the linear fit, the root mean square (RMS) and the mean bias between ISAS and *in situ* data are indicated for each latitude band in each plots.

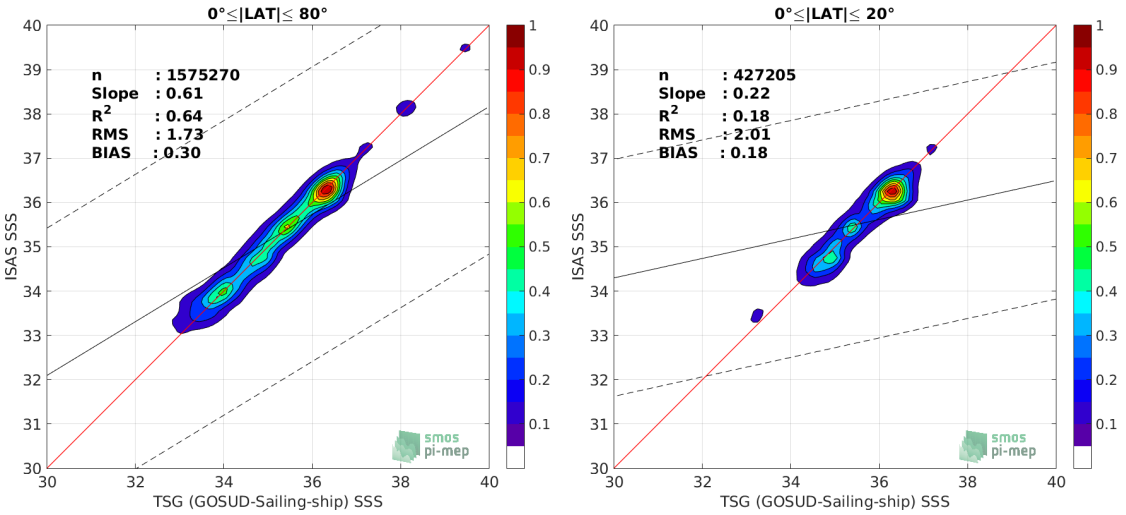

(a) $0° \leq |\text{LAT}| \leq 80°$

(b) $0° \leq |\text{LAT}| \leq 20°$

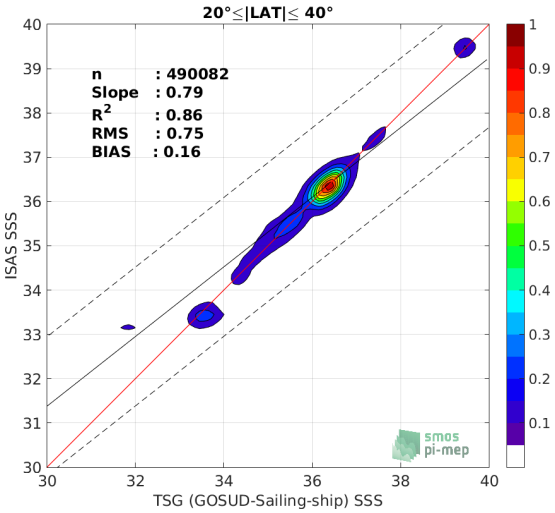

(c) $20° \leq |\text{LAT}| \leq 40°$

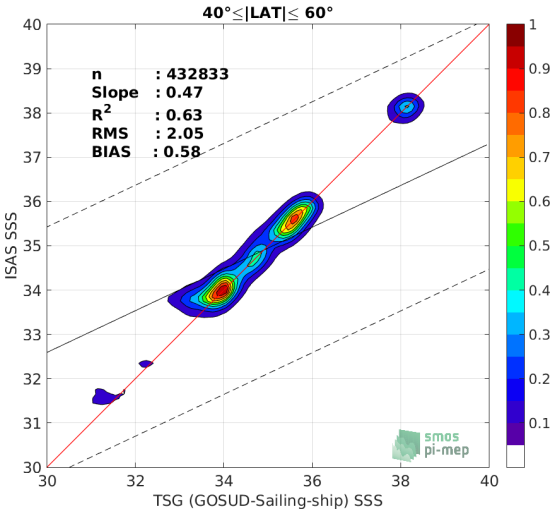

(d) $40° \leq |\text{LAT}| \leq 60°$

Figure 32: Contour maps of the concentration of ISAS SSS (y-axis) versus TSG (GOSUD-Sailing-ship) SSS (x-axis) at match-up pairs for different latitude bands. For each plot, the red line shows x=y. The black thin and dashed lines indicate a linear fit through the data cloud and the ±95% confidence levels, respectively. The number match-up pairs n, the slope and R^2 coefficient of the linear fit, the root mean square (RMS) and the mean bias between ISAS and *in situ* data are indicated for each latitude band in each plots.

2.3.10 Time series of the monthly median and Std of the difference ΔSSS sorted by latitudinal bands

In Figure 33, time series of the monthly median (red curves) of ΔSSS (ISAS - TSG (GOSUD-Sailing-ship)) and ±1 Std (black vertical thick bars) as function of time for all the collected Pi-MEP match-up pairs estimated for the full *in situ* dataset period are shown for different latitude bands: (a) 80°S-80°N, (b) 20°S-20°N, (c) 40°S-20°S and 20°N-40°N and (d) 60°S-40°S

and 40°N-60°N.

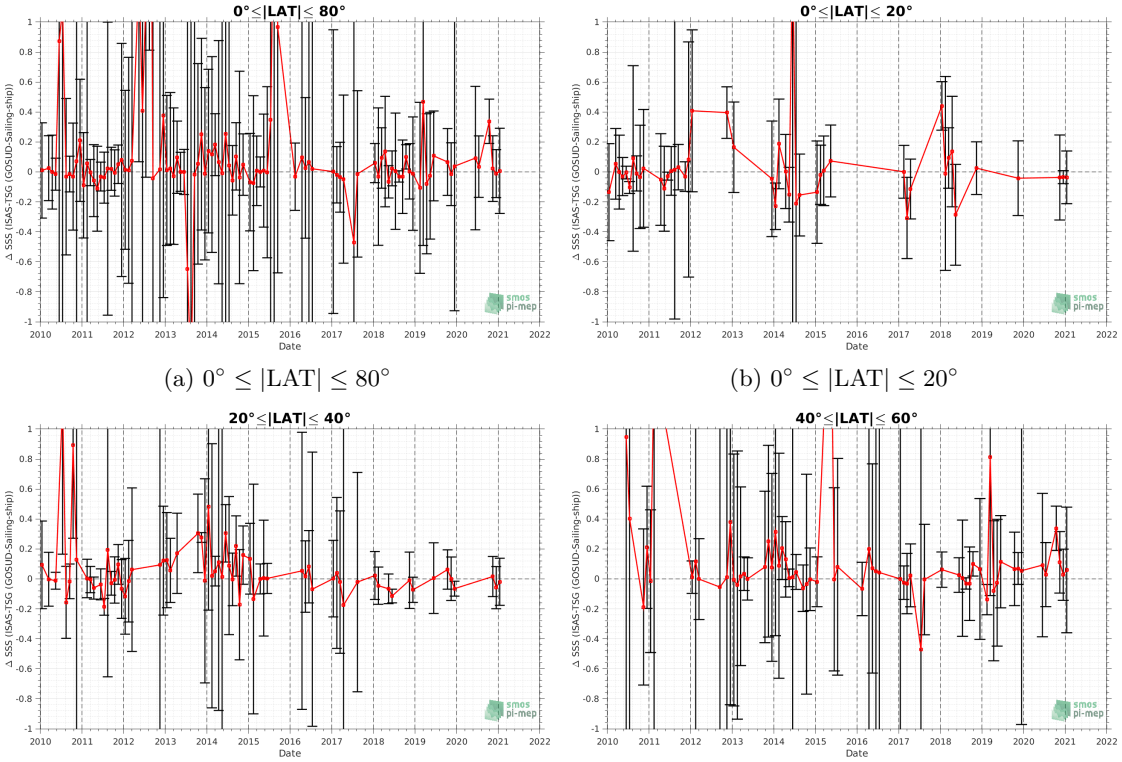

(a) $0° \leq |\text{LAT}| \leq 80°$

(b) $0° \leq |\text{LAT}| \leq 20°$

(c) $20° \leq |\text{LAT}| \leq 40°$

(d) $40° \leq |\text{LAT}| \leq 60°$

Figure 33: Monthly median (red curves) of ΔSSS (ISAS - TSG (GOSUD-Sailing-ship)) and ±1 Std (black vertical thick bars) as function of time for all the collected Pi-MEP match-up pairs for the full *in situ* dataset period are shown for different latitude bands: (a) 80°S-80°N, (b) 20°S-20°N, (c) 40°S-20°S and 20°N-40°N and (d) 60°S-40°S and 40°N-60°N.

2.3.11 ΔSSS sorted as geophysical conditions

In Figure 34, we classify the match-up differences ΔSSS (ISAS - *in situ*) as function of the geophysical conditions at match-up points. The mean and std of ΔSSS (ISAS - TSG (GOSUD-Sailing-ship)) is thus evaluated as function of the

- *in situ* SSS values per bins of width 0.2,
- *in situ* SST values per bins of width 1°C,
- ASCAT daily wind values per bins of width 1 m/s,
- CMORPH 3-hourly rain rates per bins of width 1 mm/h, and,
- distance to coasts per bins of width 50 km,
- *in situ* measurement depth (if relevant).

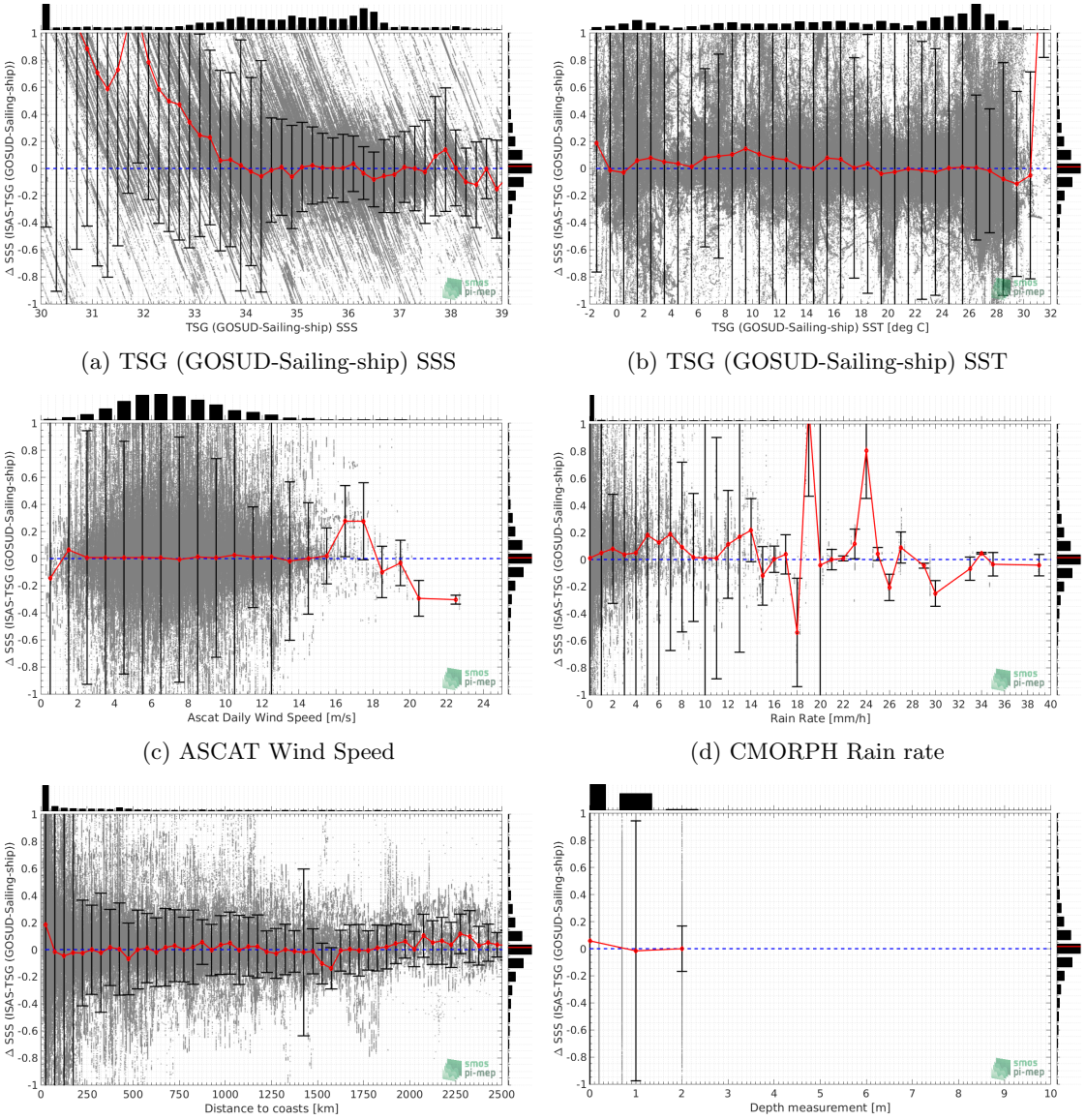

(a) TSG (GOSUD-Sailing-ship) SSS

(b) TSG (GOSUD-Sailing-ship) SST

(c) ASCAT Wind Speed

(d) CMORPH Rain rate

(e) Distance to coast

(f) Depth

Figure 34: Δ SSS (ISAS - TSG (GOSUD-Sailing-ship)) sorted as geophysical conditions: TSG (GOSUD-Sailing-ship) SSS a), TSG (GOSUD-Sailing-ship) SST b), ASCAT Wind speed c), CMORPH rain rate d), distance to coast (e) and depth measurements (f).

2.3.12 ΔSSS maps and statistics for different geophysical conditions

In Figures 35 and 36, we focus on sub-datasets of the match-up differences ΔSSS (ISAS - *in situ*) for the following specific geophysical conditions:

- **C1**:if the local value at *in situ* location of estimated rain rate is zero, mean daily wind is in the range [3, 12] m/s, the SST is $> 5°$C and distance to coast is > 800 km.
- **C2**:if the local value at *in situ* location of estimated rain rate is zero, mean daily wind is

in the range [3, 12] m/s.

- **C3**:if the local value at *in situ* location of estimated rain rate is high (ie. > 1 mm/h) and mean daily wind is low (ie. < 4 m/s).
- **C5**:if the *in situ* data is located where the climatological SSS standard deviation is low (ie. above < 0.2).
- **C6**:if the *in situ* data is located where the climatological SSS standard deviation is high (ie. above > 0.2).

For each of these conditions, the temporal mean (gridded over spatial boxes of size 1°x1°) and the histogram of the difference ΔSSS (ISAS - *in situ*) are presented.

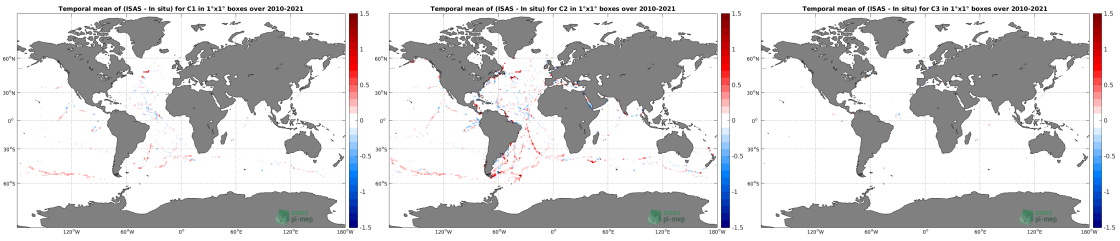

(a) RR=0 mm/h, 3< U_{10} <12 m/s, SST>5°C, distance to coast > 800 km (b) RR=0 mm/h, 3< U_{10} <12 m/s (c) RR>1mm/h and U_{10} <4m/s

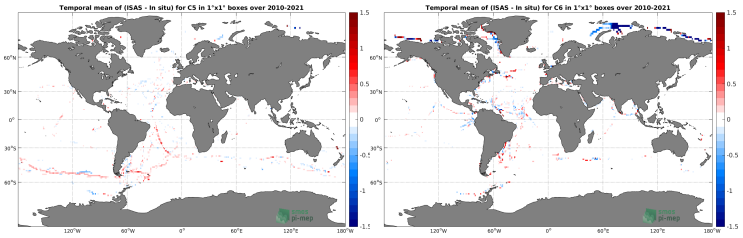

(d) WOA2013 SSS Std<0.2 (e) WOA2013 SSS Std>0.2

Figure 35: Temporal mean gridded over spatial boxes of size 1°x1° of ΔSSS (ISAS - TSG (GOSUD-Sailing-ship)) for 5 different subdatasets corresponding to:RR=0 mm/h, 3< U_{10} <12 m/s, SST>5°C, distance to coast > 800 km (a), RR=0 mm/h, 3< U_{10} <12 m/s (b), RR>1mm/h and U_{10} <4m/s (c),WOA2013 SSS Std<0.2 (d),WOA2013 SSS Std>0.2 (e).

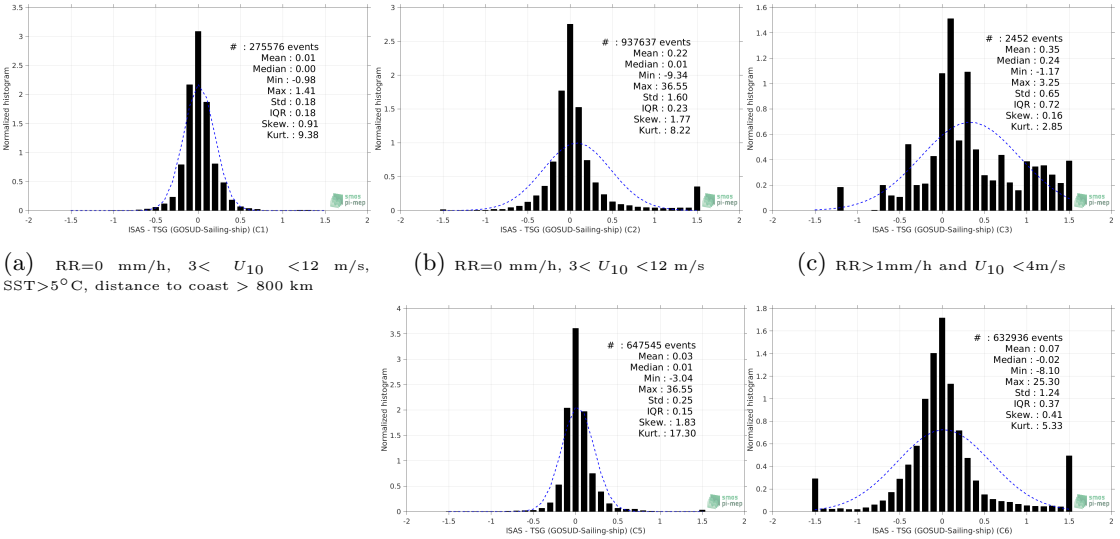

(a) RR=0 mm/h, 3< U_{10} <12 m/s, SST>5°C, distance to coast > 800 km (b) RR=0 mm/h, 3< U_{10} <12 m/s (c) RR>1mm/h and U_{10} <4m/s

(d) WOA2013 SSS Std<0.2 (e) WOA2013 SSS Std>0.2

Figure 36: Normalized histogram of ΔSSS (ISAS - TSG (GOSUD-Sailing-ship)) for 5 different subdatasets corresponding to:RR=0 mm/h, 3< U_{10} <12 m/s, SST>5°C, distance to coast > 800 km (a), RR=0 mm/h, 3< U_{10} <12 m/s (b), RR>1mm/h and U_{10} <4m/s (c),WOA2013 SSS Std<0.2 (d),WOA2013 SSS Std>0.2 (e).

2.3.13 Summary

Table 1 shows the mean, median, standard deviation (Std), root mean square (RMS), interquartile range (IQR), correlation coefficient (r^2) and robust standard deviation (Std*) of the match-up differences ΔSSS (ISAS - TSG (GOSUD-Sailing-ship)) for the following conditions:

- all: All the match-up pairs satellite/in situ SSS values are used to derive the statistics
- C1: only pairs where RR=0 mm/h, 3< U_{10} <12 m/s, SST>5°C, distance to coast > 800 km
- C2: only pairs where RR=0 mm/h, 3< U_{10} <12 m/s
- C3: only pairs where RR>1mm/h and U_{10} <4m/s
- C5: only pairs where WOA2013 SSS Std<0.2
- C6: only pairs where WOA2013 SSS Std>0.2
- C7a: only pairs with a distance to coast < 150 km.
- C7b: only pairs with a distance to coast in the range [150, 800] km.
- C7c: only pairs with a distance to coast > 800 km.
- C8a: only pairs where SST is < 5°C.
- C8b: only pairs where SST is in the range [5, 15]°C.
- C8c: only pairs where SST is > 15°C.

- C9a: only pairs where SSS is < 33.
- C9b: only pairs where SSS is in the range [33, 37].
- C9c: only pairs where SSS is > 37.

Table 1: Statistics of ΔSSS (ISAS - TSG (GOSUD-Sailing-ship))

Condition	#	Median	Mean	Std	RMS	IQR	r^2	Std*
all	1576333	0.02	0.30	1.79	1.81	0.30	0.614	0.21
C1	275576	0.00	0.01	0.18	0.18	0.18	0.971	0.13
C2	937637	0.01	0.22	1.60	1.61	0.23	0.563	0.16
C3	2452	0.24	0.35	0.65	0.74	0.72	0.940	0.44
C5	647545	0.01	0.03	0.25	0.26	0.15	0.961	0.11
C6	632936	-0.02	0.07	1.24	1.24	0.37	0.793	0.27
C7a	682646	0.08	0.71	2.62	2.71	0.78	0.536	0.41
C7b	506386	-0.01	-0.02	0.54	0.54	0.20	0.900	0.15
C7c	387171	0.00	0.02	0.22	0.22	0.18	0.960	0.13
C8a	218628	0.05	-0.02	1.47	1.47	0.60	0.721	0.44
C8b	322858	0.05	0.58	1.85	1.94	0.38	0.643	0.22
C8c	983777	0.00	0.21	1.76	1.77	0.23	0.457	0.17
C9a	242798	1.00	1.97	4.04	4.49	2.22	0.123	1.44
C9b	1201251	0.00	0.00	0.48	0.48	0.22	0.819	0.17
C9c	132284	0.00	0.01	0.33	0.33	0.21	0.850	0.16

Table 1 numerical values can be downloaded as a csv file here.

2.4 TSG (SAMOS)

2.4.1 Introduction

The TSG-SAMOS dataset corresponds to "Research" quality data from the US Shipboard Automated Meteorological and Oceanographic System (SAMOS) initiative (Smith et al. (2009)). Data are available at http://samos.coaps.fsu.edu/html/. Adjusted values when available and only collected TSG data that exhibit quality flags=1 and 2 were used. After visual inspection, data from the NANCY FOSTER (ID="WTER", IMO="008993227") with date 2011/03/21 and all data from the ATLANTIS (ID="KAQP", IMO="009105798") for year 2010 has been removed from this dataset.

2.4.2 Number of SSS data as a function of time and distance to coast

Figure 37 shows the time (a) and distance to coast (b) distributions of the TSG (SAMOS) *in situ* dataset.

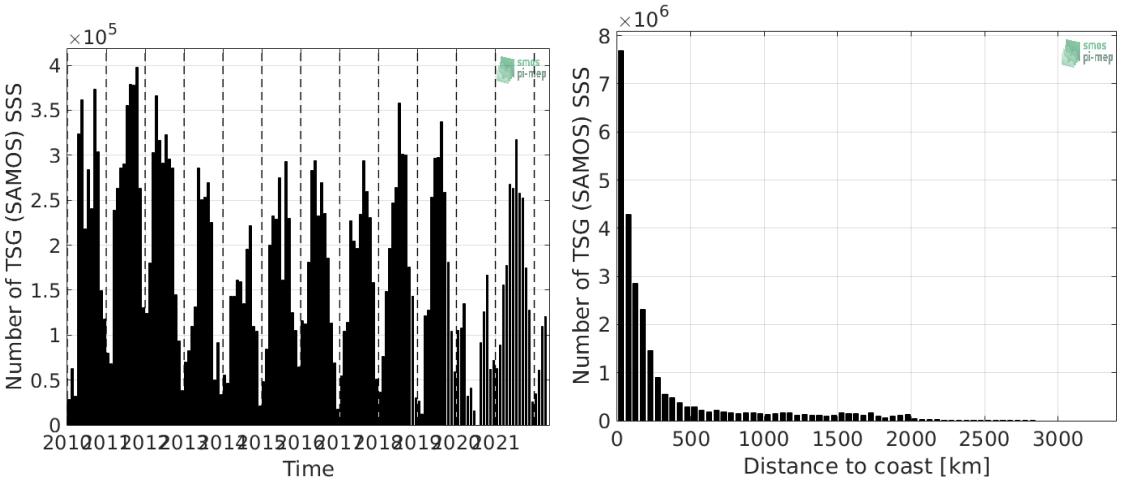

(a) (b)

Figure 37: Number of SSS from TSG (SAMOS) as a function of time (a) and distance to coast (b).

2.4.3 Histograms of SSS

Figure 38 shows the SSS distribution of the TSG (SAMOS) (a) and colocalized ISAS (b) dataset.

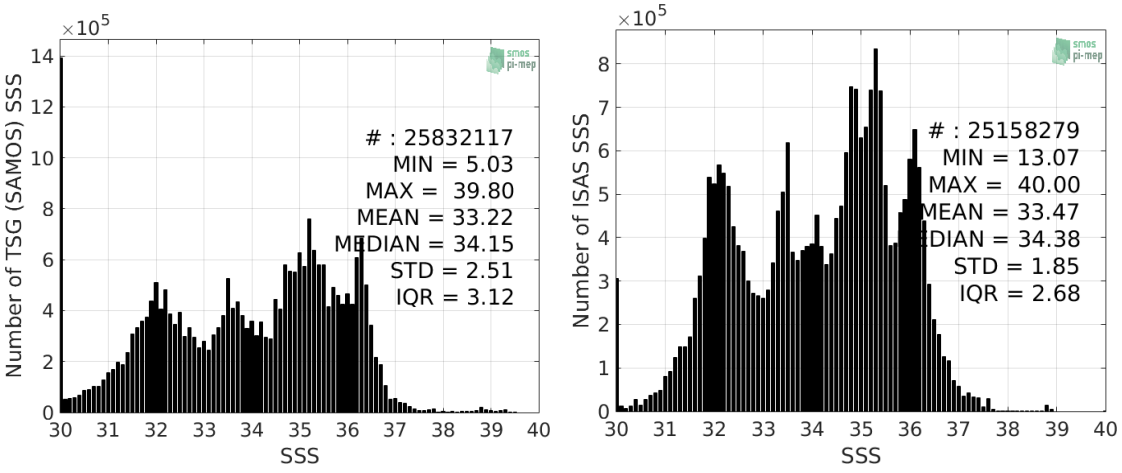

(a) (b)

Figure 38: Histograms of SSS from TSG (SAMOS) (a) and ISAS (b) per bins of 0.1.

2.4.4 Distribution of *in situ* SSS depth measurements

In Figure 39, we show the depth distribution of the *in situ* salinity dataset (a) and the spatial distribution of the depth temporal mean in 1°x1° boxes and considering the full *in situ* dataset period (b).

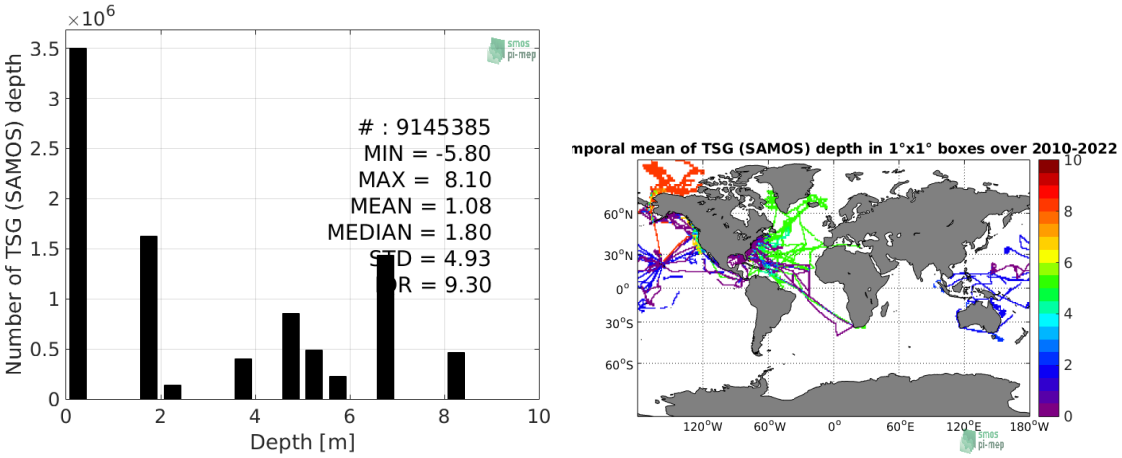

(a) (b)

Figure 39: Depth distribution of the upper level SSS measurements from TSG (SAMOS) (a) and spatial distribution of the *in situ* SSS depth measurements showing the mean value in 1°x1° boxes and considering the full *in situ* dataset period (b).

2.4.5 Spatial distribution of SSS

In Figure 40, the number of TSG (SAMOS) SSS measurements in 1°x1° boxes is shown.

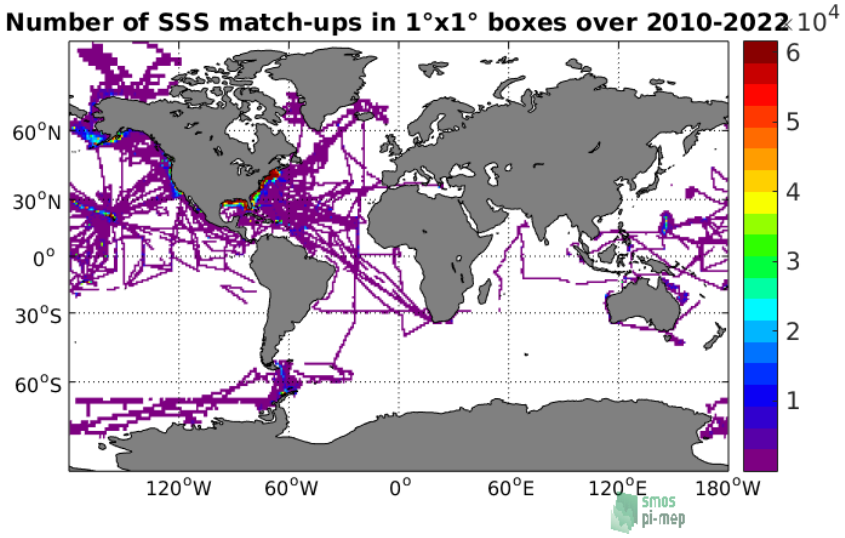

Figure 40: Number of SSS from TSG (SAMOS) in 1°x1° boxes.

2.4.6 Spatial Maps of the Temporal mean and Std of *in situ* and ISAS SSS and of the difference (ΔSSS)

In Figure 41, maps of temporal mean (left) and standard deviation (right) of ISAS (top), TSG (SAMOS) *in situ* dataset (middle) and the difference ΔSSS(ISAS -TSG (SAMOS)) (bottom) are shown. The temporal mean and std are calculated using all match-up pairs falling in spatial boxes of size 1°x1° over the full TSG (SAMOS) dataset period.

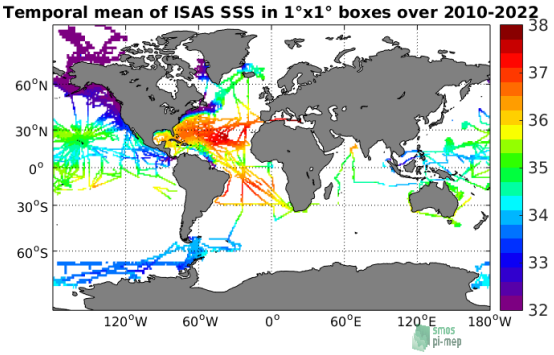

(a) MEAN(ISAS SSS)

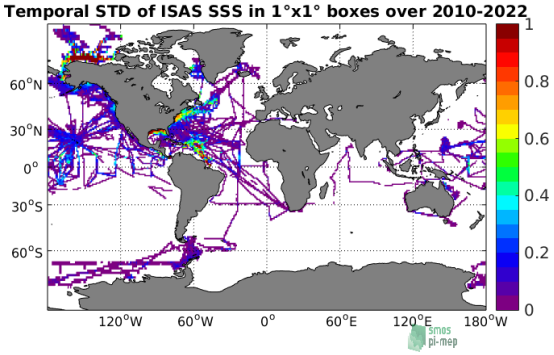

(b) Std(ISAS SSS)

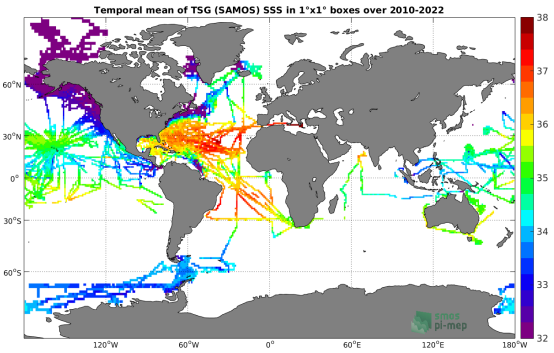

(c) MEAN(TSG (SAMOS) SSS)

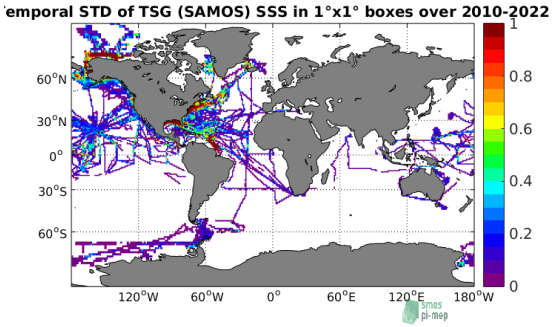

(d) Std(TSG (SAMOS) SSS)

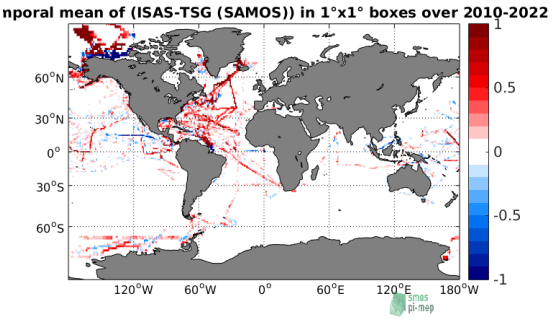

(e) MEAN(ΔSSS) (ISAS - TSG (SAMOS))

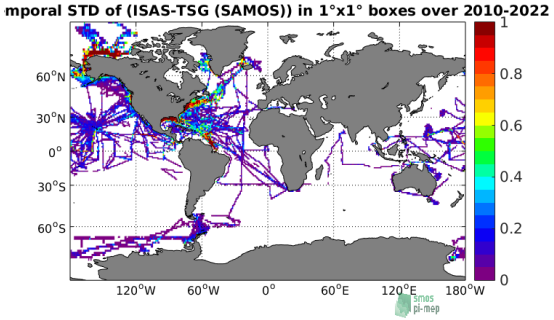

(f) Std(ΔSSS) (ISAS - TSG (SAMOS))

Figure 41: Temporal mean (left) and Std (right) of SSS from ISAS (top), TSG (SAMOS) (middle), and of ΔSSS (ISAS - TSG (SAMOS)). Only match-up pairs are used to generate these maps.

2.4.7 Time series of the monthly median and Std of *in situ* and ISAS SSS and of the difference (ΔSSS)

In the top panel of Figure 42, we show the time series of the monthly median SSS estimated for both ISAS SSS product (in black) and the TSG (SAMOS) *in situ* dataset (in blue) at the collected Pi-MEP match-up pairs.

In the middle panel of Figure 42, we show the time series of the monthly median of ΔSSS (ISAS - TSG (SAMOS)) for the collected Pi-MEP match-up pairs.

In the bottom panel of Figure 42, we show the time series of the monthly standard deviation of the ΔSSS (ISAS - TSG (SAMOS)) for the collected Pi-MEP match-up pairs.

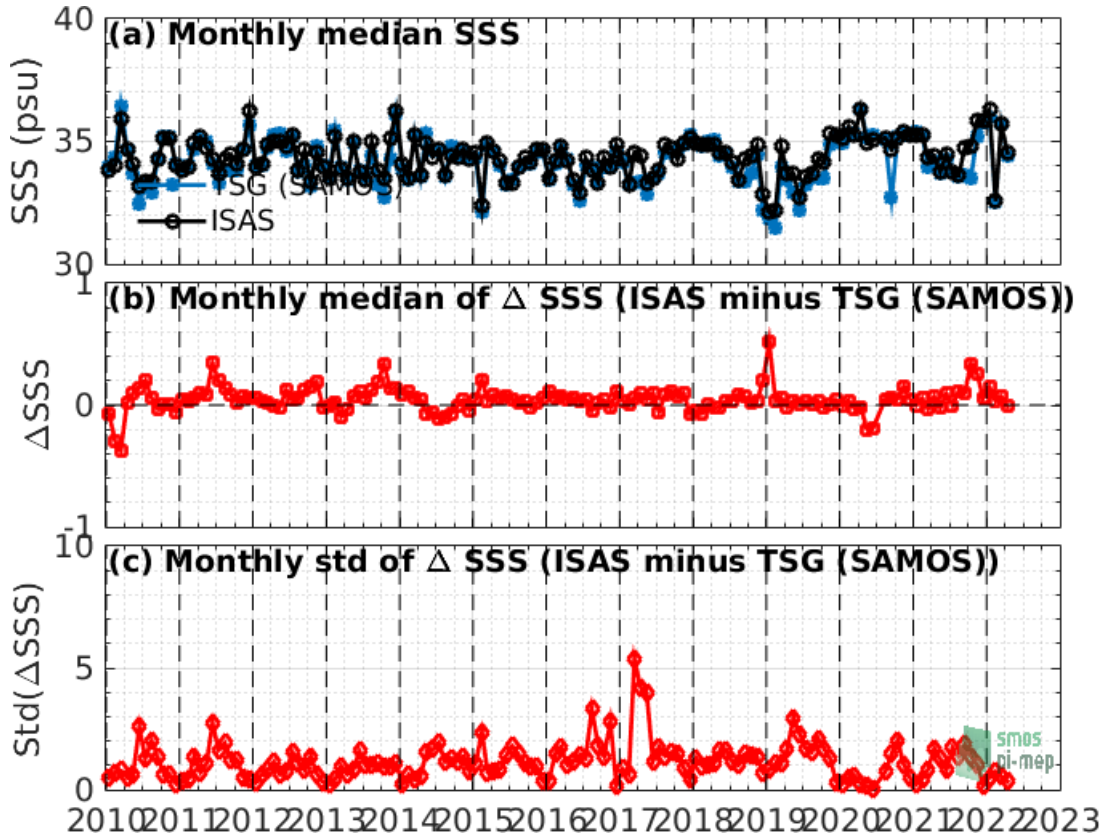

Figure 42: Time series of the monthly median SSS (top), median of ΔSSS (ISAS - TSG (SAMOS)) and Std of ΔSSS (ISAS - TSG (SAMOS)) considering all match-ups collected by the Pi-MEP.

2.4.8 Zonal mean and Std of *in situ* and ISAS SSS and of the difference ΔSSS

In Figure 43 left panel, we show the zonal mean SSS considering all Pi-MEP match-up pairs for both ISAS SSS product (in black) and the TSG (SAMOS) *in situ* dataset (in blue). The full *in situ* dataset period is used to derive the mean.

In the right panel of Figure 43, we show the zonal mean of ΔSSS (ISAS - TSG (SAMOS)) for all the collected Pi-MEP match-up pairs estimated over the full *in situ* dataset period.

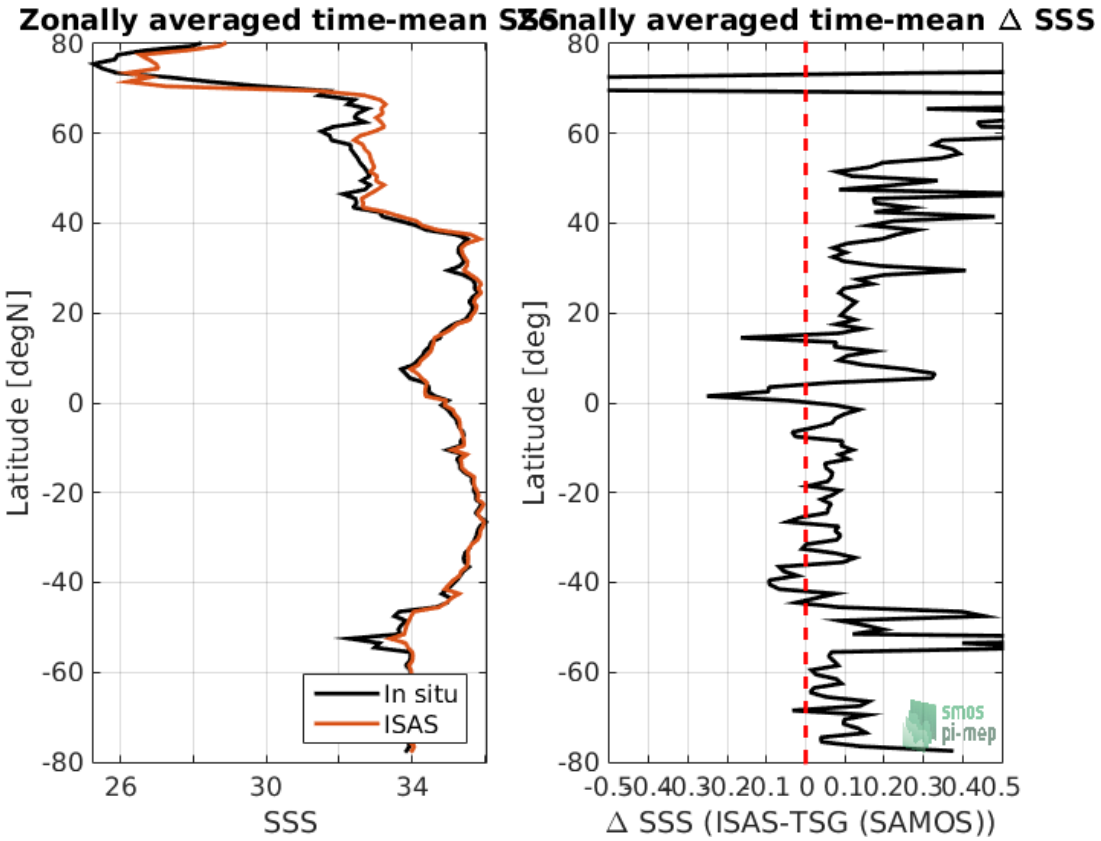

Figure 43: Left panel: Zonal mean SSS from ISAS product (black) and from TSG (SAMOS) (blue). Right panel: Zonal mean of ΔSSS (ISAS - TSG (SAMOS)) for all the collected Pi-MEP match-up pairs estimated over the full *in situ* dataset period.

2.4.9 Scatterplots of ISAS vs *in situ* SSS by latitudinal bands

In Figure 44, contour maps of the concentration of ISAS SSS (y-axis) versus TSG (SAMOS) SSS (x-axis) at match-up pairs for different latitude bands: (a) 80°S-80°N, (b) 20°S-20°N, (c) 40°S-20°S and 20°N-40°N and (d) 60°S-40°S and 40°N-60°N. For each plot, the red line shows x=y. The black thin and dashed lines indicate a linear fit through the data cloud and the ±95% confidence levels, respectively. The number match-up pairs n, the slope and R^2 coefficient of the linear fit, the root mean square (RMS) and the mean bias between ISAS and *in situ* data are indicated for each latitude band in each plots.

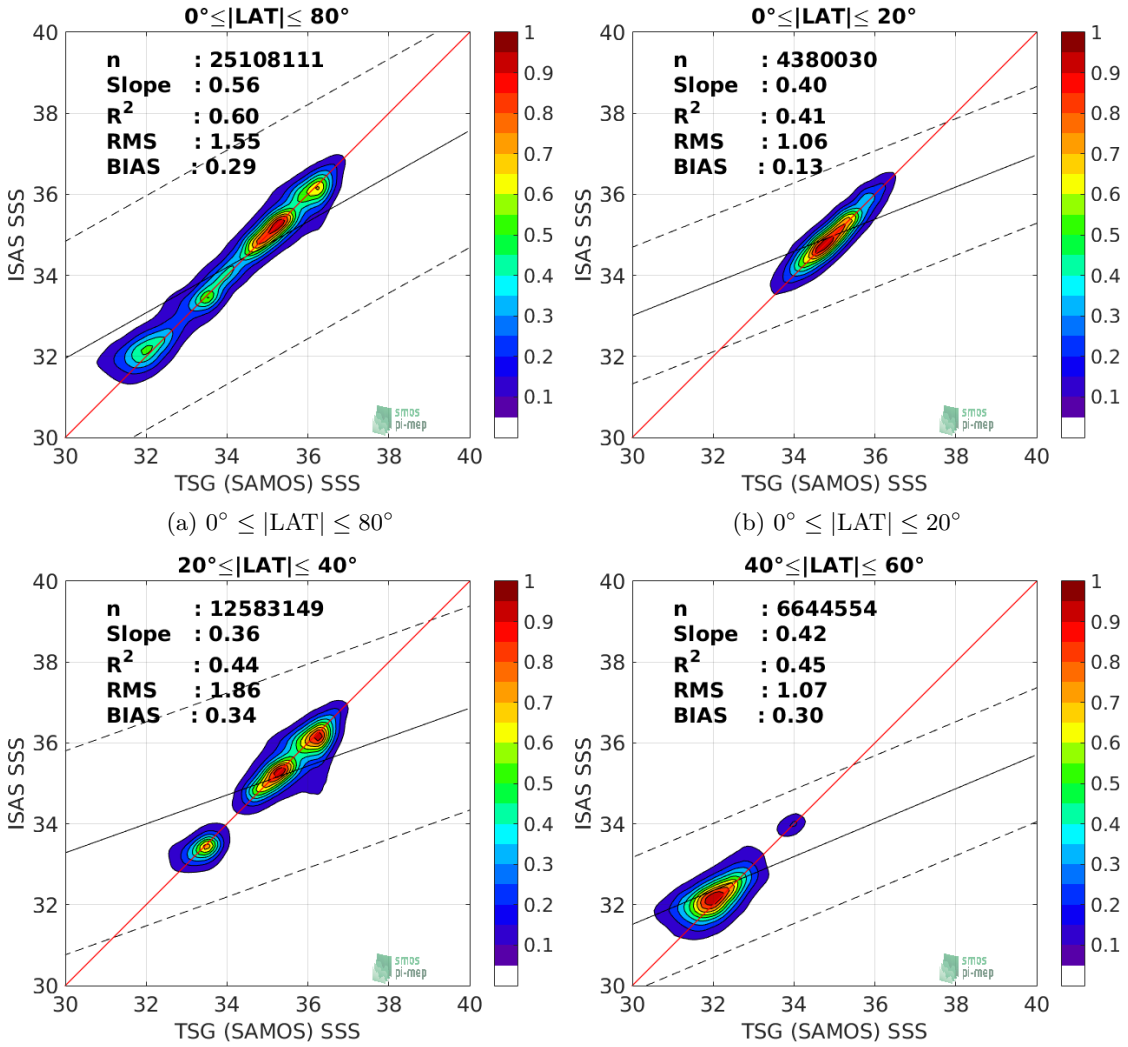

(a) $0° \leq |\text{LAT}| \leq 80°$

(b) $0° \leq |\text{LAT}| \leq 20°$

(c) $20° \leq |\text{LAT}| \leq 40°$

(d) $40° \leq |\text{LAT}| \leq 60°$

Figure 44: Contour maps of the concentration of ISAS SSS (y-axis) versus TSG (SAMOS) SSS (x-axis) at match-up pairs for different latitude bands. For each plot, the red line shows x=y. The black thin and dashed lines indicate a linear fit through the data cloud and the ±95% confidence levels, respectively. The number match-up pairs n, the slope and R^2 coefficient of the linear fit, the root mean square (RMS) and the mean bias between ISAS and *in situ* data are indicated for each latitude band in each plots.

2.4.10 Time series of the monthly median and Std of the difference ΔSSS sorted by latitudinal bands

In Figure 45, time series of the monthly median (red curves) of ΔSSS (ISAS - TSG (SAMOS)) and ±1 Std (black vertical thick bars) as function of time for all the collected Pi-MEP match-up pairs estimated for the full *in situ* dataset period are shown for different latitude bands: (a) 80°S-80°N, (b) 20°S-20°N, (c) 40°S-20°S and 20°N-40°N and (d) 60°S-40°S and 40°N-60°N.

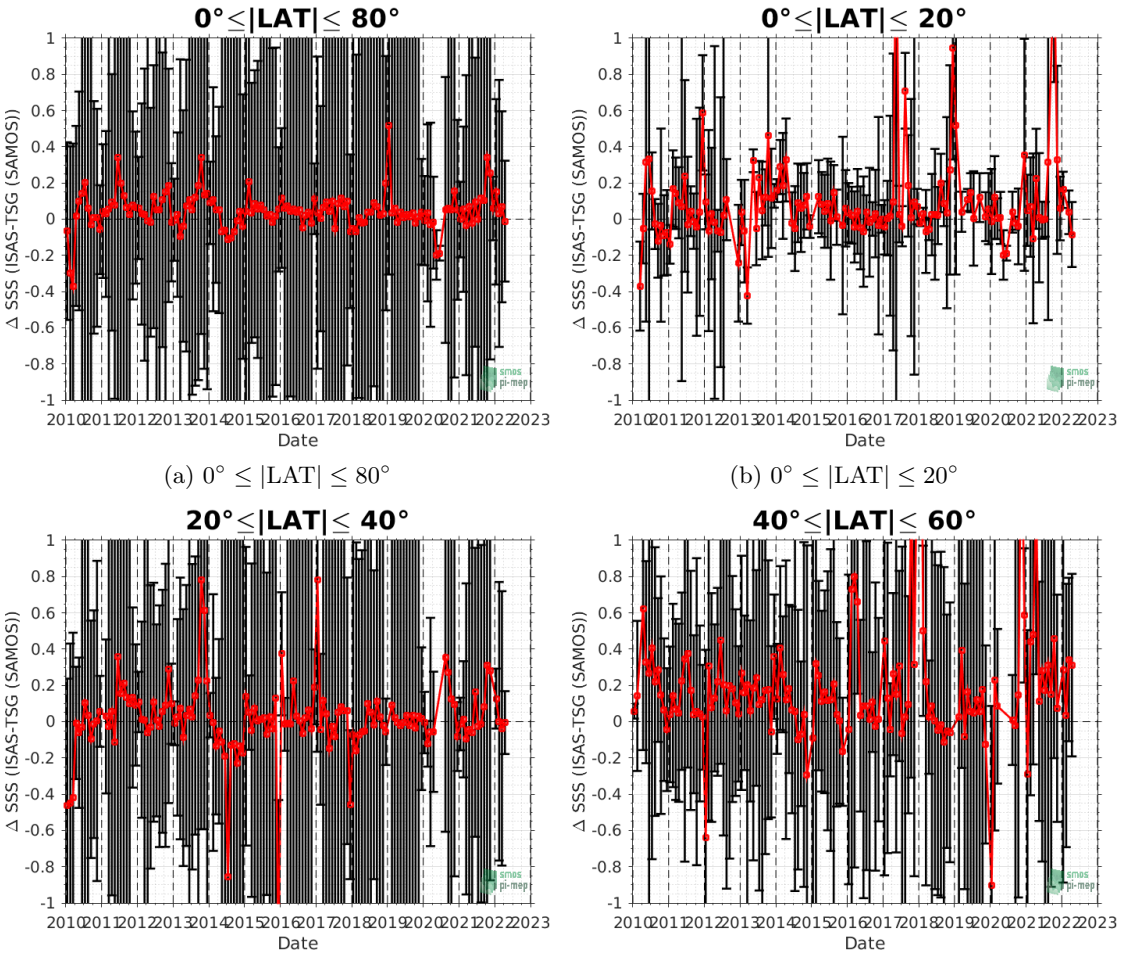

(a) $0° \leq |\text{LAT}| \leq 80°$

(b) $0° \leq |\text{LAT}| \leq 20°$

(c) $20° \leq |\text{LAT}| \leq 40°$

(d) $40° \leq |\text{LAT}| \leq 60°$

Figure 45: Monthly median (red curves) of ΔSSS (ISAS - TSG (SAMOS)) and ±1 Std (black vertical thick bars) as function of time for all the collected Pi-MEP match-up pairs for the full *in situ* dataset period are shown for different latitude bands: (a) 80°S-80°N, (b) 20°S-20°N, (c) 40°S-20°S and 20°N-40°N and (d) 60°S-40°S and 40°N-60°N.

2.4.11 ΔSSS sorted as geophysical conditions

In Figure 46, we classify the match-up differences ΔSSS (ISAS - *in situ*) as function of the geophysical conditions at match-up points. The mean and std of ΔSSS (ISAS - TSG (SAMOS)) is thus evaluated as function of the

- *in situ* SSS values per bins of width 0.2,
- *in situ* SST values per bins of width 1°C,
- ASCAT daily wind values per bins of width 1 m/s,
- CMORPH 3-hourly rain rates per bins of width 1 mm/h, and,
- distance to coasts per bins of width 50 km,

- *in situ* measurement depth (if relevant).

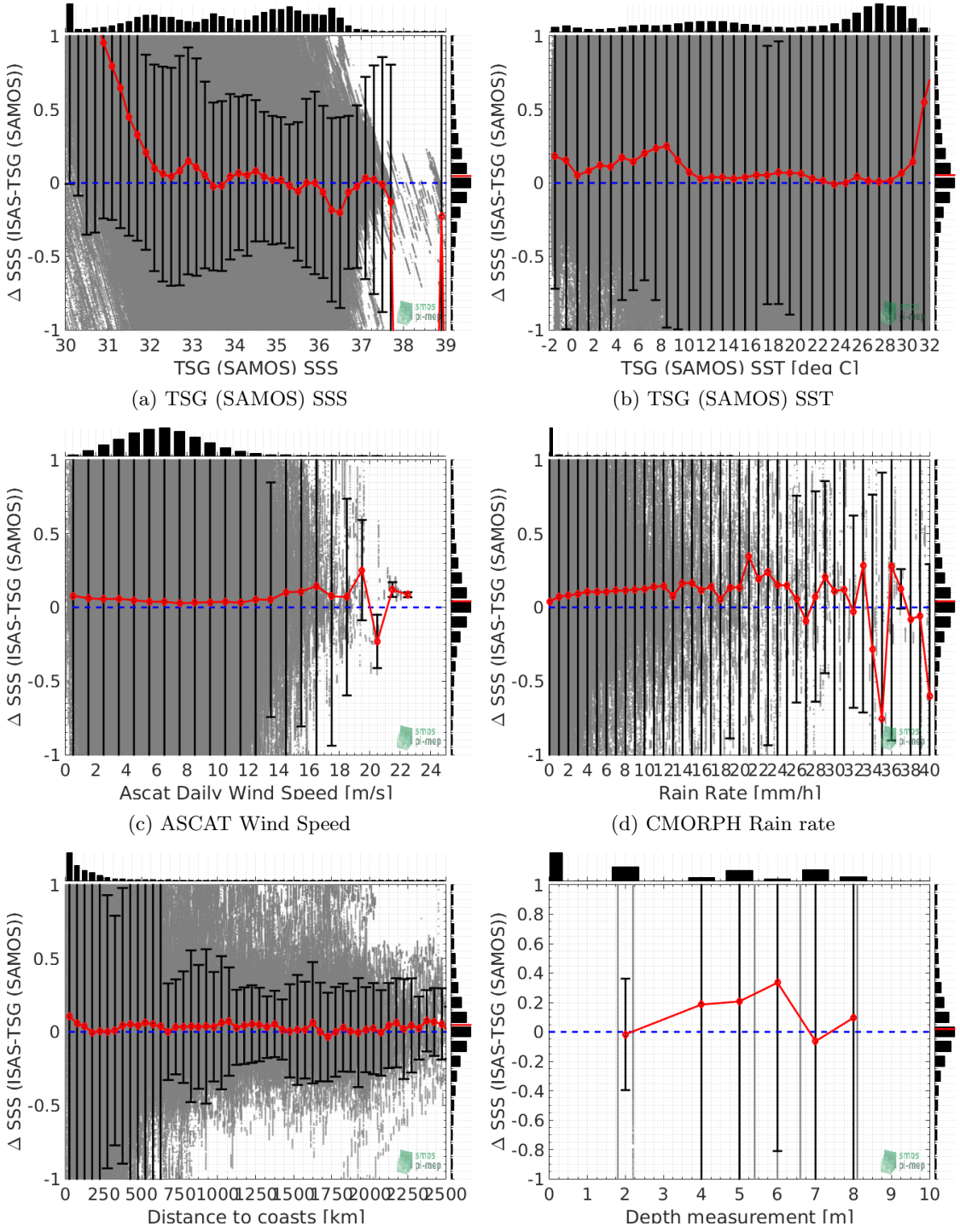

(a) TSG (SAMOS) SSS

(b) TSG (SAMOS) SST

(c) ASCAT Wind Speed

(d) CMORPH Rain rate

(e) Distance to coast

(f) Depth

Figure 46: Δ SSS (ISAS - TSG (SAMOS)) sorted as geophysical conditions: TSG (SAMOS) SSS a), TSG (SAMOS) SST b), ASCAT Wind speed c), CMORPH rain rate d), distance to coast (e) and depth measurements (f).

2.4.12 ΔSSS maps and statistics for different geophysical conditions

In Figures 47 and 48, we focus on sub-datasets of the match-up differences ΔSSS (ISAS - *in situ*) for the following specific geophysical conditions:

- **C1**:if the local value at *in situ* location of estimated rain rate is zero, mean daily wind is in the range [3, 12] m/s, the SST is > 5°C and distance to coast is > 800 km.
- **C2**:if the local value at *in situ* location of estimated rain rate is zero, mean daily wind is in the range [3, 12] m/s.
- **C3**:if the local value at *in situ* location of estimated rain rate is high (ie. > 1 mm/h) and mean daily wind is low (ie. < 4 m/s).
- **C5**:if the *in situ* data is located where the climatological SSS standard deviation is low (ie. above < 0.2).
- **C6**:if the *in situ* data is located where the climatological SSS standard deviation is high (ie. above > 0.2).

For each of these conditions, the temporal mean (gridded over spatial boxes of size 1°x1°) and the histogram of the difference ΔSSS (ISAS - *in situ*) are presented.

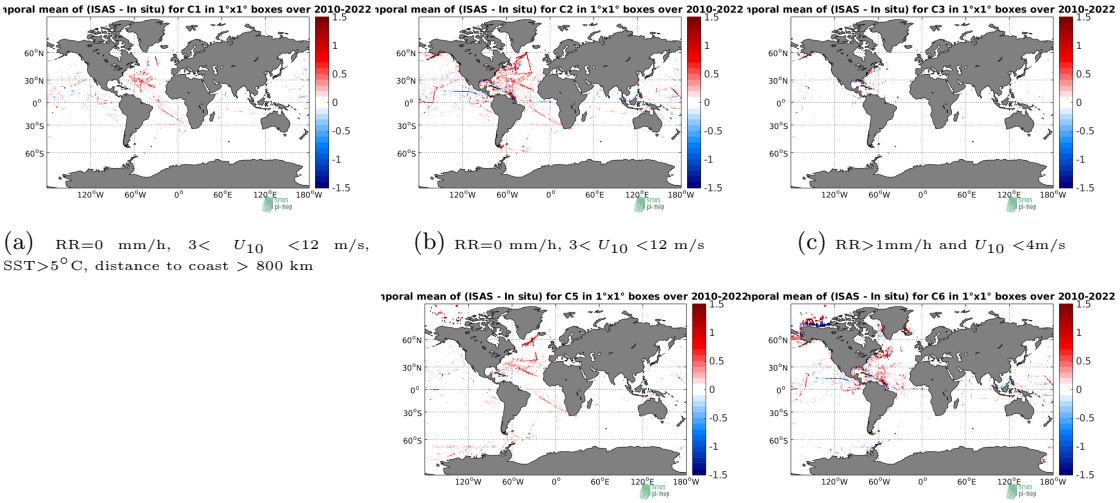

(a) RR=0 mm/h, 3< U_{10} <12 m/s, SST>5°C, distance to coast > 800 km

(b) RR=0 mm/h, 3< U_{10} <12 m/s

(c) RR>1mm/h and U_{10} <4m/s

(d) WOA2013 SSS Std<0.2

(e) WOA2013 SSS Std>0.2

Figure 47: Temporal mean gridded over spatial boxes of size 1°x1° of ΔSSS (ISAS - TSG (SAMOS)) for 5 different subdatasets corresponding to:RR=0 mm/h, 3< U_{10} <12 m/s, SST>5°C, distance to coast > 800 km (a), RR=0 mm/h, 3< U_{10} <12 m/s (b), RR>1mm/h and U_{10} <4m/s (c),WOA2013 SSS Std<0.2 (d),WOA2013 SSS Std>0.2 (e).

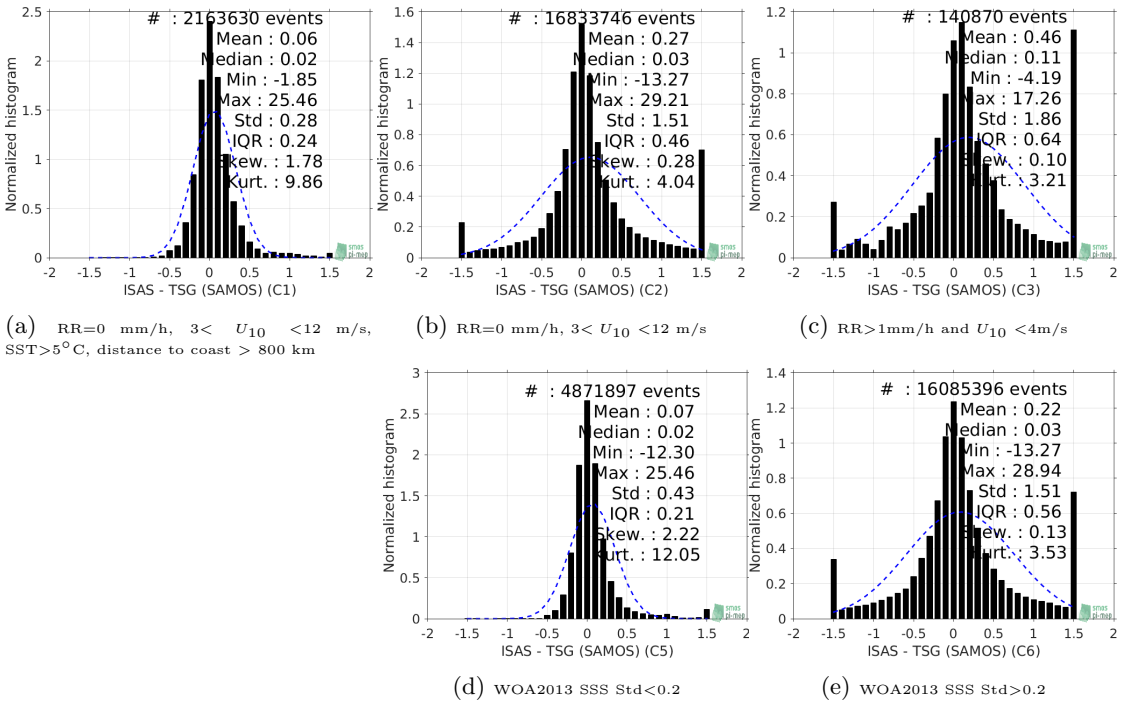

(a) RR=0 mm/h, 3< U_{10} <12 m/s, SST>5°C, distance to coast > 800 km (b) RR=0 mm/h, 3< U_{10} <12 m/s (c) RR>1mm/h and U_{10} <4m/s (d) WOA2013 SSS Std<0.2 (e) WOA2013 SSS Std>0.2

Figure 48: Normalized histogram of ΔSSS (ISAS - TSG (SAMOS)) for 5 different subdatasets corresponding to:RR=0 mm/h, 3< U_{10} <12 m/s, SST>5°C, distance to coast > 800 km (a), RR=0 mm/h, 3< U_{10} <12 m/s (b), RR>1mm/h and U_{10} <4m/s (c),WOA2013 SSS Std<0.2 (d),WOA2013 SSS Std>0.2 (e).

2.4.13 Summary

Table 1 shows the mean, median, standard deviation (Std), root mean square (RMS), interquartile range (IQR), correlation coefficient (r^2) and robust standard deviation (Std*) of the match-up differences ΔSSS (ISAS - TSG (SAMOS)) for the following conditions:

- all: All the match-up pairs satellite/in situ SSS values are used to derive the statistics
- C1: only pairs where RR=0 mm/h, 3< U_{10} <12 m/s, SST>5°C, distance to coast > 800 km
- C2: only pairs where RR=0 mm/h, 3< U_{10} <12 m/s
- C3: only pairs where RR>1mm/h and U_{10} <4m/s
- C5: only pairs where WOA2013 SSS Std<0.2
- C6: only pairs where WOA2013 SSS Std>0.2
- C7a: only pairs with a distance to coast < 150 km.
- C7b: only pairs with a distance to coast in the range [150, 800] km.
- C7c: only pairs with a distance to coast > 800 km.
- C8a: only pairs where SST is < 5°C.

- C8b: only pairs where SST is in the range [5, 15]°C.
- C8c: only pairs where SST is > 15°C.
- C9a: only pairs where SSS is < 33.
- C9b: only pairs where SSS is in the range [33, 37].
- C9c: only pairs where SSS is > 37.

Table 1: Statistics of ΔSSS (ISAS - TSG (SAMOS))

Condition	#	Median	Mean	Std	RMS	IQR	r^2	Std*
all	25158279	0.05	0.29	1.52	1.55	0.49	0.599	0.35
C1	2163630	0.02	0.06	0.28	0.28	0.24	0.912	0.17
C2	16833746	0.03	0.27	1.51	1.53	0.46	0.573	0.33
C3	140870	0.11	0.46	1.86	1.91	0.64	0.471	0.46
C5	4871897	0.02	0.07	0.43	0.43	0.21	0.887	0.16
C6	16085396	0.03	0.22	1.51	1.52	0.56	0.584	0.41
C7a	14192913	0.08	0.44	1.78	1.84	0.66	0.493	0.46
C7b	7593243	0.02	0.11	1.26	1.27	0.41	0.635	0.31
C7c	3346082	0.03	0.09	0.35	0.36	0.25	0.914	0.18
C8a	1970988	0.13	0.21	1.14	1.16	0.50	0.726	0.34
C8b	5971517	0.09	0.29	1.20	1.23	0.64	0.405	0.46
C8c	15499688	0.03	0.32	1.67	1.70	0.44	0.490	0.31
C9a	8251827	0.36	1.01	2.36	2.56	1.16	0.054	0.71
C9b	16629233	-0.01	-0.04	0.56	0.56	0.34	0.759	0.25
C9c	277219	-0.08	-1.06	1.58	1.90	2.85	0.067	0.36

Table 1 numerical values can be downloaded as a csv file here.

2.5 TSG (LEGOS-Survostral)

2.5.1 Introduction

The TSG-LEGOS-Survostral dataset corresponds to delayed mode regional data from TSG installed on the Astrolabe vessel (IPEV) during the round trips between Hobart (Tasmania) and the French Antarctic base at Dumont d'Urville (Morrow and Kestenare (2014)). It is provided by the Survostral project and available via ftp. Adjusted values when available and only collected TSG data that exhibit quality flags=1 and 2 were used.

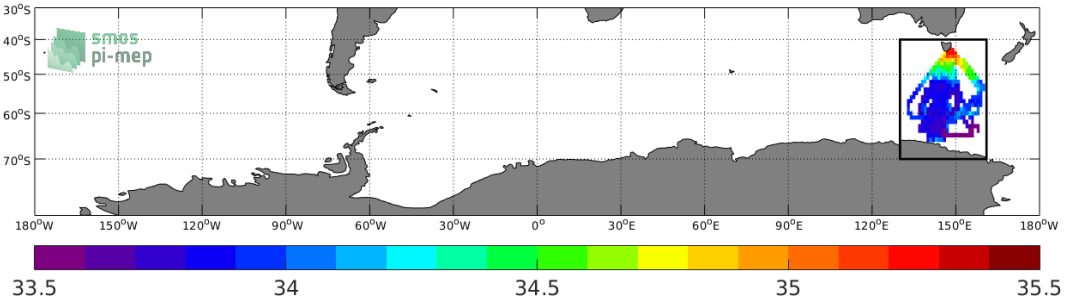

Figure 49: Location of the TSG (LEGOS-Survostral) dataset.

2.5.2 Number of SSS data as a function of time and distance to coast

Figure 50 shows the time (a) and distance to coast (b) distributions of the TSG (LEGOS-Survostral) *in situ* dataset.

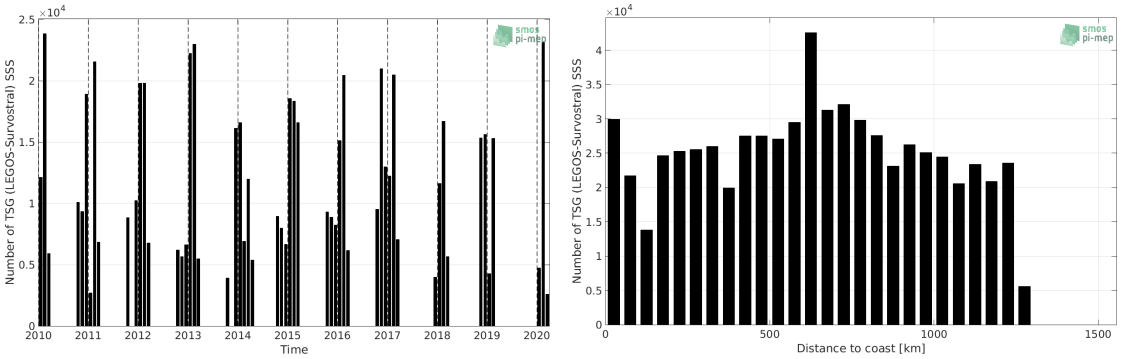

(a) (b)

Figure 50: Number of SSS from TSG (LEGOS-Survostral) as a function of time (a) and distance to coast (b).

2.5.3 Histograms of SSS

Figure 51 shows the SSS distribution of the TSG (LEGOS-Survostral) (a) and colocalized ISAS (b) dataset.

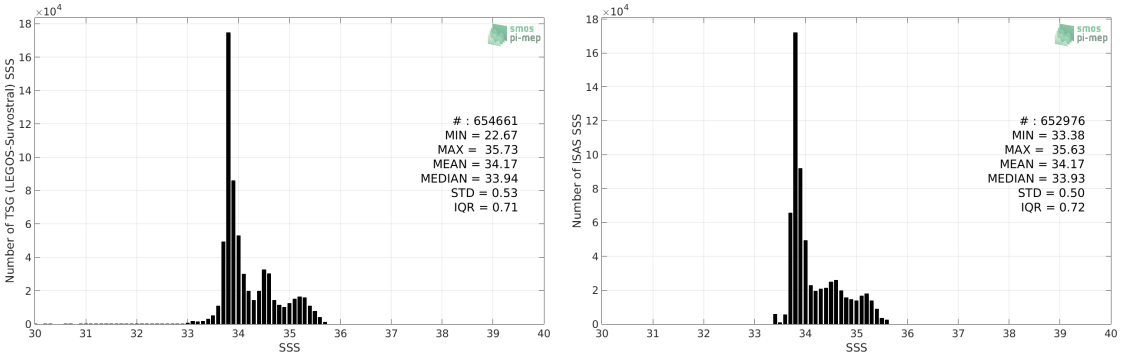

(a) (b)

Figure 51: Histograms of SSS from TSG (LEGOS-Survostral) (a) and ISAS (b) per bins of 0.1.

2.5.4 Distribution of *in situ* SSS depth measurements

In Figure 52, we show the depth distribution of the *in situ* salinity dataset (a) and the spatial distribution of the depth temporal mean in 1°x1° boxes and considering the full *in situ* dataset period (b).

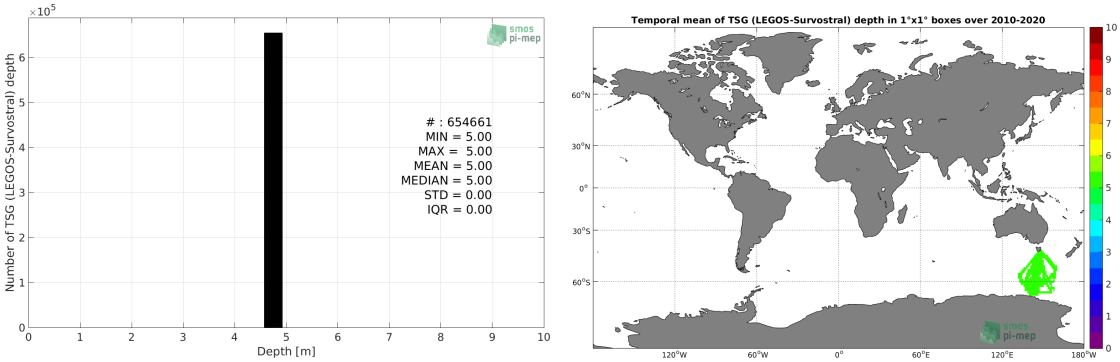

(a) (b)

Figure 52: Depth distribution of the upper level SSS measurements from TSG (LEGOS-Survostral) (a) and spatial distribution of the *in situ* SSS depth measurements showing the mean value in 1°x1° boxes and considering the full *in situ* dataset period (b).

2.5.5 Spatial distribution of SSS

In Figure 53, the number of TSG (LEGOS-Survostral) SSS measurements in 1°x1° boxes is shown.

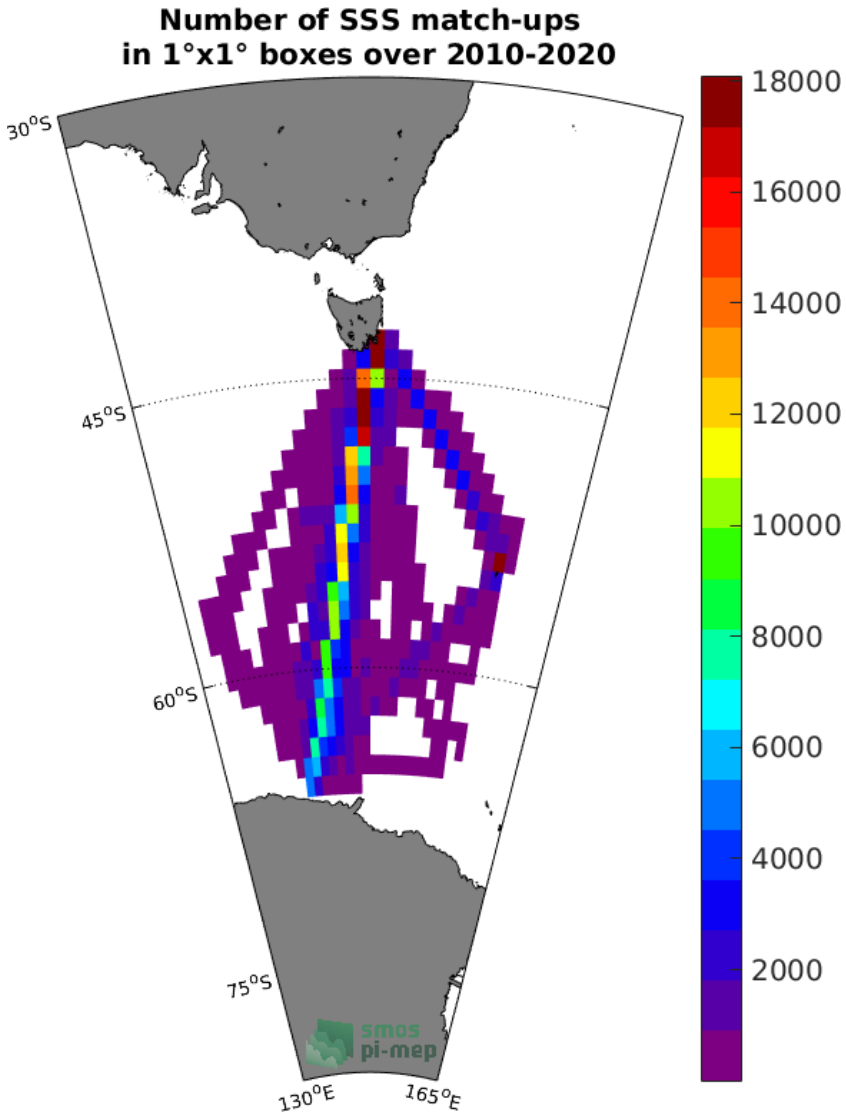

Figure 53: Number of SSS from TSG (LEGOS-Survostral) in 1°x1° boxes.

2.5.6 Spatial Maps of the Temporal mean and Std of *in situ* and ISAS SSS and of the difference (ΔSSS)

In Figure 54, maps of temporal mean (left) and standard deviation (right) of ISAS (top), TSG (LEGOS-Survostral) *in situ* dataset (middle) and the difference ΔSSS(ISAS -TSG (LEGOS-Survostral)) (bottom) are shown. The temporal mean and std are calculated using all match-up pairs falling in spatial boxes of size 1°x1° over the full TSG (LEGOS-Survostral) dataset period.

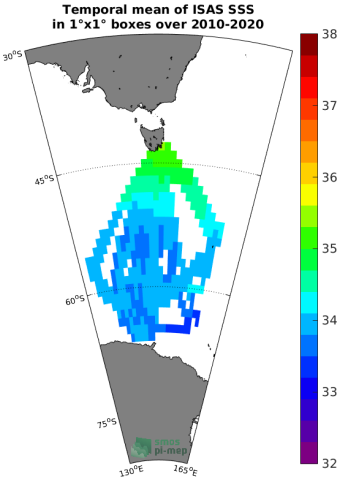

(a) MEAN(ISAS SSS)

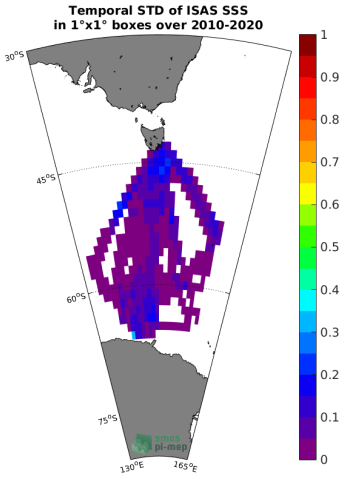

(b) Std(ISAS SSS)

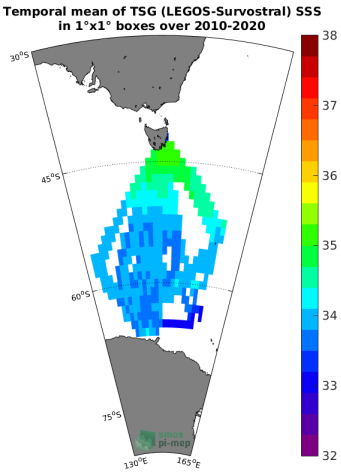

(c) MEAN(TSG (LEGOS-Survostral) SSS)

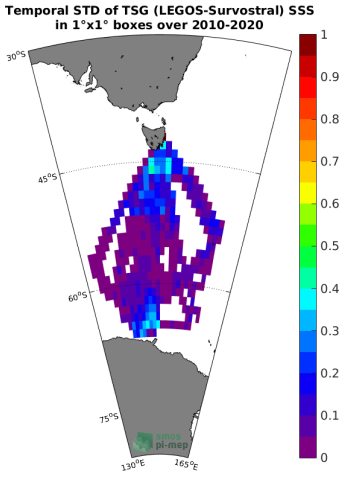

(d) Std(TSG (LEGOS-Survostral) SSS)

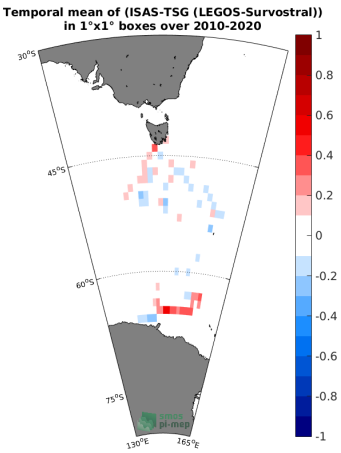

(e) MEAN(ΔSSS) (ISAS - TSG (LEGOS-Survostral))

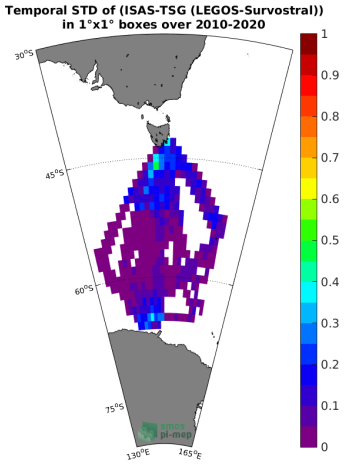

(f) Std(ΔSSS) (ISAS - TSG (LEGOS-Survostral))

Figure 54: Temporal mean (left) and Std (right) of SSS from ISAS (top), TSG (LEGOS-Survostral) (middle), and of ΔSSS (ISAS - TSG (LEGOS-Survostral)). Only match-up pairs are used to generate these maps.

2.5.7 Time series of the monthly median and Std of *in situ* and ISAS SSS and of the difference (ΔSSS)

In the top panel of Figure 55, we show the time series of the monthly median SSS estimated for both ISAS SSS product (in black) and the TSG (LEGOS-Survostral) *in situ* dataset (in blue) at the collected Pi-MEP match-up pairs.

In the middle panel of Figure 55, we show the time series of the monthly median of ΔSSS (ISAS - TSG (LEGOS-Survostral)) for the collected Pi-MEP match-up pairs.

In the bottom panel of Figure 55, we show the time series of the monthly standard deviation of the ΔSSS (ISAS - TSG (LEGOS-Survostral)) for the collected Pi-MEP match-up pairs.

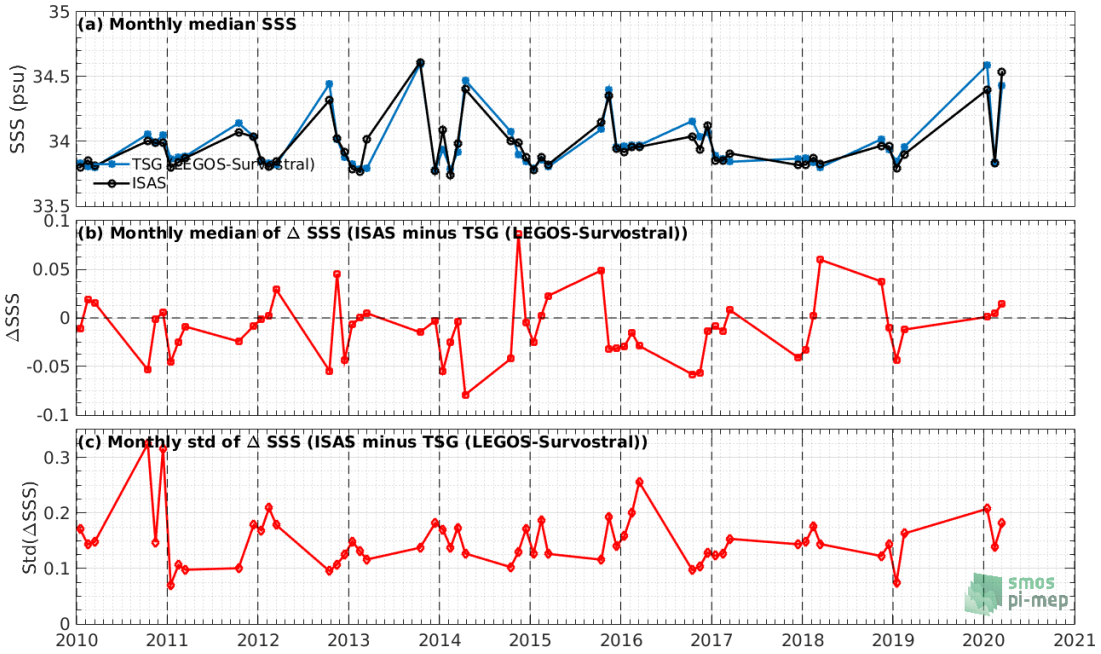

Figure 55: Time series of the monthly median SSS (top), median of ΔSSS (ISAS - TSG (LEGOS-Survostral)) and Std of ΔSSS (ISAS - TSG (LEGOS-Survostral)) considering all match-ups collected by the Pi-MEP.

2.5.8 Zonal mean and Std of *in situ* and ISAS SSS and of the difference ΔSSS

In Figure 56 left panel, we show the zonal mean SSS considering all Pi-MEP match-up pairs for both ISAS SSS product (in black) and the TSG (LEGOS-Survostral) *in situ* dataset (in blue). The full *in situ* dataset period is used to derive the mean.

In the right panel of Figure 56, we show the zonal mean of ΔSSS (ISAS - TSG (LEGOS-Survostral)) for all the collected Pi-MEP match-up pairs estimated over the full *in situ* dataset period.

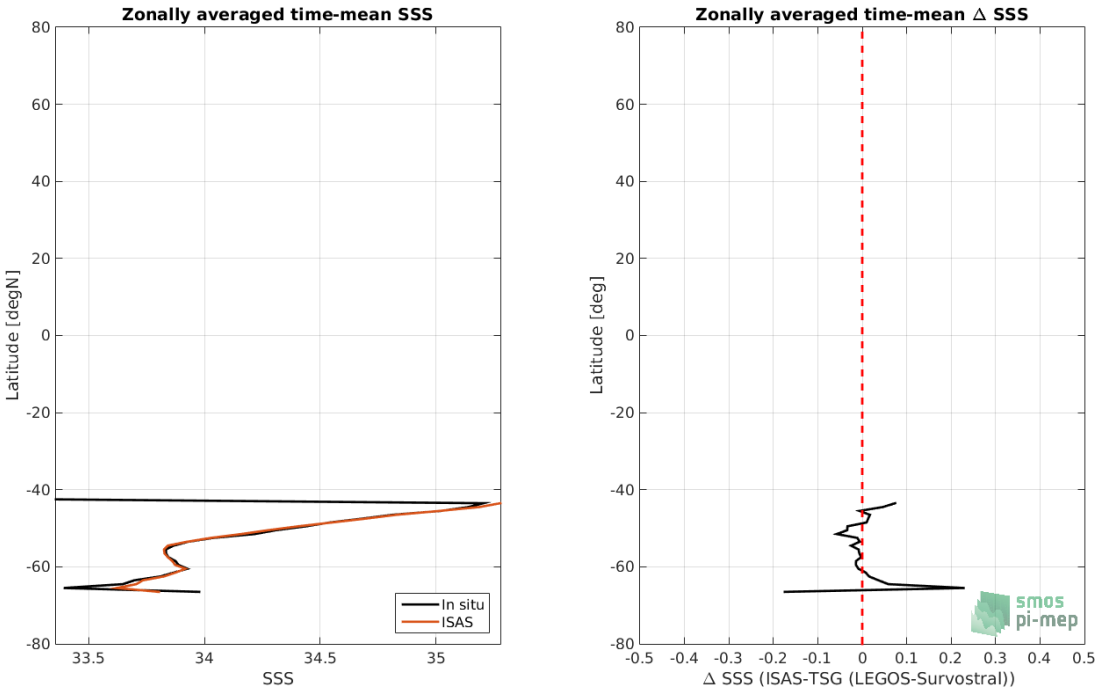

Figure 56: Left panel: Zonal mean SSS from ISAS product (black) and from TSG (LEGOS-Survostral) (blue). Right panel: Zonal mean of ΔSSS (ISAS - TSG (LEGOS-Survostral)) for all the collected Pi-MEP match-up pairs estimated over the full *in situ* dataset period.

2.5.9 Scatterplots of ISAS vs *in situ* SSS by latitudinal bands

In Figure 57, contour maps of the concentration of ISAS SSS (y-axis) versus TSG (LEGOS-Survostral) SSS (x-axis) at match-up pairs for different latitude bands: (a) 80°S-80°N, (b) 20°S-20°N, (c) 40°S-20°S and 20°N-40°N and (d) 60°S-40°S and 40°N-60°N. For each plot, the red line shows x=y. The black thin and dashed lines indicate a linear fit through the data cloud and the ±95% confidence levels, respectively. The number match-up pairs n, the slope and R^2 coefficient of the linear fit, the root mean square (RMS) and the mean bias between ISAS and *in situ* data are indicated for each latitude band in each plots.

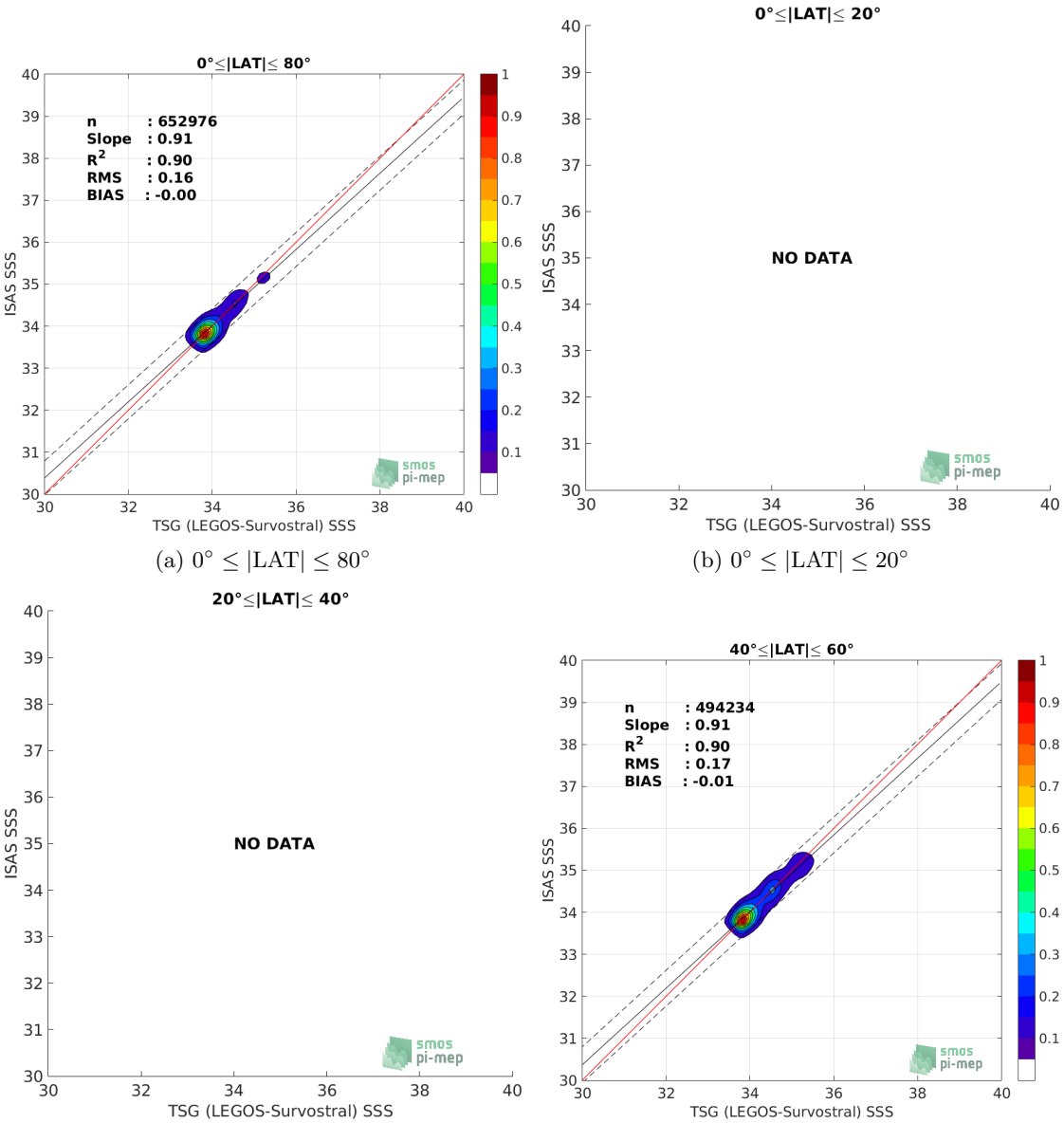

(a) $0° \leq |\text{LAT}| \leq 80°$

(b) $0° \leq |\text{LAT}| \leq 20°$

(c) $20° \leq |\text{LAT}| \leq 40°$

(d) $40° \leq |\text{LAT}| \leq 60°$

Figure 57: Contour maps of the concentration of ISAS SSS (y-axis) versus TSG (LEGOS-Survostral) SSS (x-axis) at match-up pairs for different latitude bands. For each plot, the red line shows x=y. The black thin and dashed lines indicate a linear fit through the data cloud and the ±95% confidence levels, respectively. The number match-up pairs n, the slope and R^2 coefficient of the linear fit, the root mean square (RMS) and the mean bias between ISAS and *in situ* data are indicated for each latitude band in each plots.

2.5.10 Time series of the monthly median and Std of the difference ΔSSS sorted by latitudinal bands

In Figure 58, time series of the monthly median (red curves) of ΔSSS (ISAS - TSG (LEGOS-Survostral)) and ±1 Std (black vertical thick bars) as function of time for all the collected Pi-MEP match-up pairs estimated for the full *in situ* dataset period are shown for different latitude bands: (a) 80°S-80°N, (b) 20°S-20°N, (c) 40°S-20°S and 20°N-40°N and (d) 60°S-40°S and 40°N-60°N.

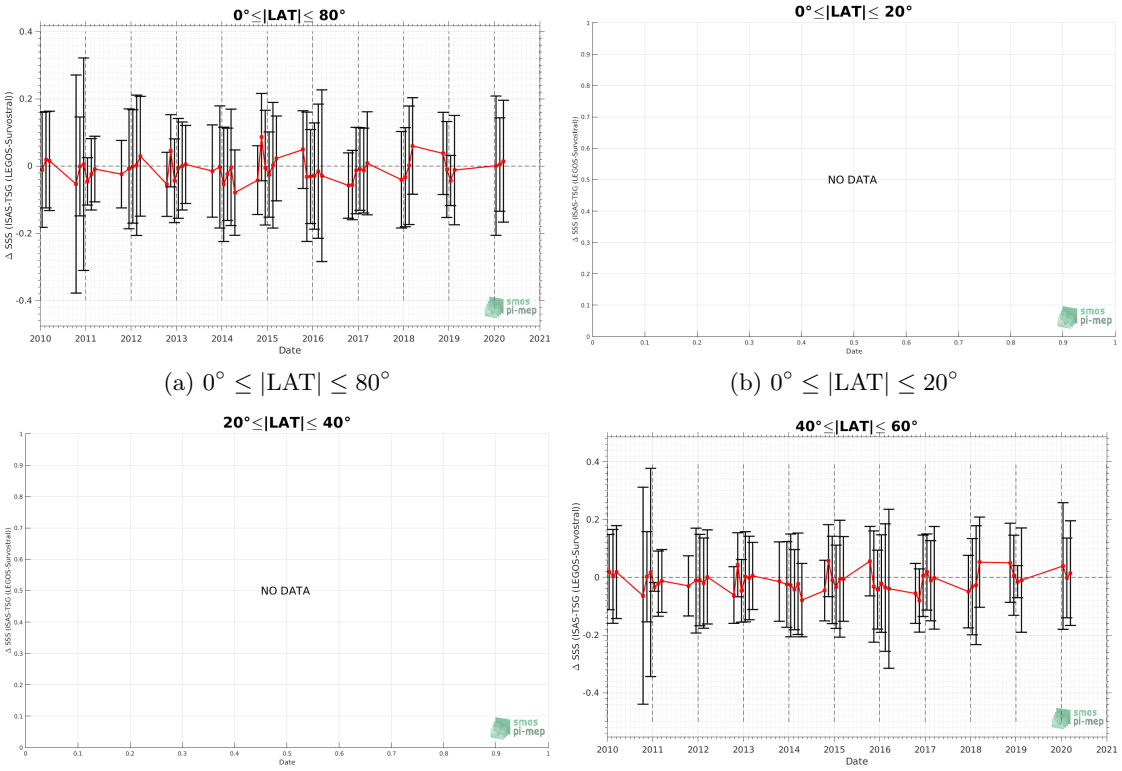

(a) 0° ≤ |LAT| ≤ 80°

(b) 0° ≤ |LAT| ≤ 20°

(c) 20° ≤ |LAT| ≤ 40°

(d) 40° ≤ |LAT| ≤ 60°

Figure 58: Monthly median (red curves) of ΔSSS (ISAS - TSG (LEGOS-Survostral)) and ±1 Std (black vertical thick bars) as function of time for all the collected Pi-MEP match-up pairs for the full *in situ* dataset period are shown for different latitude bands: (a) 80°S-80°N, (b) 20°S-20°N, (c) 40°S-20°S and 20°N-40°N and (d) 60°S-40°S and 40°N-60°N.

2.5.11 ΔSSS sorted as geophysical conditions

In Figure 59, we classify the match-up differences ΔSSS (ISAS - *in situ*) as function of the geophysical conditions at match-up points. The mean and std of ΔSSS (ISAS - TSG (LEGOS-Survostral)) is thus evaluated as function of the

- *in situ* SSS values per bins of width 0.2,
- *in situ* SST values per bins of width 1°C,
- ASCAT daily wind values per bins of width 1 m/s,

- CMORPH 3-hourly rain rates per bins of width 1 mm/h, and,
- distance to coasts per bins of width 50 km,
- *in situ* measurement depth (if relevant).

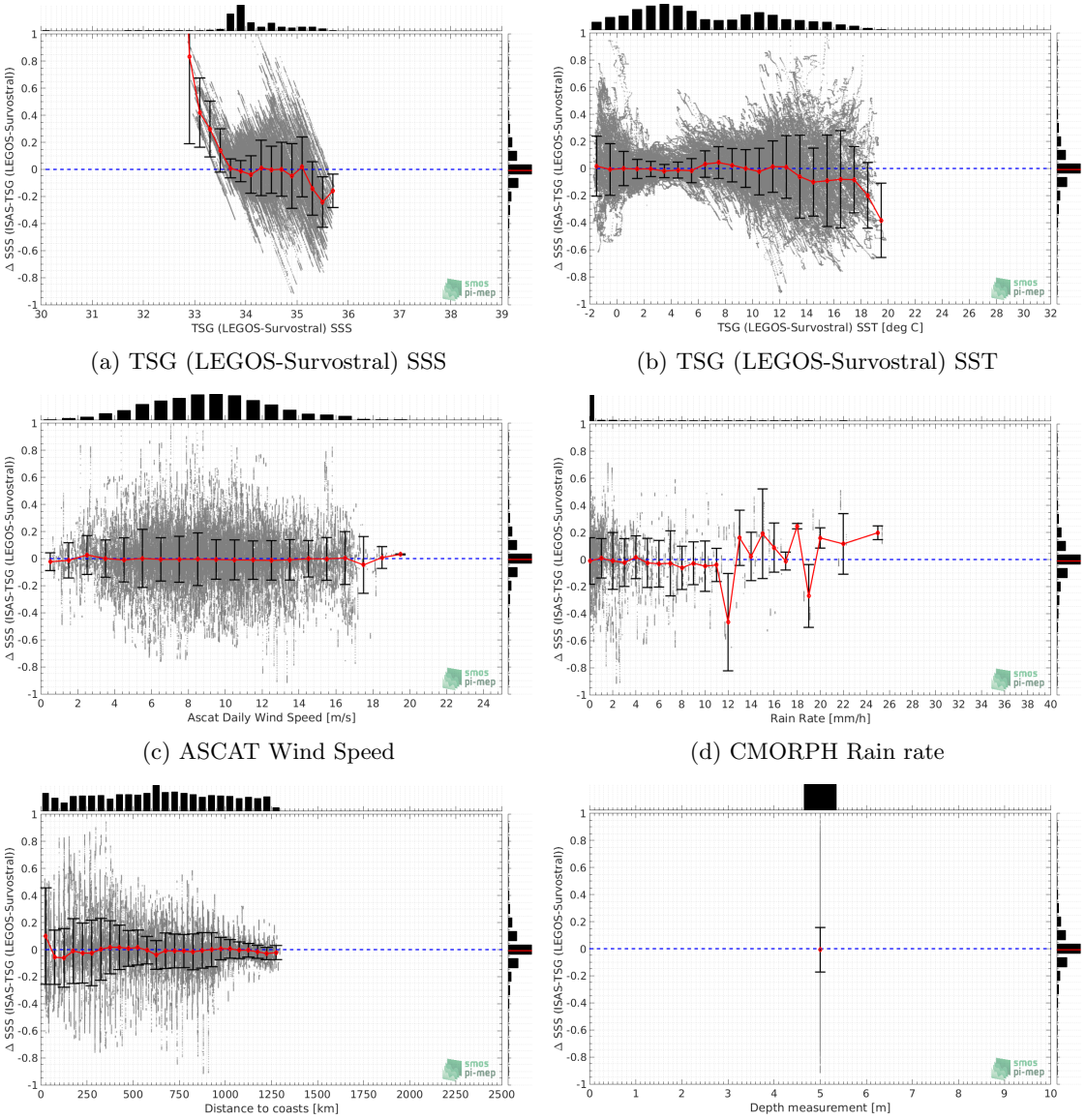

(a) TSG (LEGOS-Survostral) SSS

(b) TSG (LEGOS-Survostral) SST

(c) ASCAT Wind Speed

(d) CMORPH Rain rate

(e) Distance to coast

(f) Depth

Figure 59: Δ SSS (ISAS - TSG (LEGOS-Survostral)) sorted as geophysical conditions: TSG (LEGOS-Survostral) SSS a), TSG (LEGOS-Survostral) SST b), ASCAT Wind speed c), CMORPH rain rate d), distance to coast (e) and depth measurements (f).

2.5.12 ΔSSS maps and statistics for different geophysical conditions

In Figures 60 and 61, we focus on sub-datasets of the match-up differences ΔSSS (ISAS - *in situ*) for the following specific geophysical conditions:

- **C1**:if the local value at *in situ* location of estimated rain rate is zero, mean daily wind is in the range [3, 12] m/s, the SST is $> 5°$C and distance to coast is > 800 km.
- **C2**:if the local value at *in situ* location of estimated rain rate is zero, mean daily wind is in the range [3, 12] m/s.
- **C3**:if the local value at *in situ* location of estimated rain rate is high (ie. > 1 mm/h) and mean daily wind is low (ie. < 4 m/s).
- **C5**:if the *in situ* data is located where the climatological SSS standard deviation is low (ie. above < 0.2).
- **C6**:if the *in situ* data is located where the climatological SSS standard deviation is high (ie. above > 0.2).

For each of these conditions, the temporal mean (gridded over spatial boxes of size 1°x1°) and the histogram of the difference ΔSSS (ISAS - *in situ*) are presented.

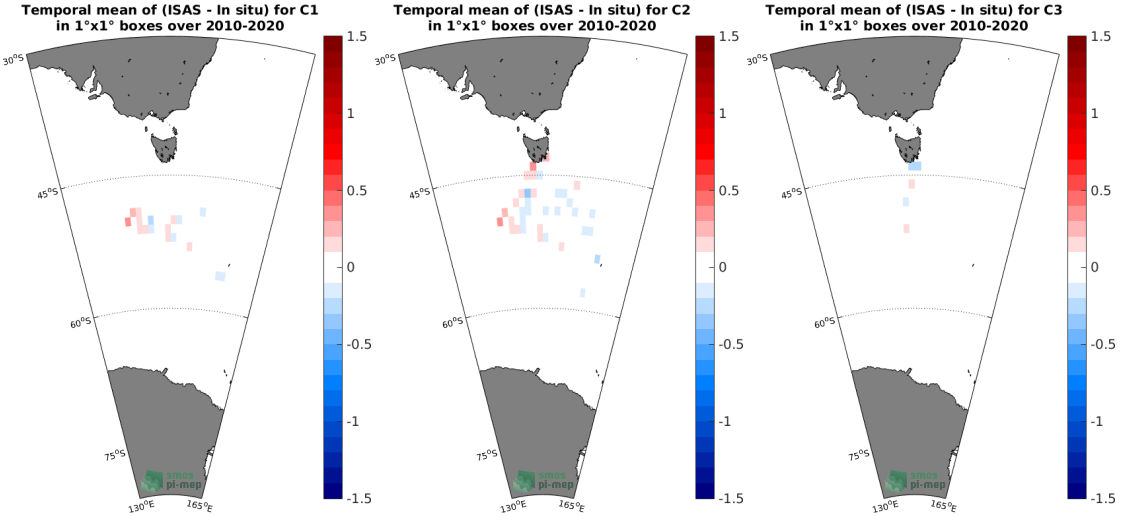

(a) RR=0 mm/h, 3< U_{10} <12 m/s, SST>5°C, distance to coast > 800 km (b) RR=0 mm/h, 3< U_{10} <12 m/s (c) RR>1mm/h and U_{10} <4m/s

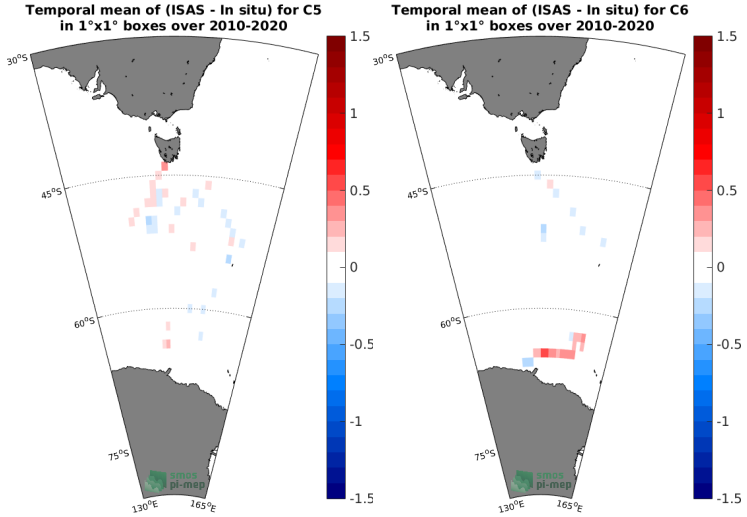

(d) WOA2013 SSS Std<0.2 (e) WOA2013 SSS Std>0.2

Figure 60: Temporal mean gridded over spatial boxes of size 1°x1° of ΔSSS (ISAS - TSG (LEGOS-Survostral)) for 5 different subdatasets corresponding to:RR=0 mm/h, 3< U_{10} <12 m/s, SST>5°C, distance to coast > 800 km (a), RR=0 mm/h, 3< U_{10} <12 m/s (b), RR>1mm/h and U_{10} <4m/s (c),WOA2013 SSS Std<0.2 (d),WOA2013 SSS Std>0.2 (e).

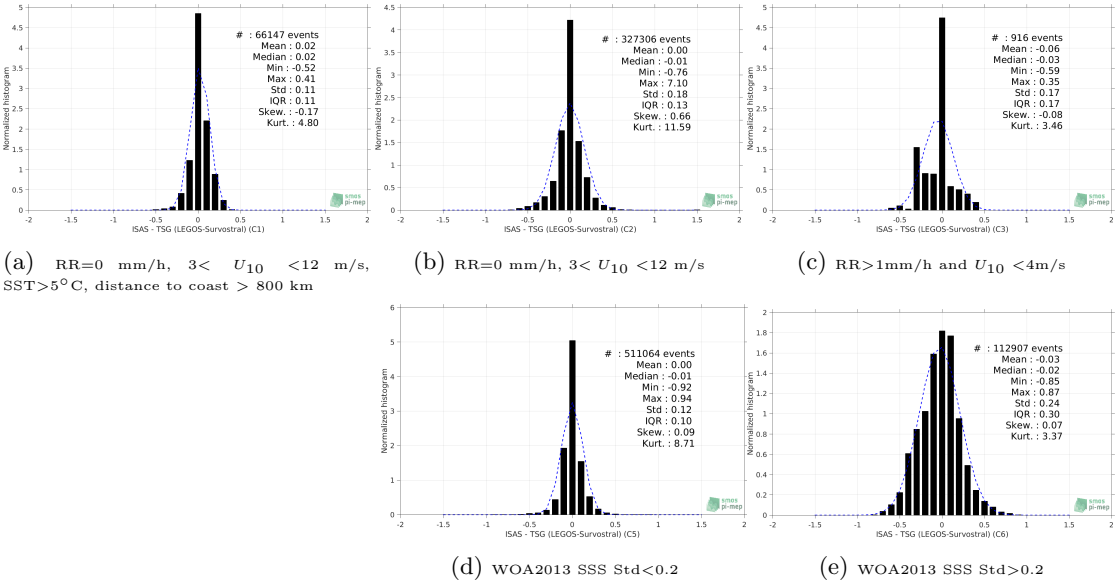

(a) RR=0 mm/h, 3< U_{10} <12 m/s, SST>5°C, distance to coast > 800 km (b) RR=0 mm/h, 3< U_{10} <12 m/s (c) RR>1mm/h and U_{10} <4m/s

(d) WOA2013 SSS Std<0.2 (e) WOA2013 SSS Std>0.2

Figure 61: Normalized histogram of ΔSSS (ISAS - TSG (LEGOS-Survostral)) for 5 different subdatasets corresponding to:RR=0 mm/h, 3< U_{10} <12 m/s, SST>5°C, distance to coast > 800 km (a), RR=0 mm/h, 3< U_{10} <12 m/s (b), RR>1mm/h and U_{10} <4m/s (c),WOA2013 SSS Std<0.2 (d),WOA2013 SSS Std>0.2 (e).

2.5.13 Summary

Table 1 shows the mean, median, standard deviation (Std), root mean square (RMS), interquartile range (IQR), correlation coefficient (r^2) and robust standard deviation (Std*) of the match-up differences ΔSSS (ISAS - TSG (LEGOS-Survostral)) for the following conditions:

- all: All the match-up pairs satellite/in situ SSS values are used to derive the statistics
- C1: only pairs where RR=0 mm/h, 3< U_{10} <12 m/s, SST>5°C, distance to coast > 800 km
- C2: only pairs where RR=0 mm/h, 3< U_{10} <12 m/s
- C3: only pairs where RR>1mm/h and U_{10} <4m/s
- C5: only pairs where WOA2013 SSS Std<0.2
- C6: only pairs where WOA2013 SSS Std>0.2
- C7a: only pairs with a distance to coast < 150 km.
- C7b: only pairs with a distance to coast in the range [150, 800] km.
- C7c: only pairs with a distance to coast > 800 km.
- C8a: only pairs where SST is < 5°C.
- C8b: only pairs where SST is in the range [5, 15]°C.
- C8c: only pairs where SST is > 15°C.

- C9a: only pairs where SSS is < 33.
- C9b: only pairs where SSS is in the range [33, 37].
- C9c: only pairs where SSS is > 37.

Table 1: Statistics of ΔSSS (ISAS - TSG (LEGOS-Survostral))

Condition	#	Median	Mean	Std	RMS	IQR	r^2	Std*
all	652976	-0.01	0.00	0.16	0.16	0.12	0.902	0.09
C1	66147	0.02	0.02	0.11	0.11	0.11	0.743	0.08
C2	327306	-0.01	0.00	0.18	0.18	0.13	0.897	0.09
C3	916	-0.03	-0.06	0.17	0.18	0.17	0.917	0.08
C5	511064	-0.01	0.00	0.12	0.12	0.10	0.923	0.07
C6	112907	-0.02	-0.03	0.24	0.24	0.30	0.855	0.22
C7a	63782	0.00	0.03	0.29	0.29	0.31	0.847	0.23
C7b	368723	-0.01	-0.01	0.17	0.17	0.15	0.898	0.11
C7c	220471	-0.01	0.00	0.09	0.09	0.08	0.738	0.06
C8a	308616	-0.01	0.00	0.10	0.10	0.08	0.520	0.06
C8b	295347	0.00	0.00	0.18	0.18	0.19	0.845	0.14
C8c	42997	-0.10	-0.07	0.32	0.33	0.38	0.004	0.28
C9a	400	0.92	1.73	1.27	2.15	1.77	0.155	0.76
C9b	652576	-0.01	0.00	0.16	0.16	0.12	0.912	0.09
C9c	0	NaN	NaN	NaN	NaN	NaN	NaN	NaN

Table 1 numerical values can be downloaded as a csv file here.

2.6 TSG (LEGOS-Survostral-Adelie)

2.6.1 Introduction

The TSG-LEGOS-Surv-Adel dataset corresponds to delayed mode regional dataset along the Adelie coast provided by the Survostral project and available via ftp. Adjusted values when available and only collected TSG data that exhibit quality flags=1 and 2 were used.

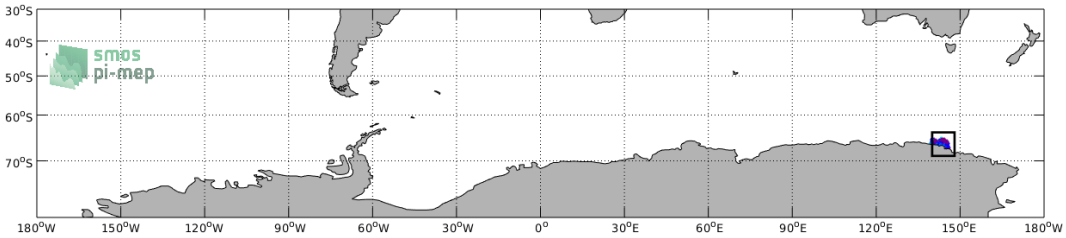

Figure 62: Location of the TSG (LEGOS-Survostral-Adelie) dataset.

2.6.2 Number of SSS data as a function of time and distance to coast

Figure 63 shows the time (a) and distance to coast (b) distributions of the TSG (LEGOS-Survostral-Adelie) *in situ* dataset.

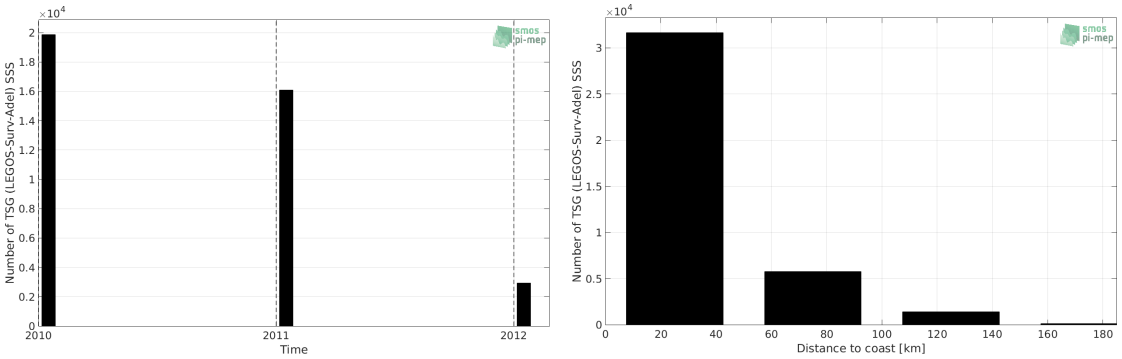

(a) (b)

Figure 63: Number of SSS from TSG (LEGOS-Survostral-Adelie) as a function of time (a) and distance to coast (b).

2.6.3 Histograms of SSS

Figure 64 shows the SSS distribution of the TSG (LEGOS-Survostral-Adelie) (a) and colocalized ISAS (b) dataset.

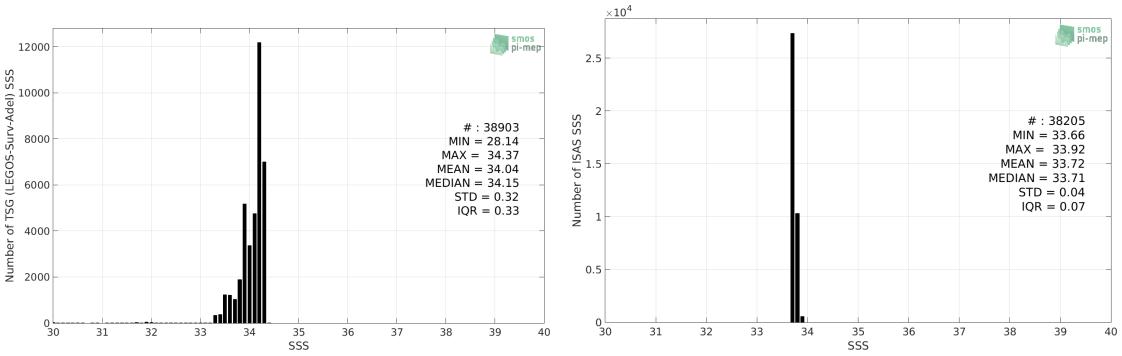

(a) (b)

Figure 64: Histograms of SSS from TSG (LEGOS-Survostral-Adelie) (a) and ISAS (b) per bins of 0.1.

2.6.4 Distribution of *in situ* SSS depth measurements

In Figure 65, we show the depth distribution of the *in situ* salinity dataset (a) and the spatial distribution of the depth temporal mean in 1°x1° boxes and considering the full *in situ* dataset period (b).

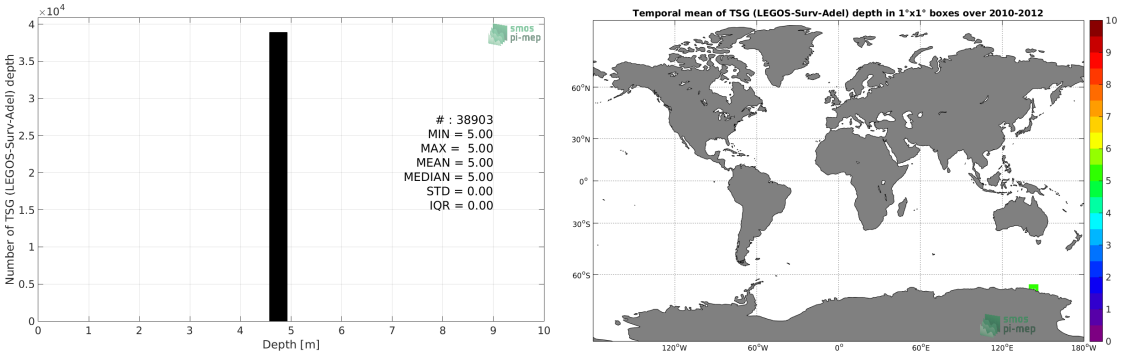

(a) (b)

Figure 65: Depth distribution of the upper level SSS measurements from TSG (LEGOS-Survostral-Adelie) (a) and spatial distribution of the *in situ* SSS depth measurements showing the mean value in 1°x1° boxes and considering the full *in situ* dataset period (b).

2.6.5 Spatial distribution of SSS

In Figure 66, the number of TSG (LEGOS-Survostral-Adelie) SSS measurements in 1°x1° boxes is shown.

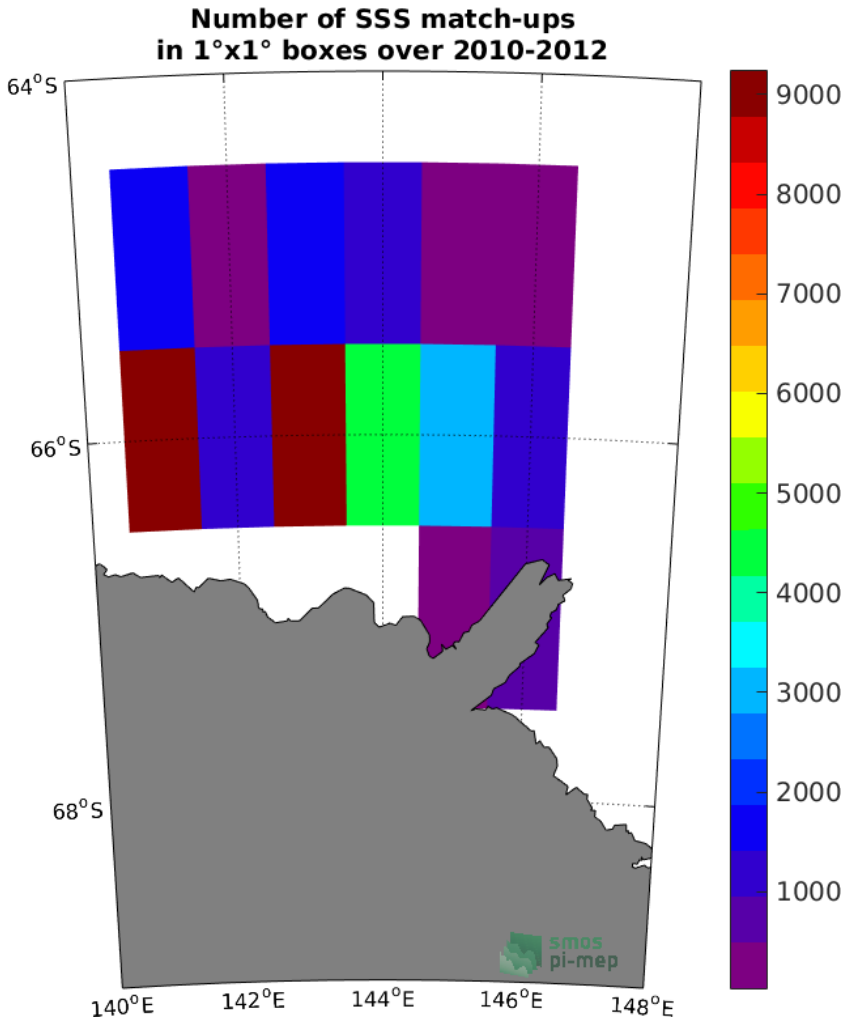

Figure 66: Number of SSS from TSG (LEGOS-Survostral-Adelie) in 1°x1° boxes.

2.6.6 Spatial Maps of the Temporal mean and Std of *in situ* and ISAS SSS and of the difference (ΔSSS)

In Figure 67, maps of temporal mean (left) and standard deviation (right) of ISAS (top), TSG (LEGOS-Survostral-Adelie) *in situ* dataset (middle) and the difference ΔSSS(ISAS -TSG (LEGOS-Survostral-Adelie)) (bottom) are shown. The temporal mean and std are calculated using all match-up pairs falling in spatial boxes of size 1°x1° over the full TSG (LEGOS-Survostral-Adelie) dataset period.

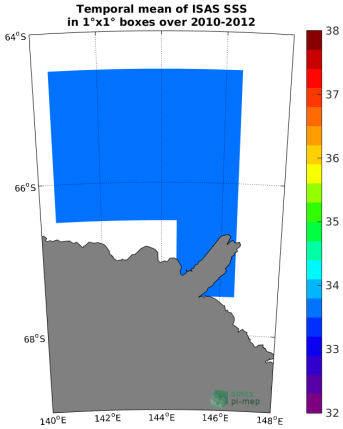

(a) MEAN(ISAS SSS)

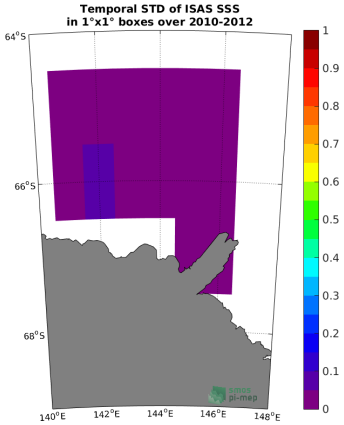

(b) Std(ISAS SSS)

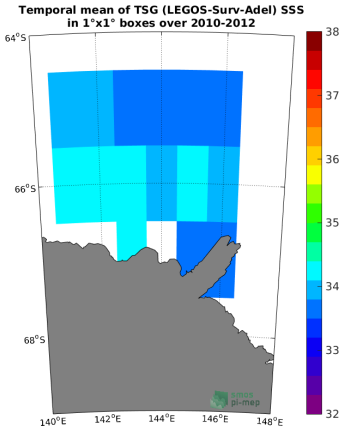

(c) MEAN(TSG (LEGOS-Survostral-Adelie) SSS)

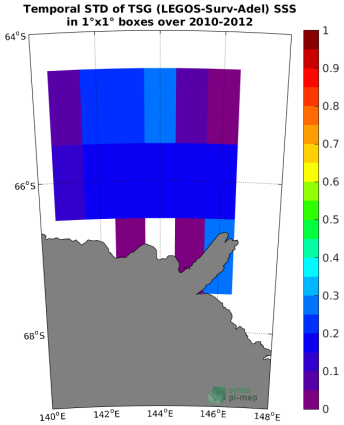

(d) Std(TSG (LEGOS-Survostral-Adelie) SSS)

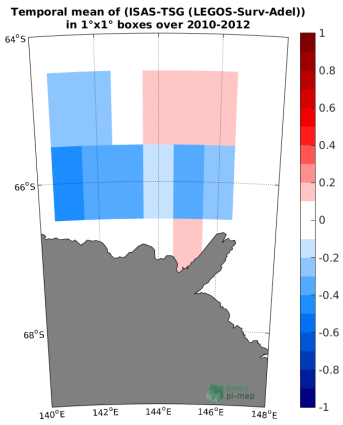

(e) MEAN(ΔSSS) (ISAS - TSG (LEGOS-Survostral-Adelie))

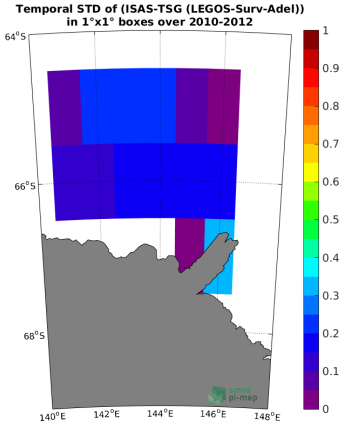

(f) Std(ΔSSS) (ISAS - TSG (LEGOS-Survostral-Adelie))

Figure 67: Temporal mean (left) and Std (right) of SSS from ISAS (top), TSG (LEGOS-Survostral-Adelie) (middle), and of ΔSSS (ISAS - TSG (LEGOS-Survostral-Adelie)). Only match-up pairs are used to generate these maps.

2.6.7 Time series of the monthly median and Std of *in situ* and ISAS SSS and of the difference (ΔSSS)

In the top panel of Figure 68, we show the time series of the monthly median SSS estimated for both ISAS SSS product (in black) and the TSG (LEGOS-Survostral-Adelie) *in situ* dataset (in blue) at the collected Pi-MEP match-up pairs.

In the middle panel of Figure 68, we show the time series of the monthly median of ΔSSS (ISAS - TSG (LEGOS-Survostral-Adelie)) for the collected Pi-MEP match-up pairs.

In the bottom panel of Figure 68, we show the time series of the monthly standard deviation of the ΔSSS (ISAS - TSG (LEGOS-Survostral-Adelie)) for the collected Pi-MEP match-up pairs.

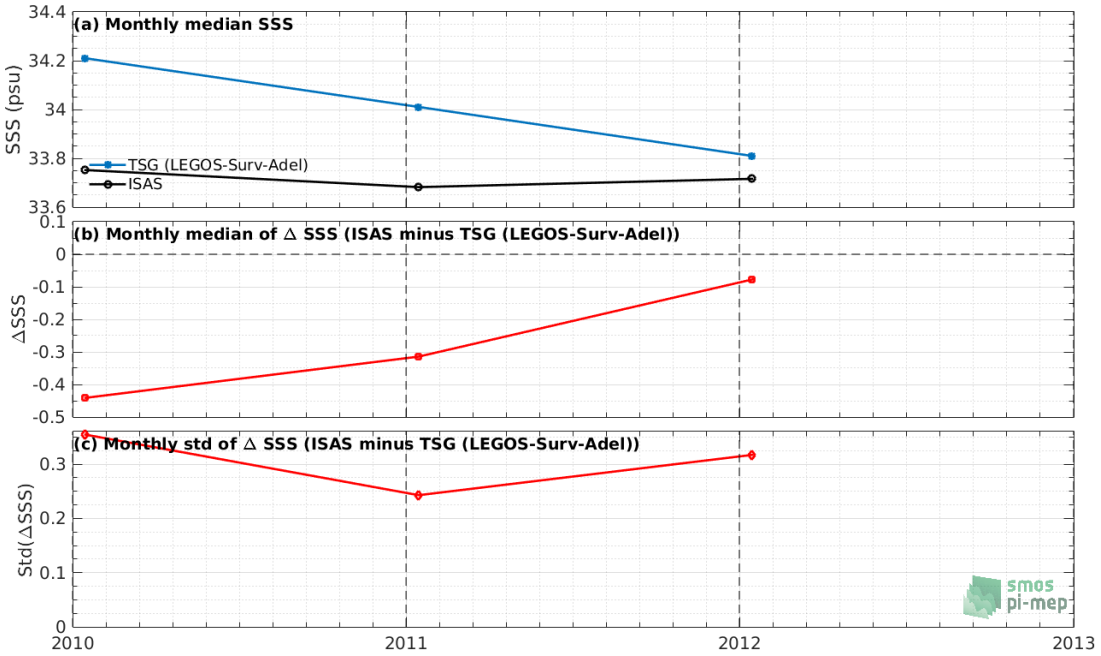

Figure 68: Time series of the monthly median SSS (top), median of ΔSSS (ISAS - TSG (LEGOS-Survostral-Adelie)) and Std of ΔSSS (ISAS - TSG (LEGOS-Survostral-Adelie)) considering all match-ups collected by the Pi-MEP.

2.6.8 Zonal mean and Std of *in situ* and ISAS SSS and of the difference ΔSSS

In Figure 69 left panel, we show the zonal mean SSS considering all Pi-MEP match-up pairs for both ISAS SSS product (in black) and the TSG (LEGOS-Survostral-Adelie) *in situ* dataset (in blue). The full *in situ* dataset period is used to derive the mean.

In the right panel of Figure 69, we show the zonal mean of ΔSSS (ISAS - TSG (LEGOS-Survostral-Adelie)) for all the collected Pi-MEP match-up pairs estimated over the full *in situ* dataset period.

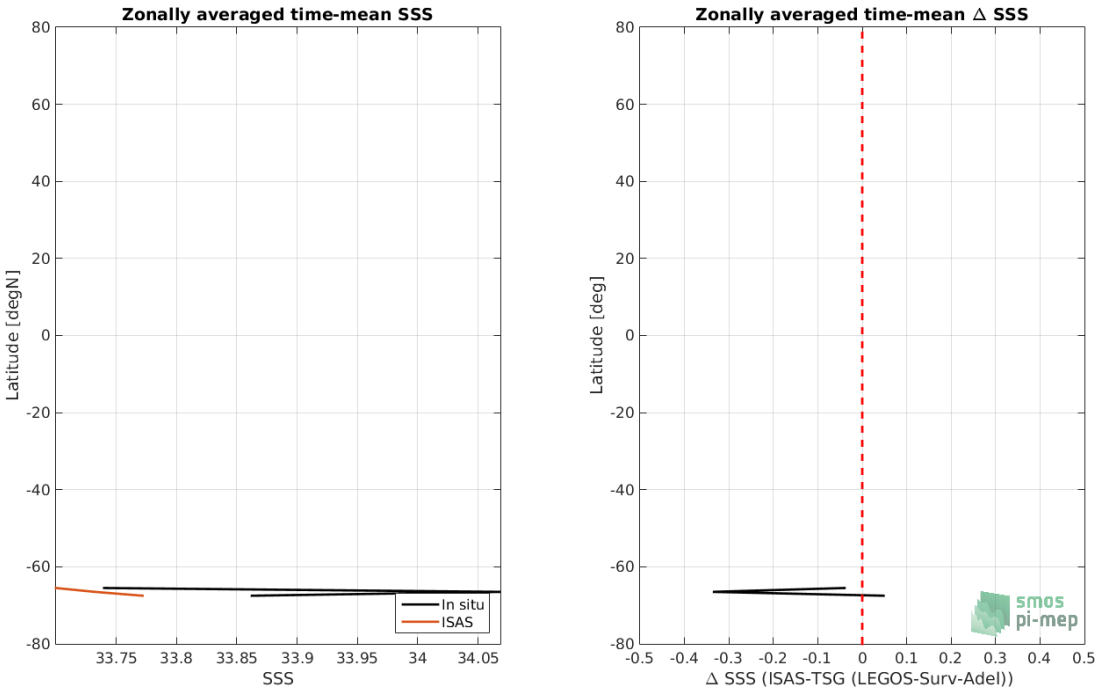

Figure 69: Left panel: Zonal mean SSS from ISAS product (black) and from TSG (LEGOS-Survostral-Adelie) (blue). Right panel: Zonal mean of ΔSSS (ISAS - TSG (LEGOS-Survostral-Adelie)) for all the collected Pi-MEP match-up pairs estimated over the full *in situ* dataset period.

2.6.9 Scatterplots of ISAS vs *in situ* SSS by latitudinal bands

In Figure 70, contour maps of the concentration of ISAS SSS (y-axis) versus TSG (LEGOS-Survostral-Adelie) SSS (x-axis) at match-up pairs for different latitude bands: (a) 80°S-80°N, (b) 20°S-20°N, (c) 40°S-20°S and 20°N-40°N and (d) 60°S-40°S and 40°N-60°N. For each plot, the red line shows x=y. The black thin and dashed lines indicate a linear fit through the data cloud and the ±95% confidence levels, respectively. The number match-up pairs n, the slope and R^2 coefficient of the linear fit, the root mean square (RMS) and the mean bias between ISAS and *in situ* data are indicated for each latitude band in each plots.

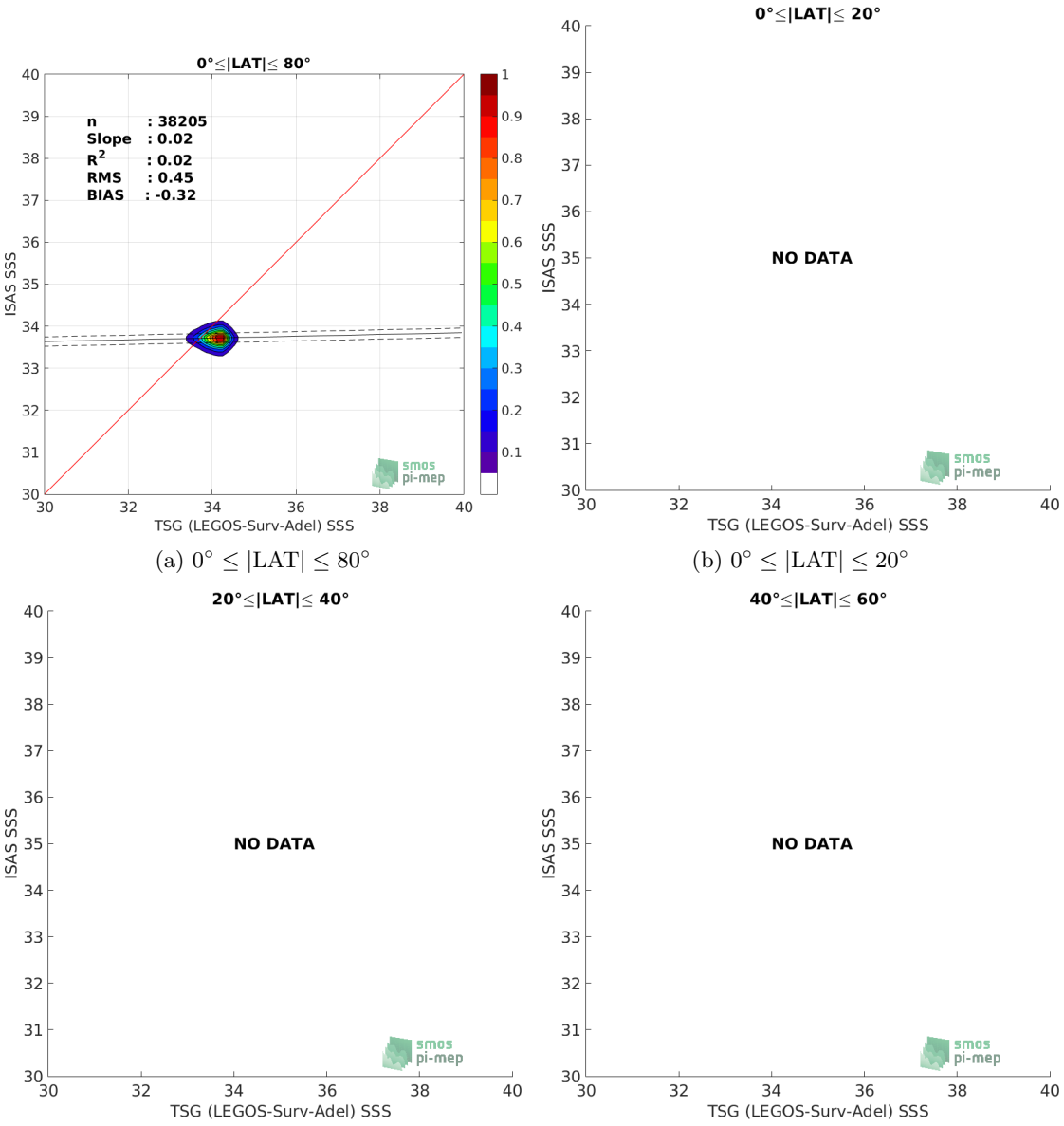

(a) $0° \leq |\text{LAT}| \leq 80°$

(b) $0° \leq |\text{LAT}| \leq 20°$

(c) $20° \leq |\text{LAT}| \leq 40°$

(d) $40° \leq |\text{LAT}| \leq 60°$

Figure 70: Contour maps of the concentration of ISAS SSS (y-axis) versus TSG (LEGOS-Survostral-Adelie) SSS (x-axis) at match-up pairs for different latitude bands. For each plot, the red line shows x=y. The black thin and dashed lines indicate a linear fit through the data cloud and the ±95% confidence levels, respectively. The number match-up pairs n, the slope and R^2 coefficient of the linear fit, the root mean square (RMS) and the mean bias between ISAS and *in situ* data are indicated for each latitude band in each plots.

2.6.10 Time series of the monthly median and Std of the difference ΔSSS sorted by latitudinal bands

In Figure 71, time series of the monthly median (red curves) of ΔSSS (ISAS - TSG (LEGOS-Survostral-Adelie)) and ±1 Std (black vertical thick bars) as function of time for all the collected Pi-MEP match-up pairs estimated for the full *in situ* dataset period are shown for different latitude bands: (a) 80°S-80°N, (b) 20°S-20°N, (c) 40°S-20°S and 20°N-40°N and (d) 60°S-40°S and 40°N-60°N.

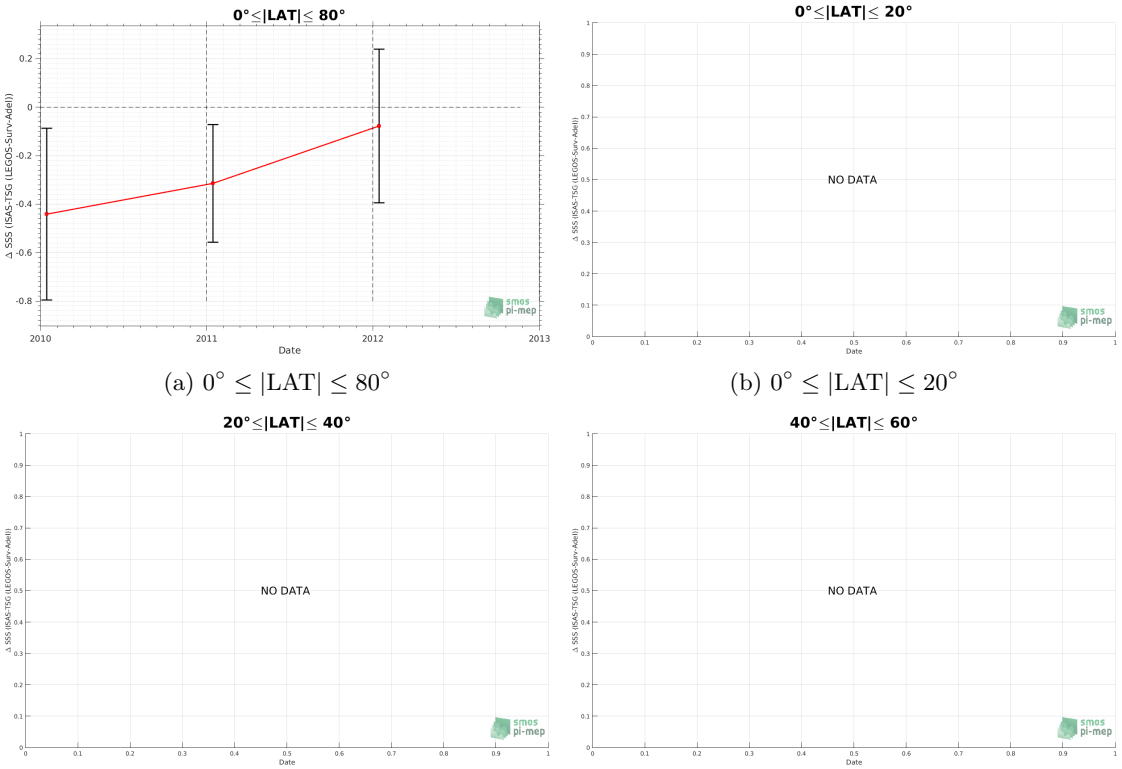

(a) $0° \leq |\text{LAT}| \leq 80°$

(b) $0° \leq |\text{LAT}| \leq 20°$

(c) $20° \leq |\text{LAT}| \leq 40°$

(d) $40° \leq |\text{LAT}| \leq 60°$

Figure 71: Monthly median (red curves) of ΔSSS (ISAS - TSG (LEGOS-Survostral-Adelie)) and ±1 Std (black vertical thick bars) as function of time for all the collected Pi-MEP match-up pairs for the full *in situ* dataset period are shown for different latitude bands: (a) 80°S-80°N, (b) 20°S-20°N, (c) 40°S-20°S and 20°N-40°N and (d) 60°S-40°S and 40°N-60°N.

2.6.11 ΔSSS sorted as geophysical conditions

In Figure 72, we classify the match-up differences ΔSSS (ISAS - *in situ*) as function of the geophysical conditions at match-up points. The mean and std of ΔSSS (ISAS - TSG (LEGOS-Survostral-Adelie)) is thus evaluated as function of the

- *in situ* SSS values per bins of width 0.2,
- *in situ* SST values per bins of width 1°C,
- ASCAT daily wind values per bins of width 1 m/s,

- CMORPH 3-hourly rain rates per bins of width 1 mm/h, and,
- distance to coasts per bins of width 50 km,
- *in situ* measurement depth (if relevant).

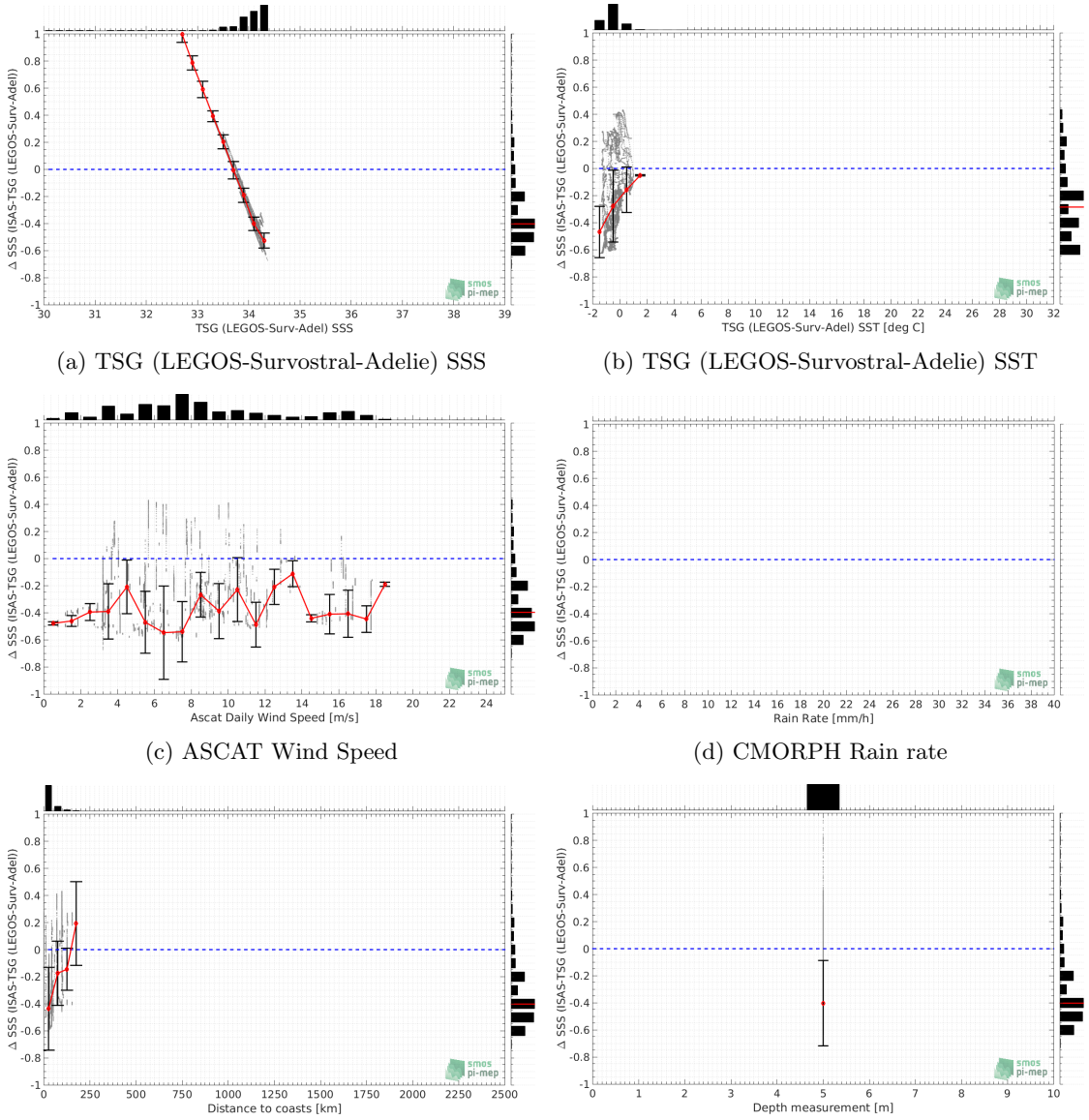

(a) TSG (LEGOS-Survostral-Adelie) SSS

(b) TSG (LEGOS-Survostral-Adelie) SST

(c) ASCAT Wind Speed

(d) CMORPH Rain rate

(e) Distance to coast

(f) Depth

Figure 72: Δ SSS (ISAS - TSG (LEGOS-Survostral-Adelie)) sorted as geophysical conditions: TSG (LEGOS-Survostral-Adelie) SSS a), TSG (LEGOS-Survostral-Adelie) SST b), ASCAT Wind speed c), CMORPH rain rate d), distance to coast (e) and depth measurements (f).

2.6.12 ΔSSS maps and statistics for different geophysical conditions

In Figures 73 and 74, we focus on sub-datasets of the match-up differences ΔSSS (ISAS - *in situ*) for the following specific geophysical conditions:

- **C1**:if the local value at *in situ* location of estimated rain rate is zero, mean daily wind is in the range [3, 12] m/s, the SST is $> 5°$C and distance to coast is > 800 km.
- **C2**:if the local value at *in situ* location of estimated rain rate is zero, mean daily wind is in the range [3, 12] m/s.
- **C3**:if the local value at *in situ* location of estimated rain rate is high (ie. > 1 mm/h) and mean daily wind is low (ie. < 4 m/s).
- **C5**:if the *in situ* data is located where the climatological SSS standard deviation is low (ie. above < 0.2).
- **C6**:if the *in situ* data is located where the climatological SSS standard deviation is high (ie. above > 0.2).

For each of these conditions, the temporal mean (gridded over spatial boxes of size 1°x1°) and the histogram of the difference ΔSSS (ISAS - *in situ*) are presented.

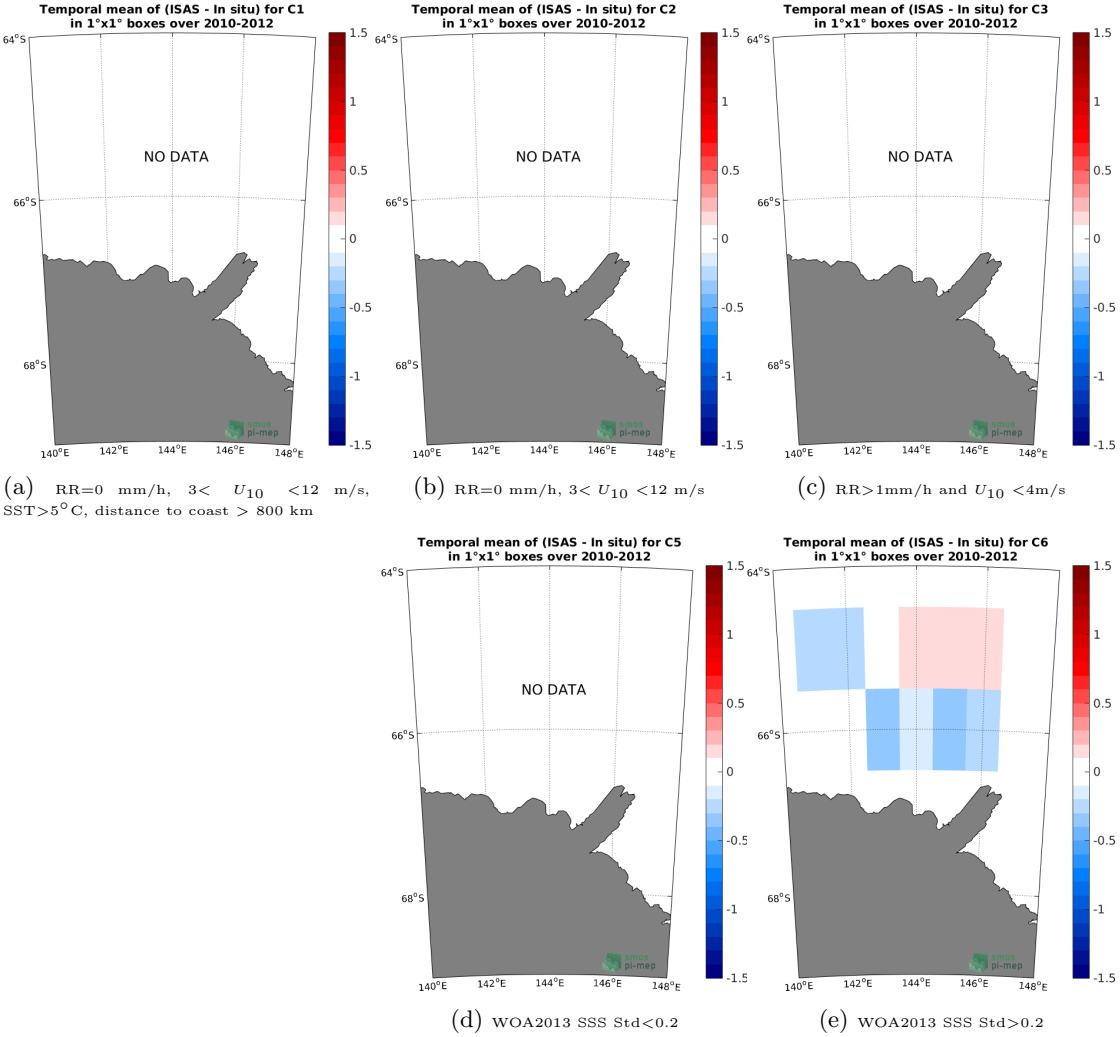

(a) RR=0 mm/h, 3< U_{10} <12 m/s, SST>5°C, distance to coast > 800 km (b) RR=0 mm/h, 3< U_{10} <12 m/s (c) RR>1mm/h and U_{10} <4m/s

(d) WOA2013 SSS Std<0.2 (e) WOA2013 SSS Std>0.2

Figure 73: Temporal mean gridded over spatial boxes of size 1°x1° of ΔSSS (ISAS - TSG (LEGOS-Survostral-Adelie)) for 5 different subdatasets corresponding to:RR=0 mm/h, 3< U_{10} <12 m/s, SST>5°C, distance to coast > 800 km (a), RR=0 mm/h, 3< U_{10} <12 m/s (b), RR>1mm/h and U_{10} <4m/s (c),WOA2013 SSS Std<0.2 (d),WOA2013 SSS Std>0.2 (e).

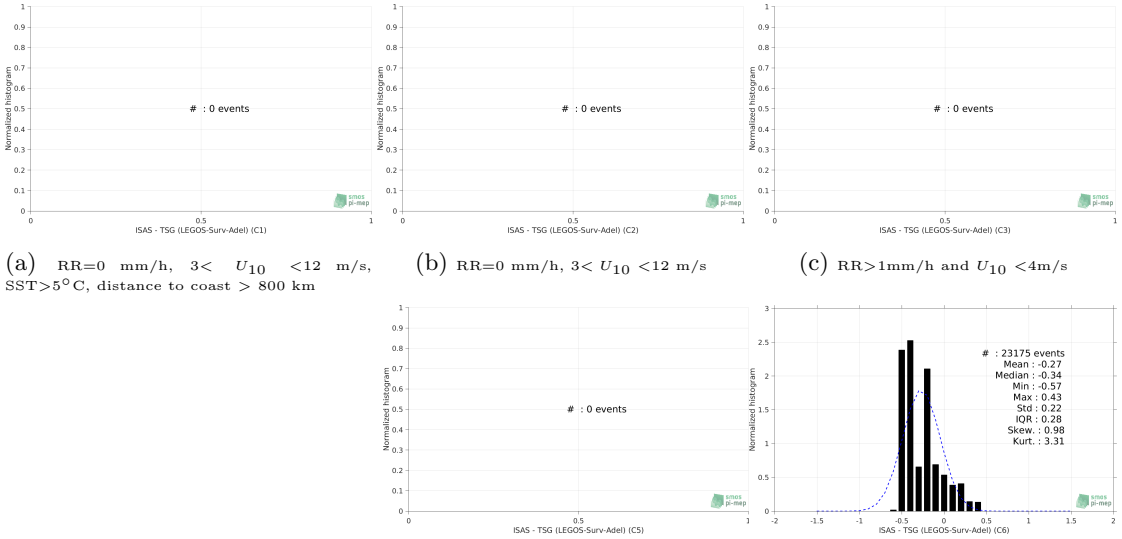

(a) RR=0 mm/h, 3< U_{10} <12 m/s, SST>5°C, distance to coast > 800 km (b) RR=0 mm/h, 3< U_{10} <12 m/s (c) RR>1mm/h and U_{10} <4m/s

(d) WOA2013 SSS Std<0.2 (e) WOA2013 SSS Std>0.2

Figure 74: Normalized histogram of ΔSSS (ISAS - TSG (LEGOS-Survostral-Adelie)) for 5 different subdatasets corresponding to:RR=0 mm/h, 3< U_{10} <12 m/s, SST>5°C, distance to coast > 800 km (a), RR=0 mm/h, 3< U_{10} <12 m/s (b), RR>1mm/h and U_{10} <4m/s (c),WOA2013 SSS Std<0.2 (d),WOA2013 SSS Std>0.2 (e).

2.6.13 Summary

Table 1 shows the mean, median, standard deviation (Std), root mean square (RMS), interquartile range (IQR), correlation coefficient (r^2) and robust standard deviation (Std*) of the match-up differences ΔSSS (ISAS - TSG (LEGOS-Survostral-Adelie)) for the following conditions:

- all: All the match-up pairs satellite/in situ SSS values are used to derive the statistics
- C1: only pairs where RR=0 mm/h, 3< U_{10} <12 m/s, SST>5°C, distance to coast > 800 km
- C2: only pairs where RR=0 mm/h, 3< U_{10} <12 m/s
- C3: only pairs where RR>1mm/h and U_{10} <4m/s
- C5: only pairs where WOA2013 SSS Std<0.2
- C6: only pairs where WOA2013 SSS Std>0.2
- C7a: only pairs with a distance to coast < 150 km.
- C7b: only pairs with a distance to coast in the range [150, 800] km.
- C7c: only pairs with a distance to coast > 800 km.
- C8a: only pairs where SST is < 5°C.
- C8b: only pairs where SST is in the range [5, 15]°C.
- C8c: only pairs where SST is > 15°C.

- C9a: only pairs where SSS is < 33.
- C9b: only pairs where SSS is in the range [33, 37].
- C9c: only pairs where SSS is > 37.

Table 1: Statistics of ΔSSS (ISAS - TSG (LEGOS-Survostral-Adelie))

Condition	#	Median	Mean	Std	RMS	IQR	r^2	Std*
all	38205	-0.40	-0.32	0.32	0.45	0.30	0.024	0.20
C1	0	NaN	NaN	NaN	NaN	NaN	NaN	NaN
C2	0	NaN	NaN	NaN	NaN	NaN	NaN	NaN
C3	0	NaN	NaN	NaN	NaN	NaN	NaN	NaN
C5	0	NaN	NaN	NaN	NaN	NaN	NaN	NaN
C6	23175	-0.34	-0.27	0.22	0.35	0.28	0.405	0.21
C7a	38109	-0.40	-0.32	0.32	0.45	0.30	0.023	0.20
C7b	96	0.19	0.00	0.31	0.31	0.65	0.991	0.12
C7c	0	NaN	NaN	NaN	NaN	NaN	NaN	NaN
C8a	18615	-0.29	-0.27	0.26	0.37	0.34	0.218	0.26
C8b	0	NaN	NaN	NaN	NaN	NaN	NaN	NaN
C8c	0	NaN	NaN	NaN	NaN	NaN	NaN	NaN
C9a	270	1.76	2.09	1.16	2.39	0.93	0.000	0.59
C9b	37935	-0.40	-0.34	0.22	0.40	0.30	0.031	0.20
C9c	0	NaN	NaN	NaN	NaN	NaN	NaN	NaN

Table 1 numerical values can be downloaded as a csv file here.

2.7 TSG (Polarstern)

2.7.1 Introduction

The TSG-POLARSTERN dataset has been gathered through the https://www.pangaea.de/ data warehouse utility using the following criteria: basis:"Polarstern" , device:"Underway cruise track measurements (CT)" , time coverage form 2010/01/01 to present. The result of the query is a collection of 79 different datasets with the following identification numbers: 736345, 742729, 753224, 753225, 753226, 753227, 758080, 760120, 760121, 761277, 770034, 770035, 770828, 776596, 776597, 780004, 802809, 802810, 802811, 802812, 803431, 808835, 808836, 808838, 809727, 810678, 816055, 819831, 823259, 839406, 839407, 839408, 848615, 858879, 858880, 858881, 858882, 858883, 858884, 858885, 863228, 863229, 863230, 863231, 863232, 863234, 873145, 873147, 873151, 873153, 873155, 873156, 873158, 887767, 889444, 889513, 889515, 889516, 889517, 889535, 889542, 889548, 895578, 895579, 895581, 898225, 898233, 898266, 905555, 905562, 905608, 905610, 905734, 930022, 930023, 930024, 930026, 930027, 930028.

2.7.2 Number of SSS data as a function of time and distance to coast

Figure 75 shows the time (a) and distance to coast (b) distributions of the TSG (Polarstern) *in situ* dataset.

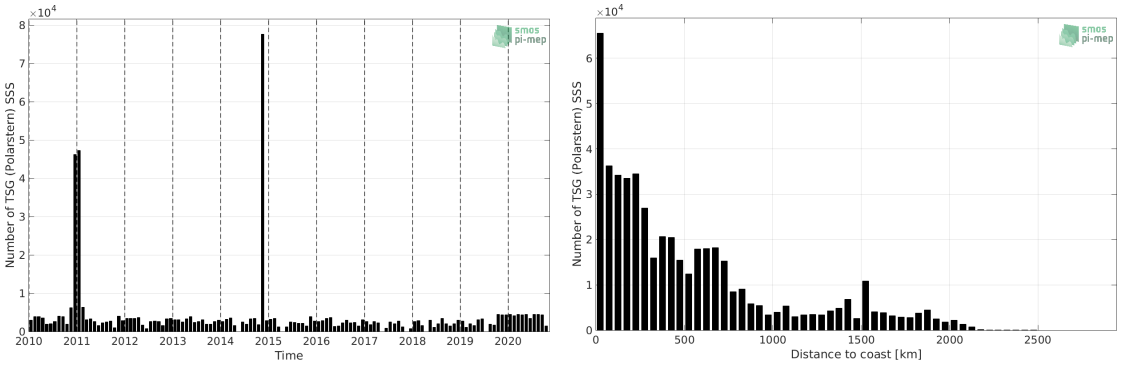

(a) (b)

Figure 75: Number of SSS from TSG (Polarstern) as a function of time (a) and distance to coast (b).

2.7.3 Histograms of SSS

Figure 76 shows the SSS distribution of the TSG (Polarstern) (a) and colocalized ISAS (b) dataset.

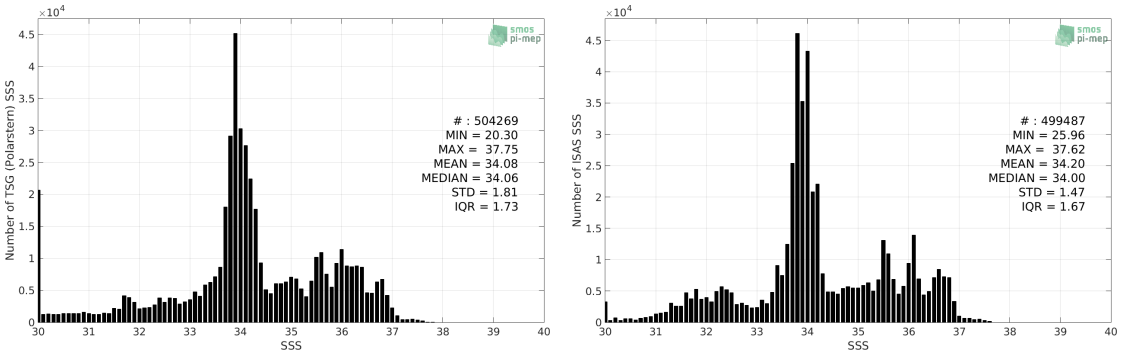

(a) (b)

Figure 76: Histograms of SSS from TSG (Polarstern) (a) and ISAS (b) per bins of 0.1.

2.7.4 Distribution of *in situ* SSS depth measurements

In Figure 77, we show the depth distribution of the *in situ* salinity dataset (a) and the spatial distribution of the depth temporal mean in 1°x1° boxes and considering the full *in situ* dataset period (b).

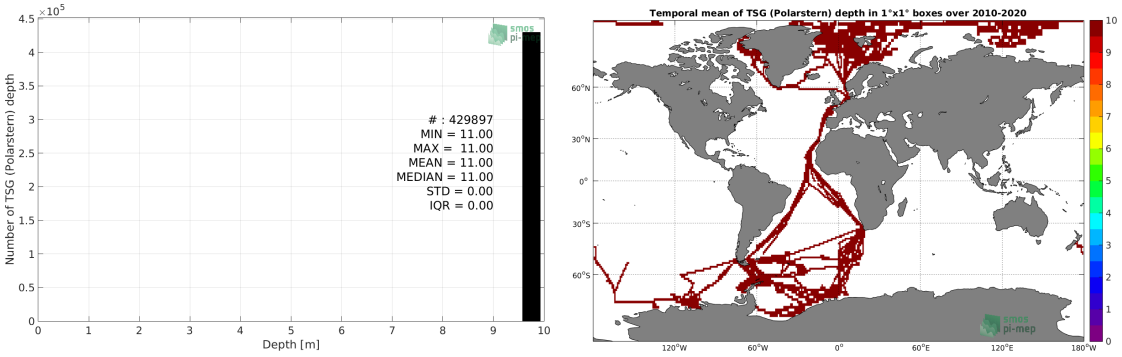

(a) (b)

Figure 77: Depth distribution of the upper level SSS measurements from TSG (Polarstern) (a) and spatial distribution of the *in situ* SSS depth measurements showing the mean value in 1°x1° boxes and considering the full *in situ* dataset period (b).

2.7.5 Spatial distribution of SSS

In Figure 78, the number of TSG (Polarstern) SSS measurements in 1°x1° boxes is shown.

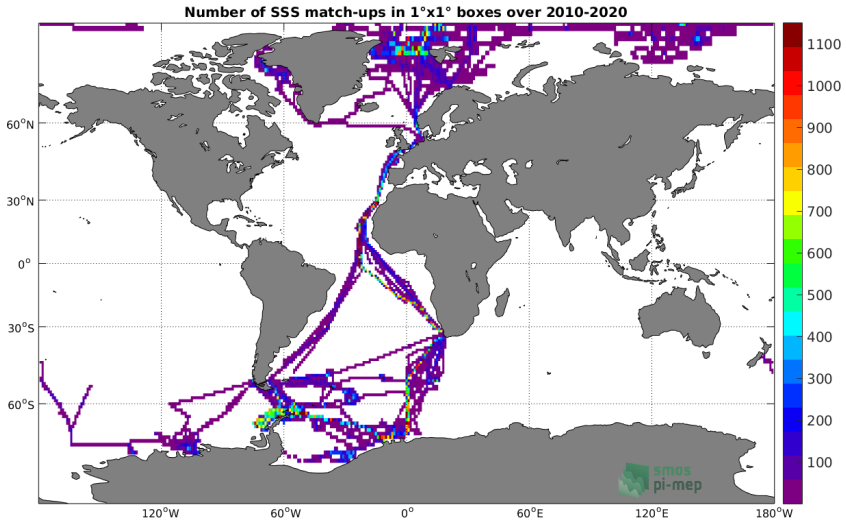

Figure 78: Number of SSS from TSG (Polarstern) in 1°x1° boxes.

2.7.6 Spatial Maps of the Temporal mean and Std of *in situ* and ISAS SSS and of the difference (ΔSSS)

In Figure 79, maps of temporal mean (left) and standard deviation (right) of ISAS (top), TSG (Polarstern) *in situ* dataset (middle) and the difference ΔSSS(ISAS -TSG (Polarstern)) (bottom) are shown. The temporal mean and std are calculated using all match-up pairs falling in spatial boxes of size 1°x1° over the full TSG (Polarstern) dataset period.

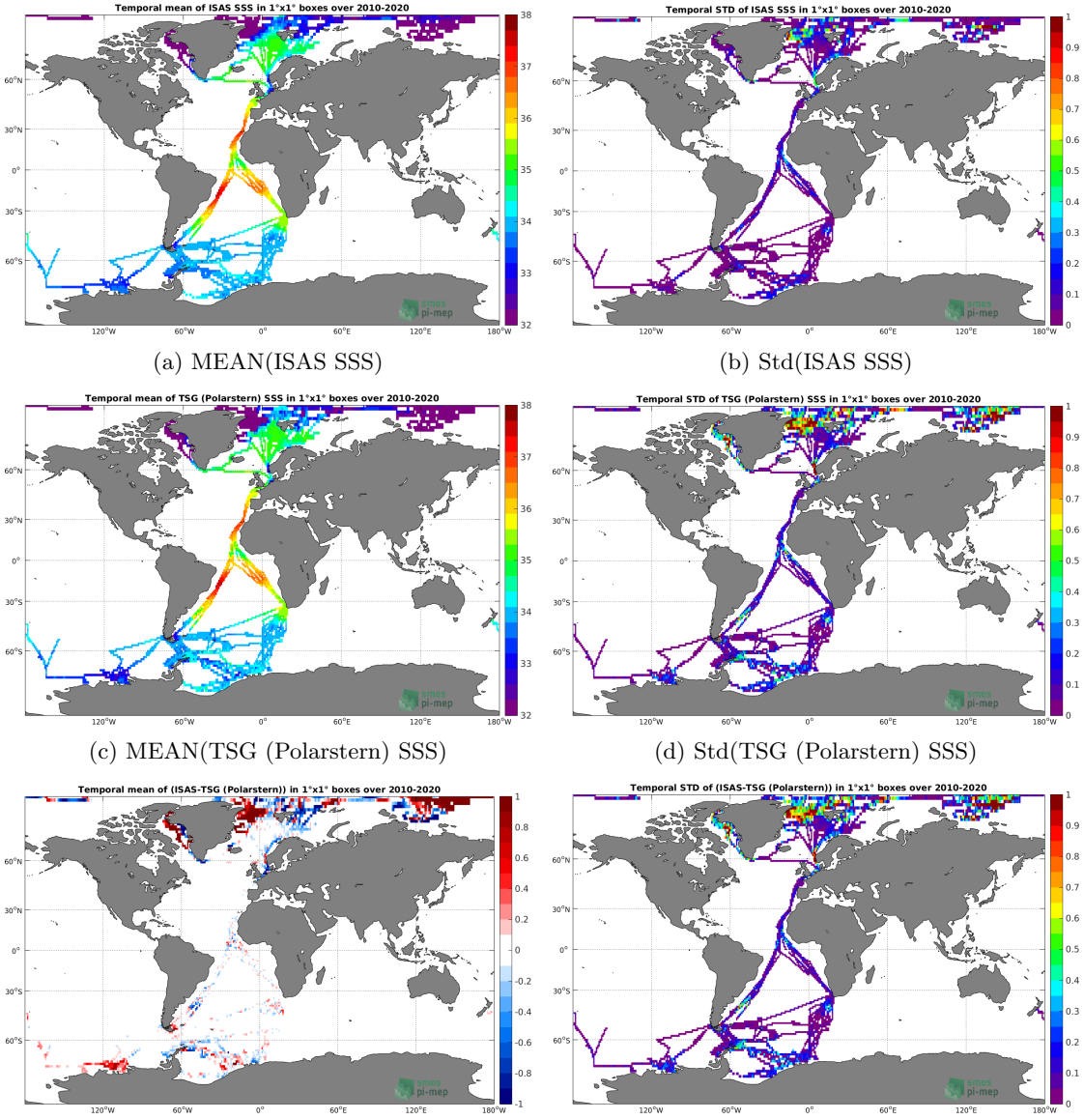

(a) MEAN(ISAS SSS)

(b) Std(ISAS SSS)

(c) MEAN(TSG (Polarstern) SSS)

(d) Std(TSG (Polarstern) SSS)

(e) MEAN(ΔSSS) (ISAS - TSG (Polarstern))

(f) Std(ΔSSS) (ISAS - TSG (Polarstern))

Figure 79: Temporal mean (left) and Std (right) of SSS from ISAS (top), TSG (Polarstern) (middle), and of ΔSSS (ISAS - TSG (Polarstern)). Only match-up pairs are used to generate these maps.

2.7.7 Time series of the monthly median and Std of *in situ* and ISAS SSS and of the difference (ΔSSS)

In the top panel of Figure 80, we show the time series of the monthly median SSS estimated for both ISAS SSS product (in black) and the TSG (Polarstern) *in situ* dataset (in blue) at the collected Pi-MEP match-up pairs.

In the middle panel of Figure 80, we show the time series of the monthly median of ΔSSS (ISAS - TSG (Polarstern)) for the collected Pi-MEP match-up pairs.

In the bottom panel of Figure 80, we show the time series of the monthly standard deviation of the ΔSSS (ISAS - TSG (Polarstern)) for the collected Pi-MEP match-up pairs.

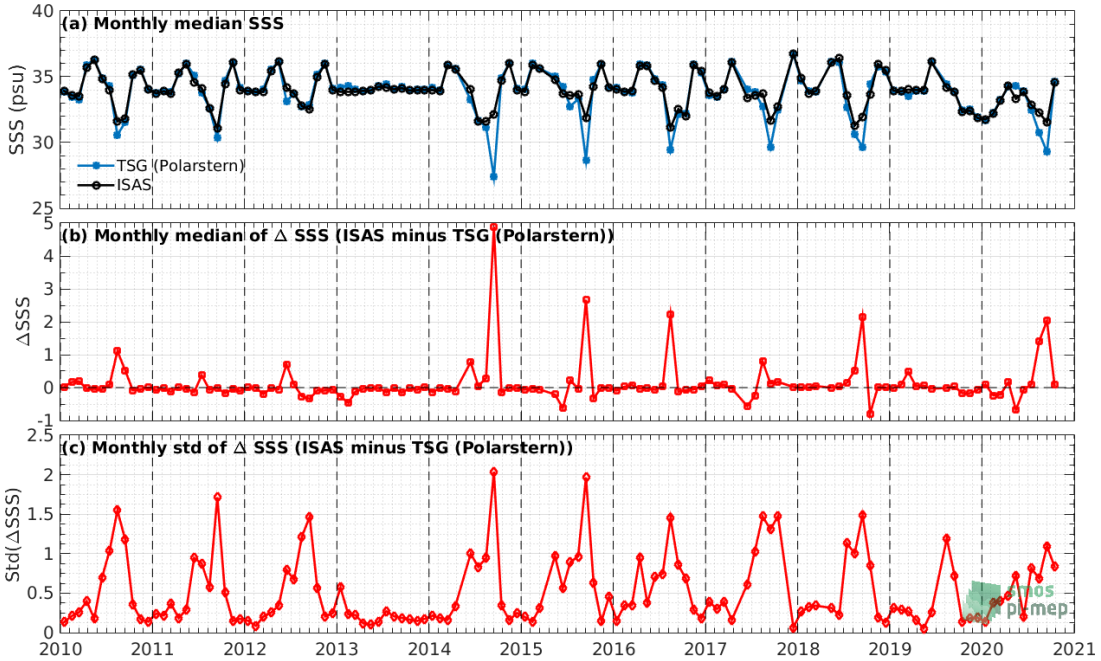

Figure 80: Time series of the monthly median SSS (top), median of ΔSSS (ISAS - TSG (Polarstern)) and Std of ΔSSS (ISAS - TSG (Polarstern)) considering all match-ups collected by the Pi-MEP.

2.7.8 Zonal mean and Std of *in situ* and ISAS SSS and of the difference ΔSSS

In Figure 81 left panel, we show the zonal mean SSS considering all Pi-MEP match-up pairs for both ISAS SSS product (in black) and the TSG (Polarstern) *in situ* dataset (in blue). The full *in situ* dataset period is used to derive the mean.

In the right panel of Figure 81, we show the zonal mean of ΔSSS (ISAS - TSG (Polarstern)) for all the collected Pi-MEP match-up pairs estimated over the full *in situ* dataset period.

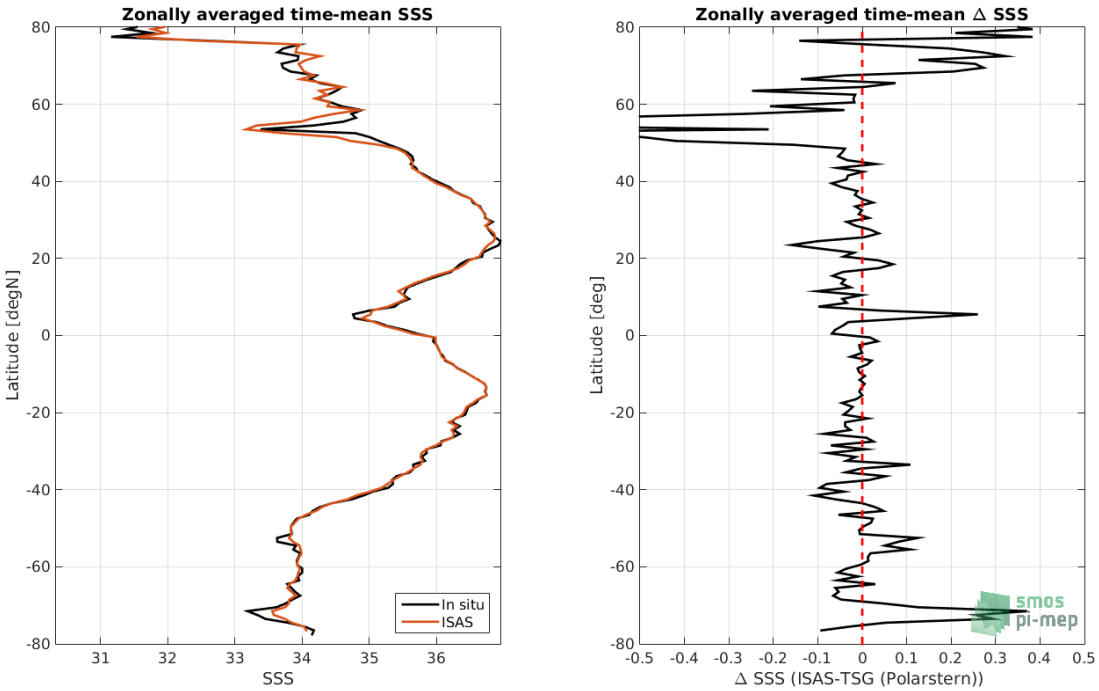

Figure 81: Left panel: Zonal mean SSS from ISAS product (black) and from TSG (Polarstern) (blue). Right panel: Zonal mean of ΔSSS (ISAS - TSG (Polarstern)) for all the collected Pi-MEP match-up pairs estimated over the full *in situ* dataset period.

2.7.9 Scatterplots of ISAS vs *in situ* SSS by latitudinal bands

In Figure 82, contour maps of the concentration of ISAS SSS (y-axis) versus TSG (Polarstern) SSS (x-axis) at match-up pairs for different latitude bands: (a) 80°S-80°N, (b) 20°S-20°N, (c) 40°S-20°S and 20°N-40°N and (d) 60°S-40°S and 40°N-60°N. For each plot, the red line shows x=y. The black thin and dashed lines indicate a linear fit through the data cloud and the ±95% confidence levels, respectively. The number match-up pairs n, the slope and R^2 coefficient of the linear fit, the root mean square (RMS) and the mean bias between ISAS and *in situ* data are indicated for each latitude band in each plots.

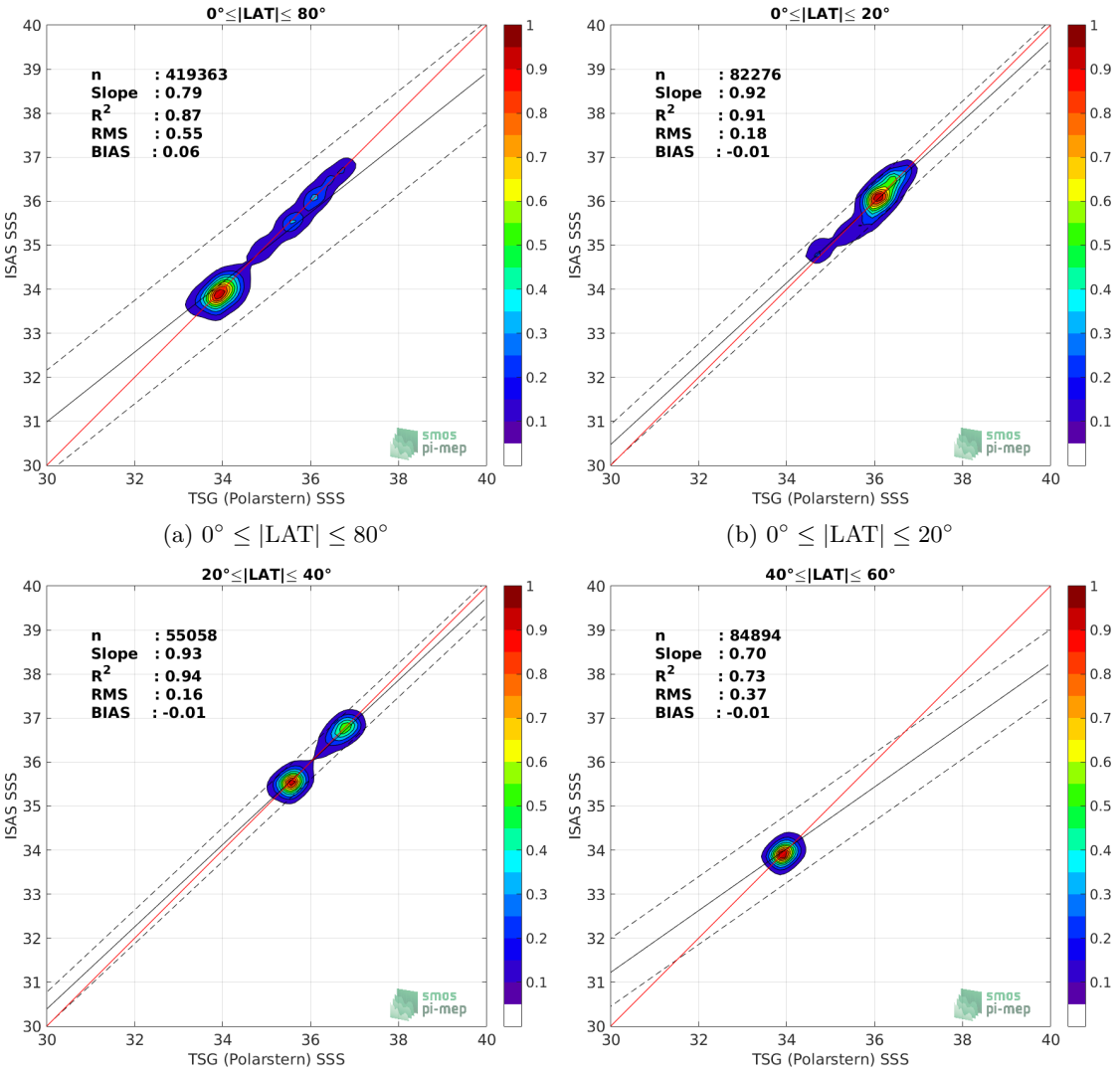

(a) $0° \leq |\text{LAT}| \leq 80°$ (b) $0° \leq |\text{LAT}| \leq 20°$

(c) $20° \leq |\text{LAT}| \leq 40°$ (d) $40° \leq |\text{LAT}| \leq 60°$

Figure 82: Contour maps of the concentration of ISAS SSS (y-axis) versus TSG (Polarstern) SSS (x-axis) at match-up pairs for different latitude bands. For each plot, the red line shows x=y. The black thin and dashed lines indicate a linear fit through the data cloud and the ±95% confidence levels, respectively. The number match-up pairs n, the slope and R^2 coefficient of the linear fit, the root mean square (RMS) and the mean bias between ISAS and *in situ* data are indicated for each latitude band in each plots.

2.7.10 Time series of the monthly median and Std of the difference ΔSSS sorted by latitudinal bands

In Figure 83, time series of the monthly median (red curves) of ΔSSS (ISAS - TSG (Polarstern)) and ±1 Std (black vertical thick bars) as function of time for all the collected Pi-MEP match-up pairs estimated for the full *in situ* dataset period are shown for different latitude bands: (a) 80°S-80°N, (b) 20°S-20°N, (c) 40°S-20°S and 20°N-40°N and (d) 60°S-40°S and 40°N-60°N.

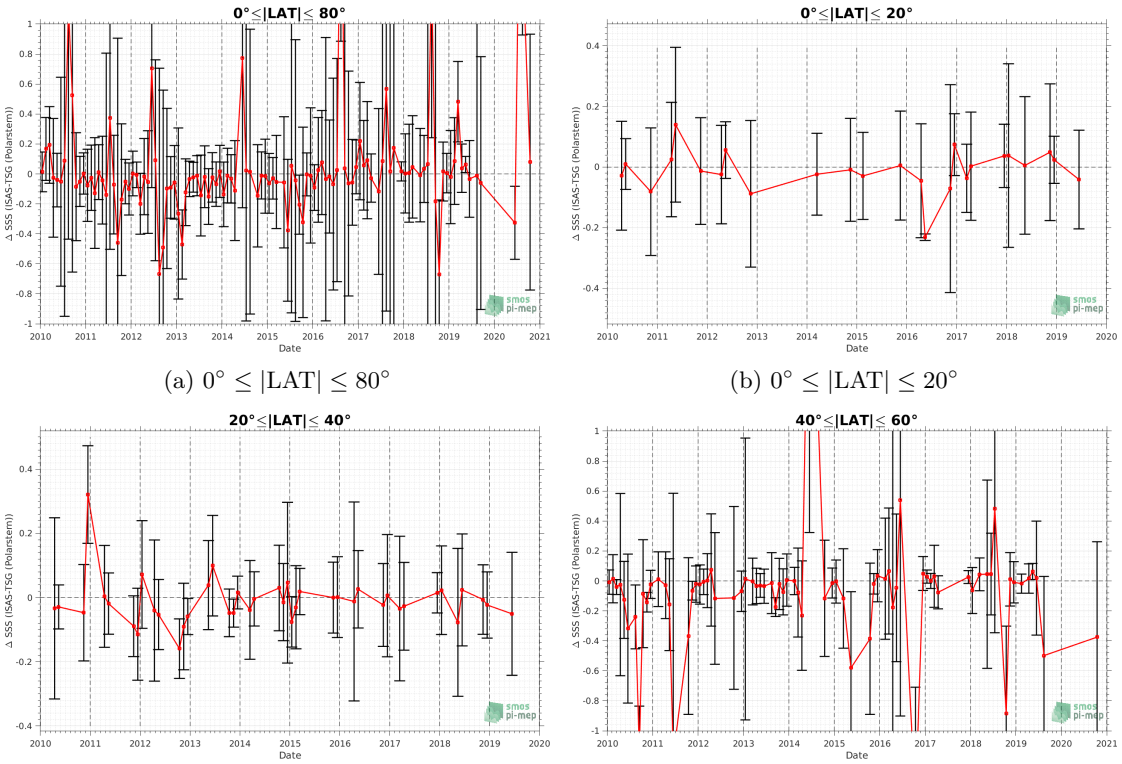

(a) $0° \leq |\text{LAT}| \leq 80°$

(b) $0° \leq |\text{LAT}| \leq 20°$

(c) $20° \leq |\text{LAT}| \leq 40°$

(d) $40° \leq |\text{LAT}| \leq 60°$

Figure 83: Monthly median (red curves) of ΔSSS (ISAS - TSG (Polarstern)) and ±1 Std (black vertical thick bars) as function of time for all the collected Pi-MEP match-up pairs for the full *in situ* dataset period are shown for different latitude bands: (a) 80°S-80°N, (b) 20°S-20°N, (c) 40°S-20°S and 20°N-40°N and (d) 60°S-40°S and 40°N-60°N.

2.7.11 ΔSSS sorted as geophysical conditions

In Figure 84, we classify the match-up differences ΔSSS (ISAS - *in situ*) as function of the geophysical conditions at match-up points. The mean and std of ΔSSS (ISAS - TSG (Polarstern)) is thus evaluated as function of the

- *in situ* SSS values per bins of width 0.2,
- *in situ* SST values per bins of width 1°C,
- ASCAT daily wind values per bins of width 1 m/s,
- CMORPH 3-hourly rain rates per bins of width 1 mm/h, and,
- distance to coasts per bins of width 50 km,
- *in situ* measurement depth (if relevant).

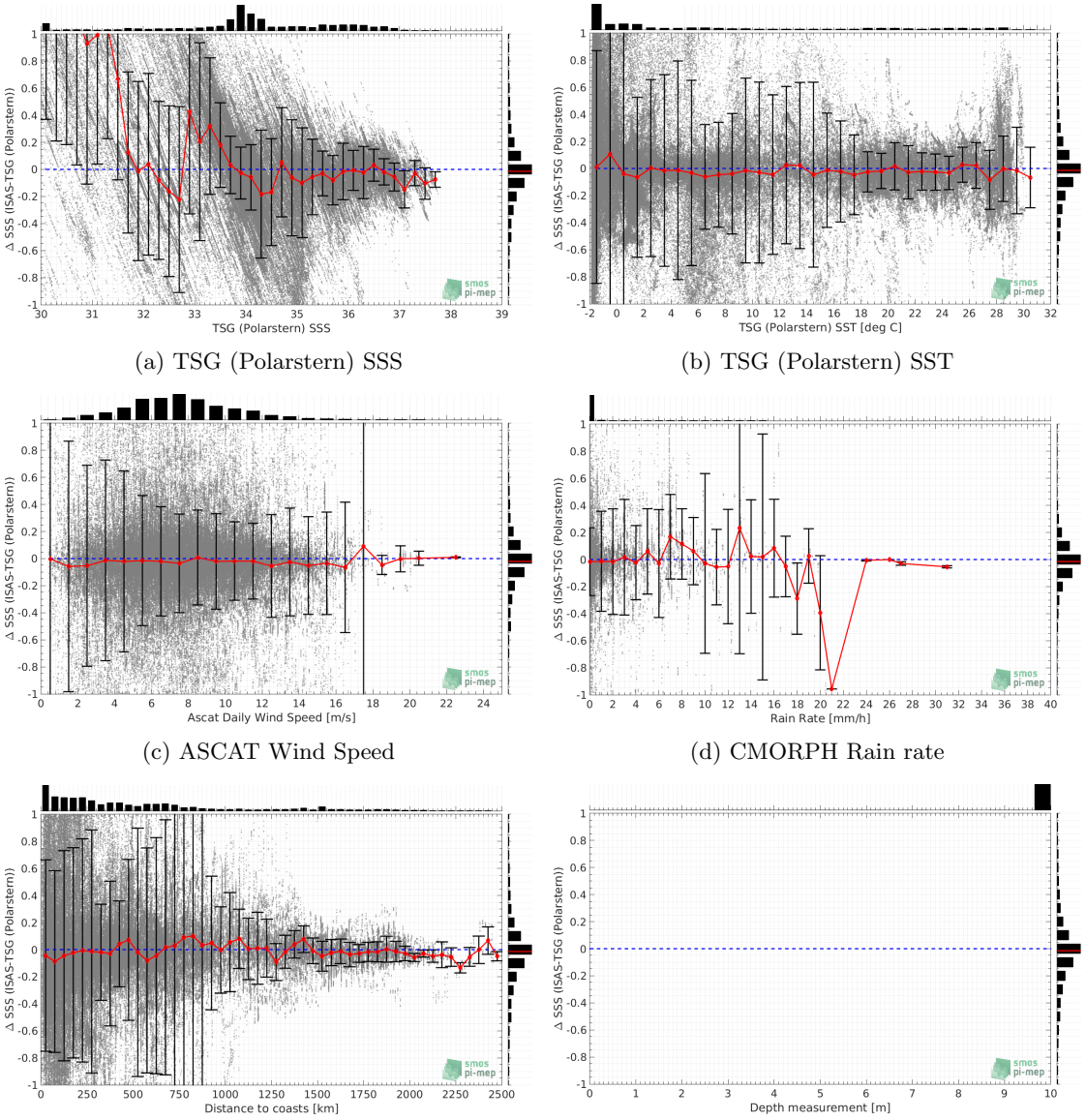

(a) TSG (Polarstern) SSS

(b) TSG (Polarstern) SST

(c) ASCAT Wind Speed

(d) CMORPH Rain rate

(e) Distance to coast

(f) Depth

Figure 84: Δ SSS (ISAS - TSG (Polarstern)) sorted as geophysical conditions: TSG (Polarstern) SSS a), TSG (Polarstern) SST b), ASCAT Wind speed c), CMORPH rain rate d), distance to coast (e) and depth measurements (f).

2.7.12 ΔSSS maps and statistics for different geophysical conditions

In Figures 85 and 86, we focus on sub-datasets of the match-up differences ΔSSS (ISAS - *in situ*) for the following specific geophysical conditions:

- **C1**:if the local value at *in situ* location of estimated rain rate is zero, mean daily wind is in the range [3, 12] m/s, the SST is $> 5°$C and distance to coast is > 800 km.
- **C2**:if the local value at *in situ* location of estimated rain rate is zero, mean daily wind is

in the range [3, 12] m/s.

- **C3**:if the local value at *in situ* location of estimated rain rate is high (ie. $>$ 1 mm/h) and mean daily wind is low (ie. $<$ 4 m/s).
- **C5**:if the *in situ* data is located where the climatological SSS standard deviation is low (ie. above $<$ 0.2).
- **C6**:if the *in situ* data is located where the climatological SSS standard deviation is high (ie. above $>$ 0.2).

For each of these conditions, the temporal mean (gridded over spatial boxes of size 1°x1°) and the histogram of the difference ΔSSS (ISAS - *in situ*) are presented.

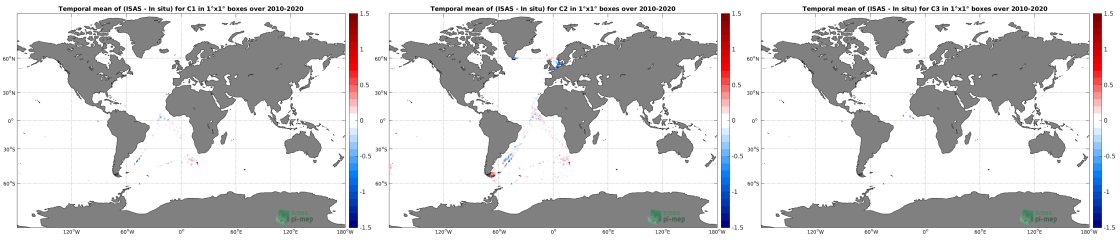

(a) RR=0 mm/h, 3< U_{10} <12 m/s, SST>5°C, distance to coast > 800 km (b) RR=0 mm/h, 3< U_{10} <12 m/s (c) RR>1mm/h and U_{10} <4m/s

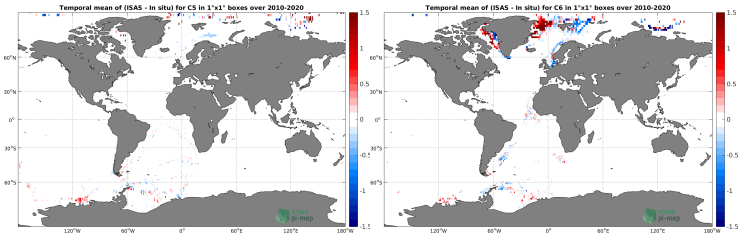

(d) WOA2013 SSS Std<0.2 (e) WOA2013 SSS Std>0.2

Figure 85: Temporal mean gridded over spatial boxes of size 1°x1° of ΔSSS (ISAS - TSG (Polarstern)) for 5 different subdatasets corresponding to:RR=0 mm/h, 3< U_{10} <12 m/s, SST>5°C, distance to coast > 800 km (a), RR=0 mm/h, 3< U_{10} <12 m/s (b), RR>1mm/h and U_{10} <4m/s (c),WOA2013 SSS Std<0.2 (d),WOA2013 SSS Std>0.2 (e).

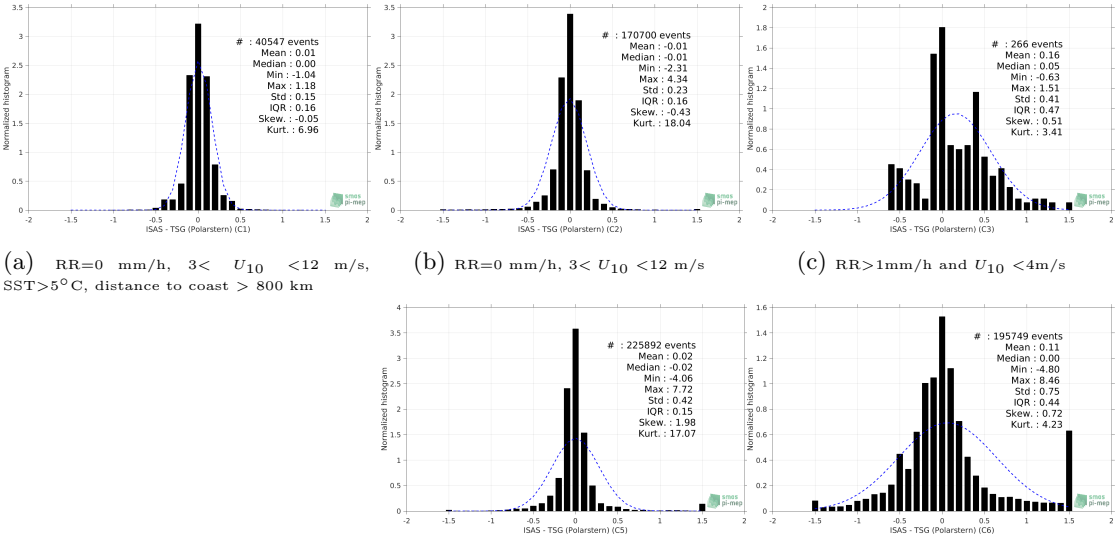

(a) RR=0 mm/h, 3< U_{10} <12 m/s, SST>5°C, distance to coast > 800 km (b) RR=0 mm/h, 3< U_{10} <12 m/s (c) RR>1mm/h and U_{10} <4m/s

(d) WOA2013 SSS Std<0.2 (e) WOA2013 SSS Std>0.2

Figure 86: Normalized histogram of ΔSSS (ISAS - TSG (Polarstern)) for 5 different subdatasets corresponding to:RR=0 mm/h, 3< U_{10} <12 m/s, SST>5°C, distance to coast > 800 km (a), RR=0 mm/h, 3< U_{10} <12 m/s (b), RR>1mm/h and U_{10} <4m/s (c),WOA2013 SSS Std<0.2 (d),WOA2013 SSS Std>0.2 (e).

2.7.13 Summary

Table 1 shows the mean, median, standard deviation (Std), root mean square (RMS), interquartile range (IQR), correlation coefficient (r^2) and robust standard deviation (Std*) of the match-up differences ΔSSS (ISAS - TSG (Polarstern)) for the following conditions:

- all: All the match-up pairs satellite/in situ SSS values are used to derive the statistics
- C1: only pairs where RR=0 mm/h, 3< U_{10} <12 m/s, SST>5°C, distance to coast > 800 km
- C2: only pairs where RR=0 mm/h, 3< U_{10} <12 m/s
- C3: only pairs where RR>1mm/h and U_{10} <4m/s
- C5: only pairs where WOA2013 SSS Std<0.2
- C6: only pairs where WOA2013 SSS Std>0.2
- C7a: only pairs with a distance to coast < 150 km.
- C7b: only pairs with a distance to coast in the range [150, 800] km.
- C7c: only pairs with a distance to coast > 800 km.
- C8a: only pairs where SST is < 5°C.
- C8b: only pairs where SST is in the range [5, 15]°C.
- C8c: only pairs where SST is > 15°C.

- C9a: only pairs where SSS is < 33.
- C9b: only pairs where SSS is in the range [33, 37].
- C9c: only pairs where SSS is > 37.

Table 1: Statistics of ΔSSS (ISAS - TSG (Polarstern))

Condition	#	Median	Mean	Std	RMS	IQR	r^2	Std*
all	499487	-0.01	0.11	0.77	0.77	0.27	0.830	0.20
C1	40547	0.00	0.01	0.15	0.15	0.16	0.973	0.12
C2	170700	-0.01	-0.01	0.23	0.23	0.16	0.956	0.12
C3	266	0.05	0.16	0.41	0.44	0.47	0.878	0.37
C5	225892	-0.02	0.02	0.42	0.42	0.15	0.912	0.11
C6	195749	0.00	0.11	0.75	0.76	0.44	0.826	0.33
C7a	131773	-0.05	0.03	0.72	0.72	0.40	0.809	0.31
C7b	257674	0.00	0.16	0.85	0.86	0.30	0.809	0.22
C7c	110003	-0.01	0.08	0.59	0.59	0.16	0.882	0.12
C8a	288338	0.00	0.21	0.95	0.97	0.40	0.662	0.28
C8b	69242	-0.04	-0.05	0.56	0.57	0.26	0.687	0.19
C8c	105979	-0.02	-0.02	0.21	0.21	0.18	0.904	0.13
C9a	85630	0.59	0.94	1.45	1.73	1.85	0.244	1.19
C9b	409548	-0.03	-0.06	0.31	0.32	0.22	0.914	0.16
C9c	4309	-0.09	-0.11	0.13	0.17	0.20	0.744	0.15

Table 1 numerical values can be downloaded as a csv file here.

2.8 TSG (NCEI-0170743)

2.8.1 Introduction

The TSG-NCEI-0170743 dataset (Aulicino et al. (2018)) contains sea surface temperature and salinity data collected from 2010 to 2017 in the South Atlantic Ocean and Southern Ocean from S.A. Agulhas and Agulhas-II research vessels, in the framework of South African National Antarctic Programme (SANAP), South African Department of Environmental Affairs (DEA) and Italian National Antarctic Research Programme (PNRA) scientific activities. Measurements have been obtained through thermosalinograph (TSG) during several cruises to both Antarctica and sub-Antarctic islands. On-board TSG devices have been regularly calibrated and continuously monitored in-between cruises; no appreciable sensor drift emerged. Independent water samples taken along the cruises have been used to validate the data; salinity measurement error was a few hundredths of a unit on the practical salinity scale. A careful quality control allowed to discard bad data for each single campaign.

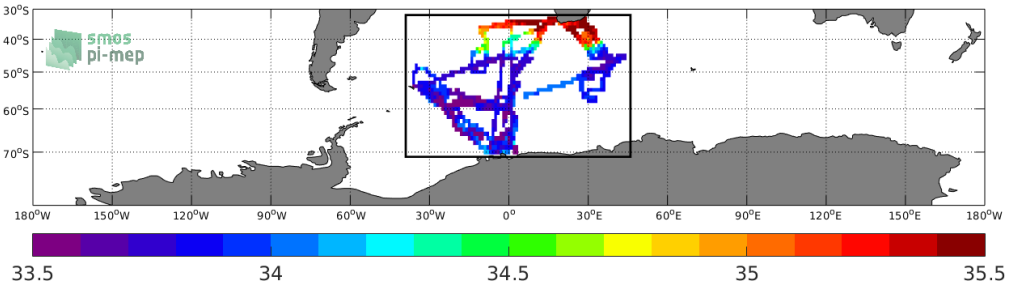

Figure 87: Location of the TSG (NCEI-0170743) dataset.

2.8.2 Number of SSS data as a function of time and distance to coast

Figure 88 shows the time (a) and distance to coast (b) distributions of the TSG (NCEI-0170743) *in situ* dataset.

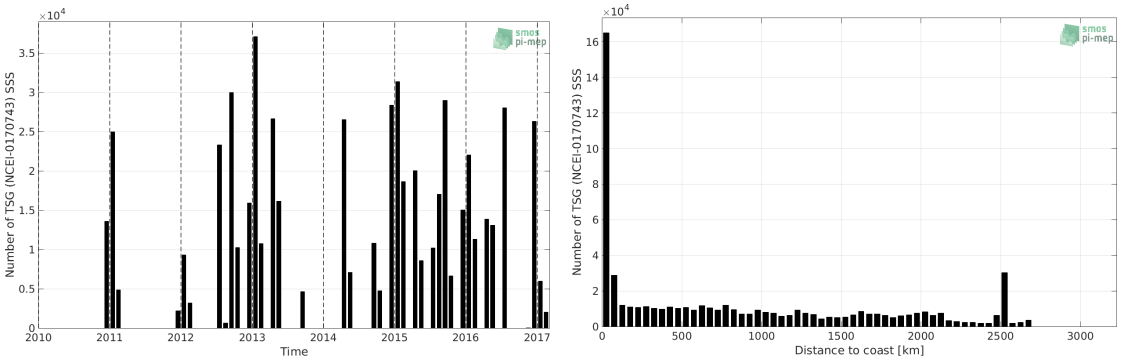

(a) (b)

Figure 88: Number of SSS from TSG (NCEI-0170743) as a function of time (a) and distance to coast (b).

2.8.3 Histograms of SSS

Figure 89 shows the SSS distribution of the TSG (NCEI-0170743) (a) and colocalized ISAS (b) dataset.

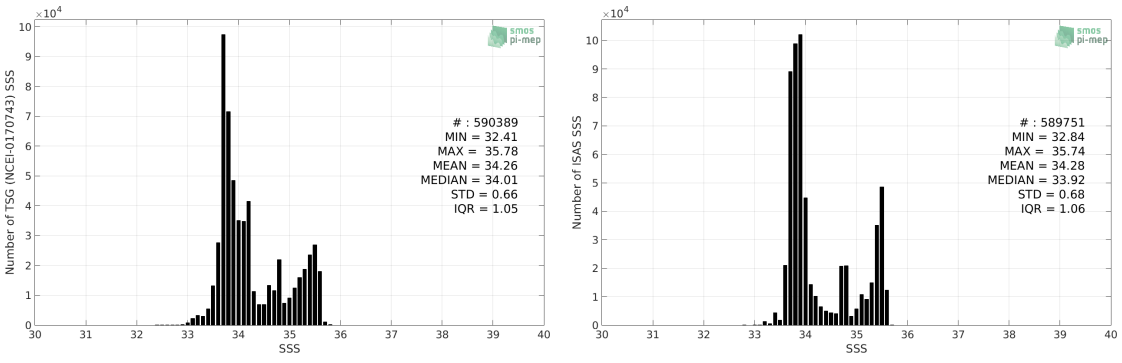

(a) (b)

Figure 89: Histograms of SSS from TSG (NCEI-0170743) (a) and ISAS (b) per bins of 0.1.

2.8.4 Distribution of *in situ* SSS depth measurements

In Figure 90, we show the depth distribution of the *in situ* salinity dataset (a) and the spatial distribution of the depth temporal mean in 1°x1° boxes and considering the full *in situ* dataset period (b).

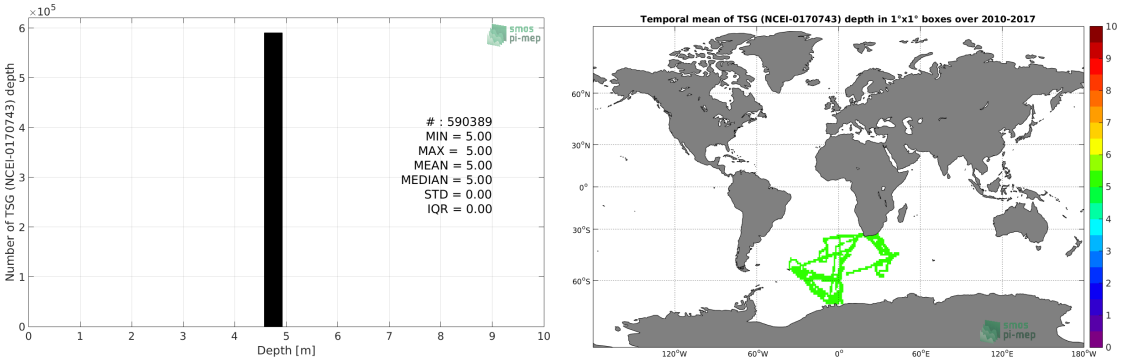

(a) (b)

Figure 90: Depth distribution of the upper level SSS measurements from TSG (NCEI-0170743) (a) and spatial distribution of the *in situ* SSS depth measurements showing the mean value in 1°x1° boxes and considering the full *in situ* dataset period (b).

2.8.5 Spatial distribution of SSS

In Figure 91, the number of TSG (NCEI-0170743) SSS measurements in 1°x1° boxes is shown.

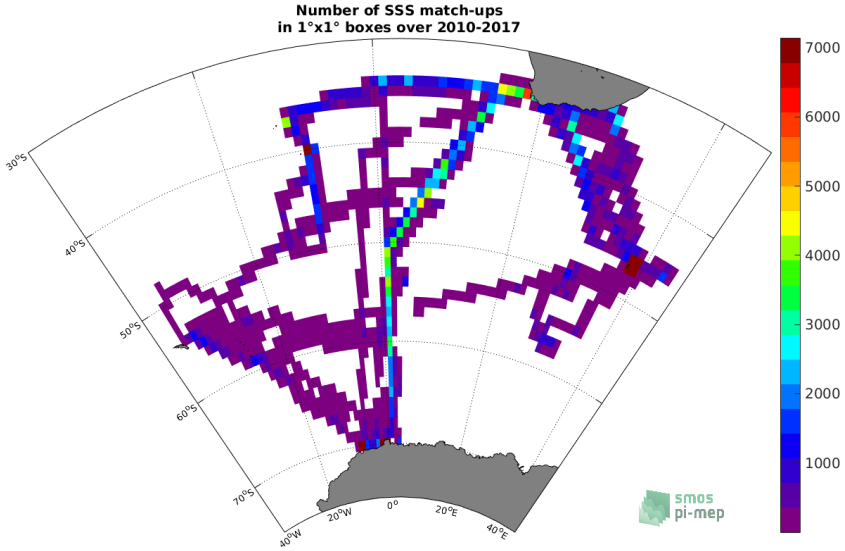

Figure 91: Number of SSS from TSG (NCEI-0170743) in 1°x1° boxes.

2.8.6 Spatial Maps of the Temporal mean and Std of *in situ* and ISAS SSS and of the difference (ΔSSS)

In Figure 92, maps of temporal mean (left) and standard deviation (right) of ISAS (top), TSG (NCEI-0170743) *in situ* dataset (middle) and the difference ΔSSS(ISAS -TSG (NCEI-0170743)) (bottom) are shown. The temporal mean and std are calculated using all match-up pairs falling in spatial boxes of size 1°x1° over the full TSG (NCEI-0170743) dataset period.

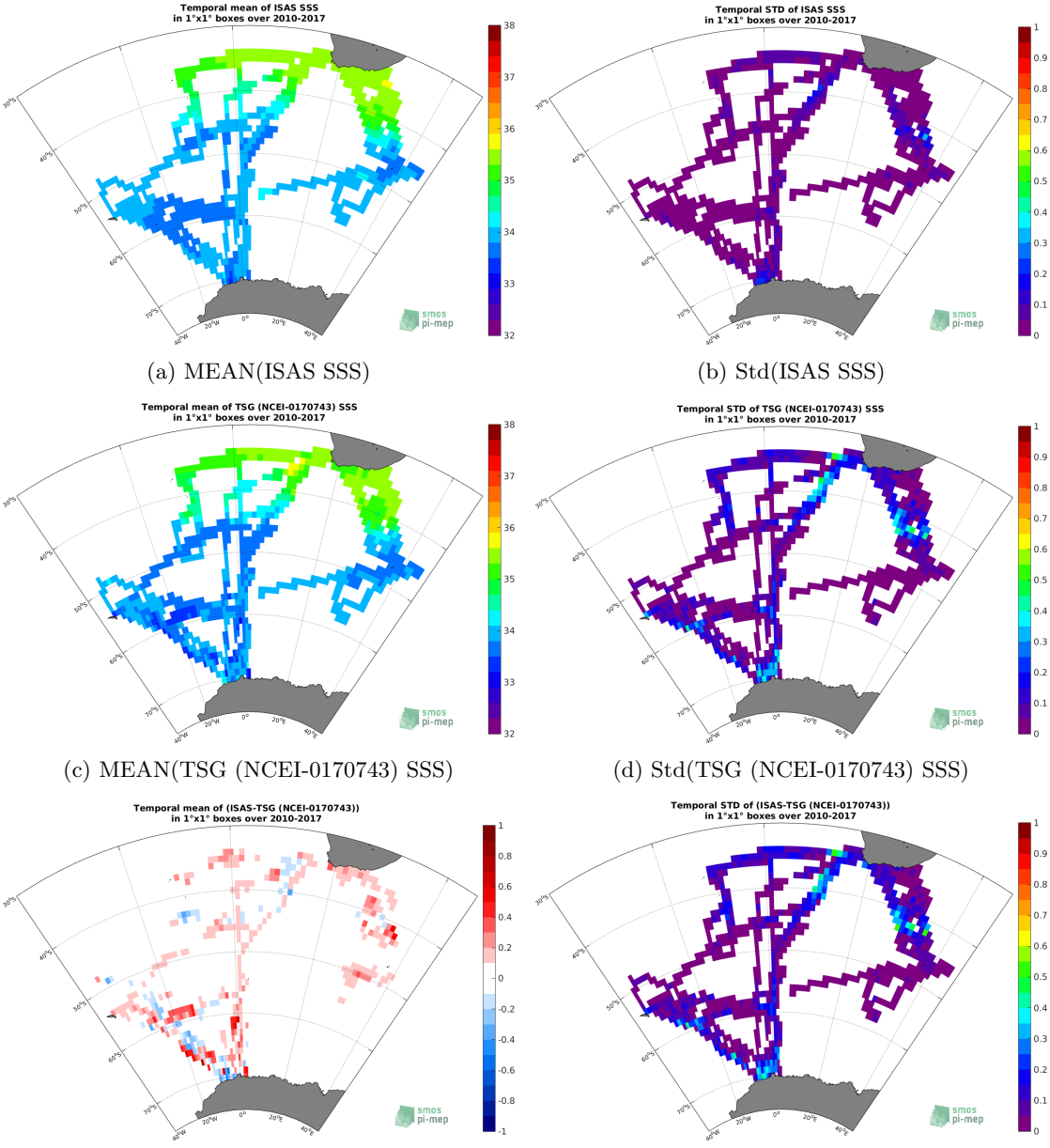

(a) MEAN(ISAS SSS)

(b) Std(ISAS SSS)

(c) MEAN(TSG (NCEI-0170743) SSS)

(d) Std(TSG (NCEI-0170743) SSS)

(e) MEAN(ΔSSS) (ISAS - TSG (NCEI-0170743))

(f) Std(ΔSSS) (ISAS - TSG (NCEI-0170743))

Figure 92: Temporal mean (left) and Std (right) of SSS from ISAS (top), TSG (NCEI-0170743) (middle), and of ΔSSS (ISAS - TSG (NCEI-0170743)). Only match-up pairs are used to generate these maps.

2.8.7 Time series of the monthly median and Std of *in situ* and ISAS SSS and of the difference (ΔSSS)

In the top panel of Figure 93, we show the time series of the monthly median SSS estimated for both ISAS SSS product (in black) and the TSG (NCEI-0170743) *in situ* dataset (in blue) at the collected Pi-MEP match-up pairs.

In the middle panel of Figure 93, we show the time series of the monthly median of ΔSSS (ISAS - TSG (NCEI-0170743)) for the collected Pi-MEP match-up pairs.

In the bottom panel of Figure 93, we show the time series of the monthly standard deviation of the ΔSSS (ISAS - TSG (NCEI-0170743)) for the collected Pi-MEP match-up pairs.

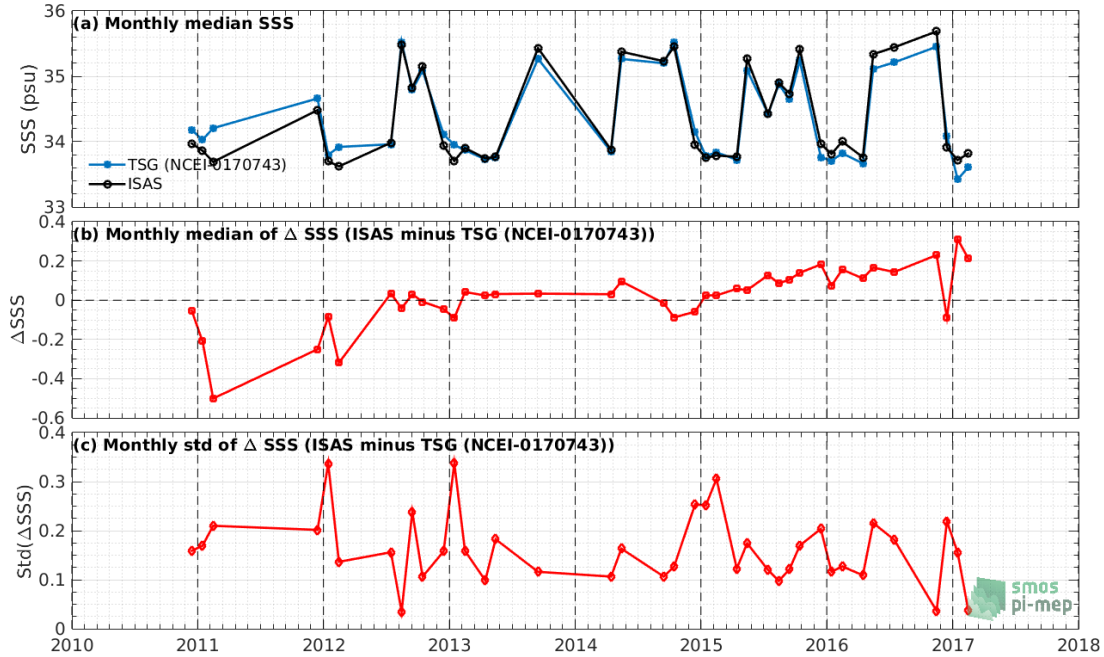

Figure 93: Time series of the monthly median SSS (top), median of ΔSSS (ISAS - TSG (NCEI-0170743)) and Std of ΔSSS (ISAS - TSG (NCEI-0170743)) considering all match-ups collected by the Pi-MEP.

2.8.8 Zonal mean and Std of *in situ* and ISAS SSS and of the difference ΔSSS

In Figure 94 left panel, we show the zonal mean SSS considering all Pi-MEP match-up pairs for both ISAS SSS product (in black) and the TSG (NCEI-0170743) *in situ* dataset (in blue). The full *in situ* dataset period is used to derive the mean.

In the right panel of Figure 94, we show the zonal mean of ΔSSS (ISAS - TSG (NCEI-0170743)) for all the collected Pi-MEP match-up pairs estimated over the full *in situ* dataset period.

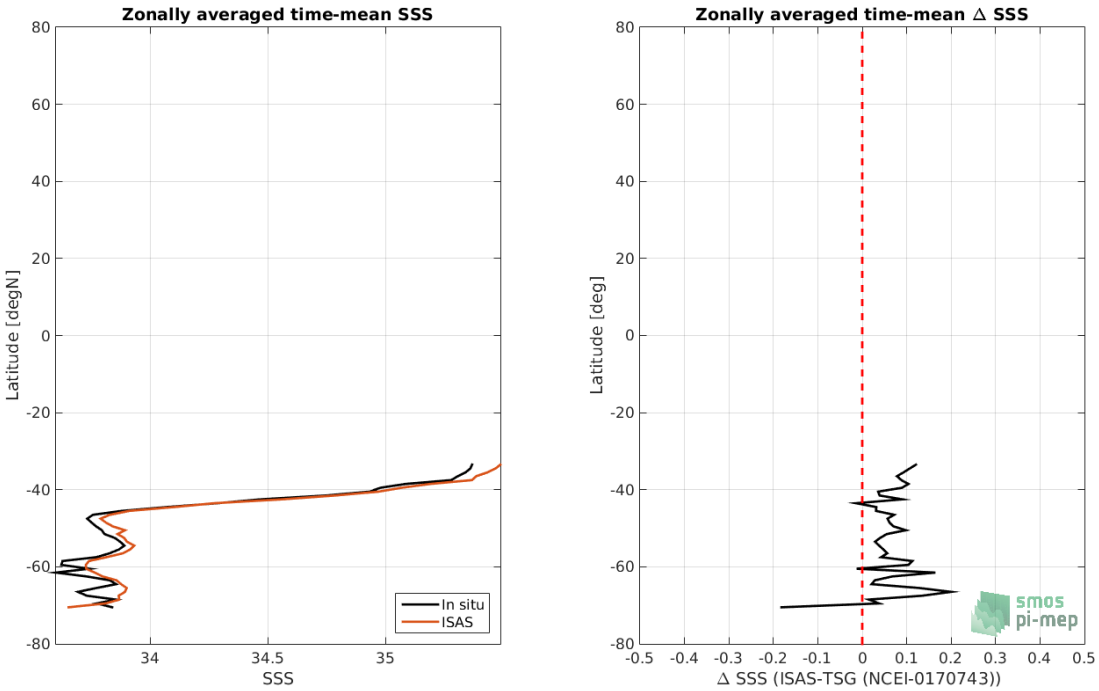

Figure 94: Left panel: Zonal mean SSS from ISAS product (black) and from TSG (NCEI-0170743) (blue). Right panel: Zonal mean of ΔSSS (ISAS - TSG (NCEI-0170743)) for all the collected Pi-MEP match-up pairs estimated over the full *in situ* dataset period.

2.8.9 Scatterplots of ISAS vs *in situ* SSS by latitudinal bands

In Figure 95, contour maps of the concentration of ISAS SSS (y-axis) versus TSG (NCEI-0170743) SSS (x-axis) at match-up pairs for different latitude bands: (a) 80°S-80°N, (b) 20°S-20°N, (c) 40°S-20°S and 20°N-40°N and (d) 60°S-40°S and 40°N-60°N. For each plot, the red line shows x=y. The black thin and dashed lines indicate a linear fit through the data cloud and the ±95% confidence levels, respectively. The number match-up pairs n, the slope and R^2 coefficient of the linear fit, the root mean square (RMS) and the mean bias between ISAS and *in situ* data are indicated for each latitude band in each plots.

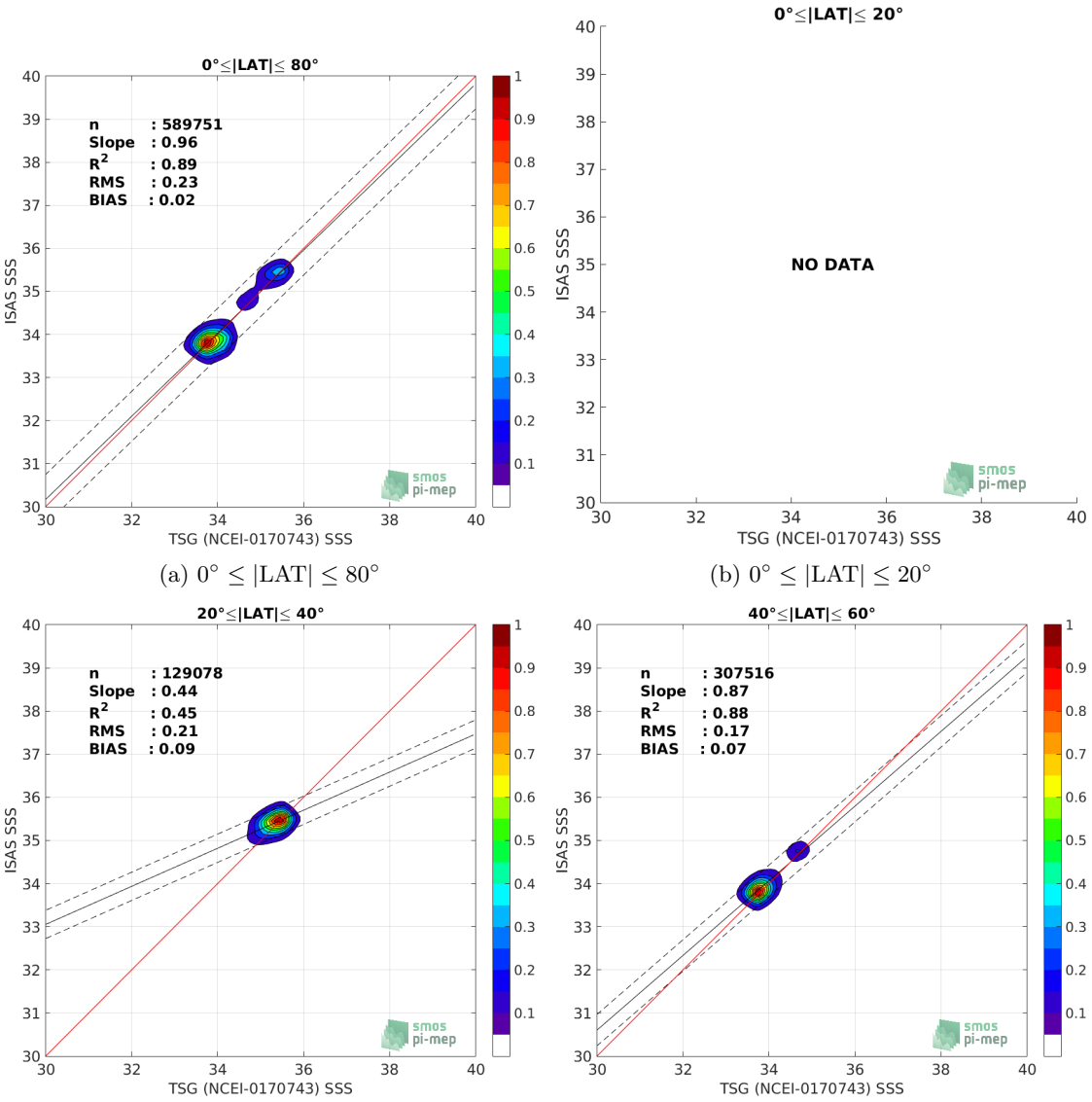

(a) $0° \leq |\text{LAT}| \leq 80°$

(b) $0° \leq |\text{LAT}| \leq 20°$

(c) $20° \leq |\text{LAT}| \leq 40°$

(d) $40° \leq |\text{LAT}| \leq 60°$

Figure 95: Contour maps of the concentration of ISAS SSS (y-axis) versus TSG (NCEI-0170743) SSS (x-axis) at match-up pairs for different latitude bands. For each plot, the red line shows x=y. The black thin and dashed lines indicate a linear fit through the data cloud and the ±95% confidence levels, respectively. The number match-up pairs n, the slope and R^2 coefficient of the linear fit, the root mean square (RMS) and the mean bias between ISAS and *in situ* data are indicated for each latitude band in each plots.

2.8.10 Time series of the monthly median and Std of the difference ΔSSS sorted by latitudinal bands

In Figure 96, time series of the monthly median (red curves) of ΔSSS (ISAS - TSG (NCEI-0170743)) and ±1 Std (black vertical thick bars) as function of time for all the collected Pi-MEP

match-up pairs estimated for the full *in situ* dataset period are shown for different latitude bands: (a) 80°S-80°N, (b) 20°S-20°N, (c) 40°S-20°S and 20°N-40°N and (d) 60°S-40°S and 40°N-60°N.

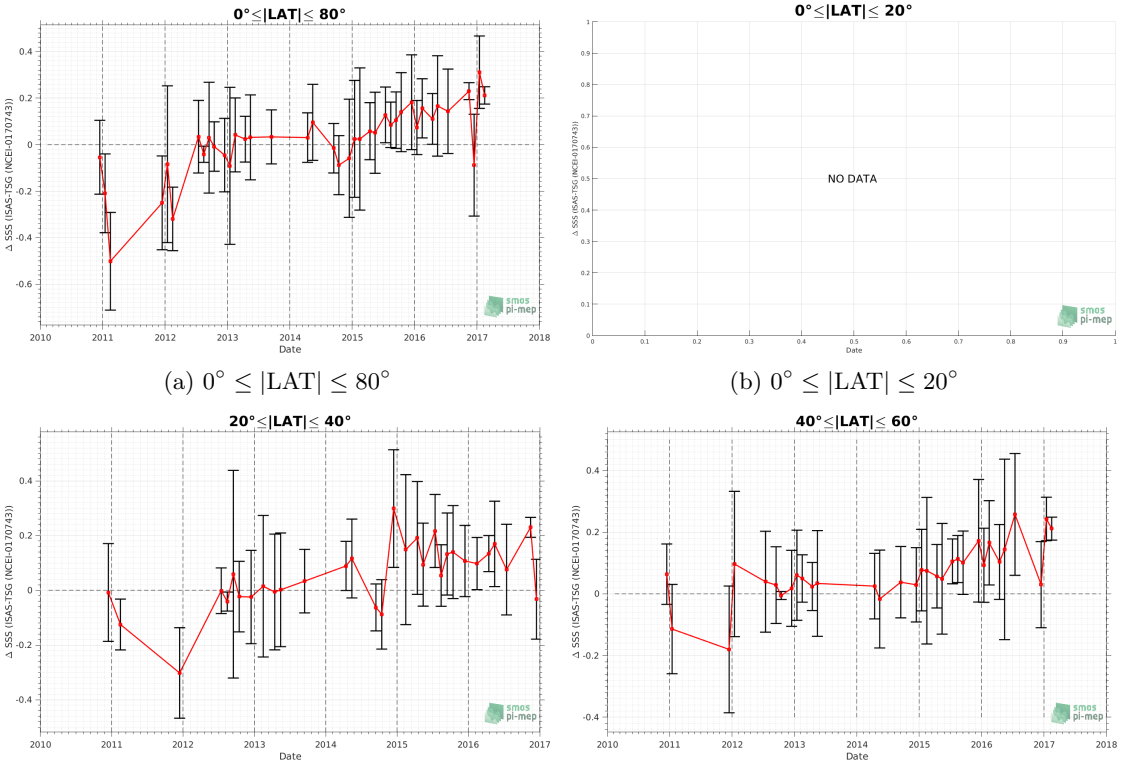

(a) $0° \leq |\text{LAT}| \leq 80°$

(b) $0° \leq |\text{LAT}| \leq 20°$

(c) $20° \leq |\text{LAT}| \leq 40°$

(d) $40° \leq |\text{LAT}| \leq 60°$

Figure 96: Monthly median (red curves) of ΔSSS (ISAS - TSG (NCEI-0170743)) and ±1 Std (black vertical thick bars) as function of time for all the collected Pi-MEP match-up pairs for the full *in situ* dataset period are shown for different latitude bands: (a) 80°S-80°N, (b) 20°S-20°N, (c) 40°S-20°S and 20°N-40°N and (d) 60°S-40°S and 40°N-60°N.

2.8.11 ΔSSS sorted as geophysical conditions

In Figure 97, we classify the match-up differences ΔSSS (ISAS - *in situ*) as function of the geophysical conditions at match-up points. The mean and std of ΔSSS (ISAS - TSG (NCEI-0170743)) is thus evaluated as function of the

- *in situ* SSS values per bins of width 0.2,
- *in situ* SST values per bins of width 1°C,
- ASCAT daily wind values per bins of width 1 m/s,
- CMORPH 3-hourly rain rates per bins of width 1 mm/h, and,
- distance to coasts per bins of width 50 km,
- *in situ* measurement depth (if relevant).

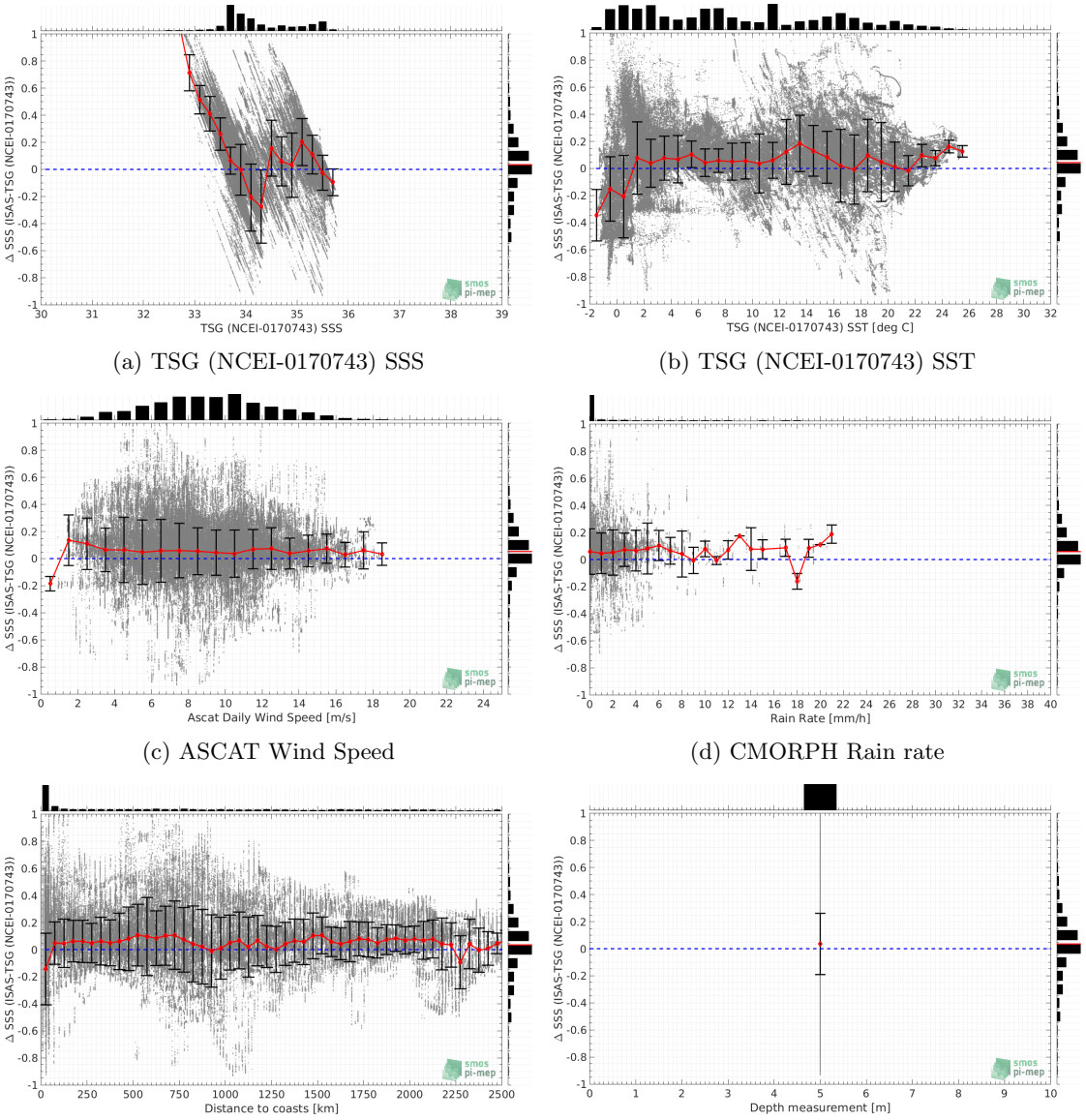

(a) TSG (NCEI-0170743) SSS

(b) TSG (NCEI-0170743) SST

(c) ASCAT Wind Speed

(d) CMORPH Rain rate

(e) Distance to coast

(f) Depth

Figure 97: Δ SSS (ISAS - TSG (NCEI-0170743)) sorted as geophysical conditions: TSG (NCEI-0170743) SSS a), TSG (NCEI-0170743) SST b), ASCAT Wind speed c), CMORPH rain rate d), distance to coast (e) and depth measurements (f).

2.8.12 ΔSSS maps and statistics for different geophysical conditions

In Figures 98 and 99, we focus on sub-datasets of the match-up differences ΔSSS (ISAS - *in situ*) for the following specific geophysical conditions:

- **C1**:if the local value at *in situ* location of estimated rain rate is zero, mean daily wind is in the range [3, 12] m/s, the SST is $> 5°$C and distance to coast is > 800 km.
- **C2**:if the local value at *in situ* location of estimated rain rate is zero, mean daily wind is

in the range [3, 12] m/s.

- **C3**:if the local value at *in situ* location of estimated rain rate is high (ie. $>$ 1 mm/h) and mean daily wind is low (ie. $<$ 4 m/s).
- **C5**:if the *in situ* data is located where the climatological SSS standard deviation is low (ie. above $<$ 0.2).
- **C6**:if the *in situ* data is located where the climatological SSS standard deviation is high (ie. above $>$ 0.2).

For each of these conditions, the temporal mean (gridded over spatial boxes of size 1°x1°) and the histogram of the difference ΔSSS (ISAS - *in situ*) are presented.

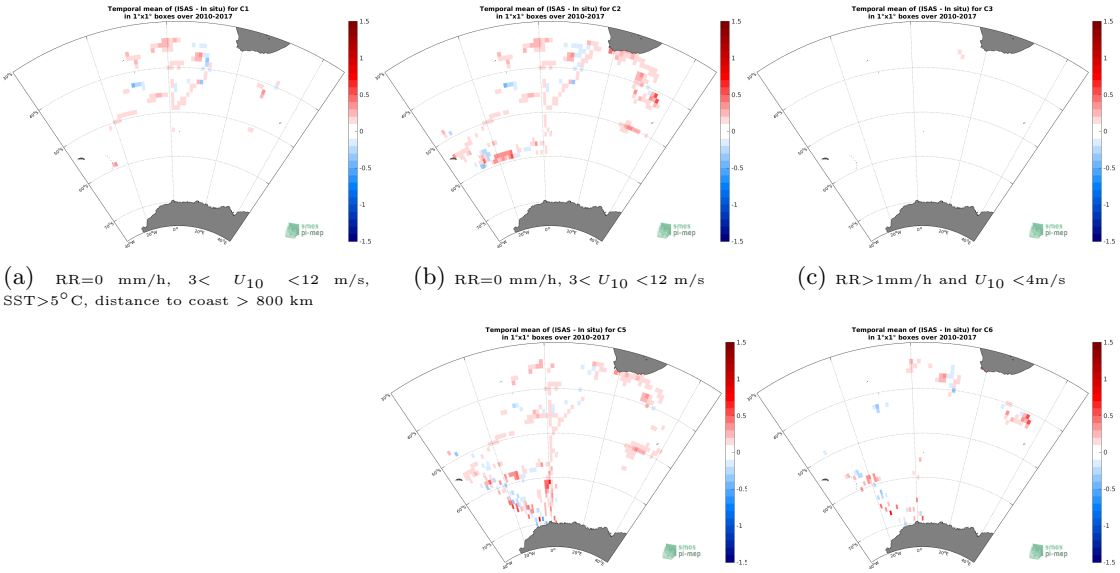

(a) RR=0 mm/h, 3< U_{10} <12 m/s, SST>5°C, distance to coast > 800 km (b) RR=0 mm/h, 3< U_{10} <12 m/s (c) RR>1mm/h and U_{10} <4m/s

(d) WOA2013 SSS Std<0.2 (e) WOA2013 SSS Std>0.2

Figure 98: Temporal mean gridded over spatial boxes of size 1°x1° of ΔSSS (ISAS - TSG (NCEI-0170743)) for 5 different subdatasets corresponding to:RR=0 mm/h, 3< U_{10} <12 m/s, SST>5°C, distance to coast > 800 km (a), RR=0 mm/h, 3< U_{10} <12 m/s (b), RR>1mm/h and U_{10} <4m/s (c),WOA2013 SSS Std<0.2 (d),WOA2013 SSS Std>0.2 (e).

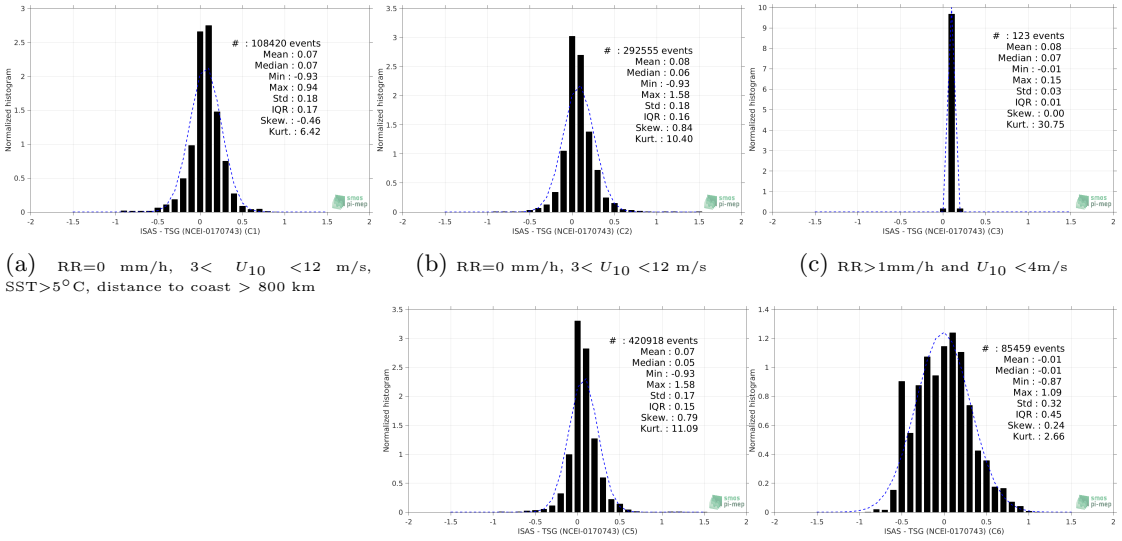

(a) RR=0 mm/h, 3< U_{10} <12 m/s, SST>5°C, distance to coast > 800 km (b) RR=0 mm/h, 3< U_{10} <12 m/s (c) RR>1mm/h and U_{10} <4m/s

(d) WOA2013 SSS Std<0.2 (e) WOA2013 SSS Std>0.2

Figure 99: Normalized histogram of ΔSSS (ISAS - TSG (NCEI-0170743)) for 5 different sub-datasets corresponding to:RR=0 mm/h, 3< U_{10} <12 m/s, SST>5°C, distance to coast > 800 km (a), RR=0 mm/h, 3< U_{10} <12 m/s (b), RR>1mm/h and U_{10} <4m/s (c),WOA2013 SSS Std<0.2 (d),WOA2013 SSS Std>0.2 (e).

2.8.13 Summary

Table 1 shows the mean, median, standard deviation (Std), root mean square (RMS), interquartile range (IQR), correlation coefficient (r^2) and robust standard deviation (Std*) of the match-up differences ΔSSS (ISAS - TSG (NCEI-0170743)) for the following conditions:

- all: All the match-up pairs satellite/in situ SSS values are used to derive the statistics
- C1: only pairs where RR=0 mm/h, 3< U_{10} <12 m/s, SST>5°C, distance to coast > 800 km
- C2: only pairs where RR=0 mm/h, 3< U_{10} <12 m/s
- C3: only pairs where RR>1mm/h and U_{10} <4m/s
- C5: only pairs where WOA2013 SSS Std<0.2
- C6: only pairs where WOA2013 SSS Std>0.2
- C7a: only pairs with a distance to coast < 150 km.
- C7b: only pairs with a distance to coast in the range [150, 800] km.
- C7c: only pairs with a distance to coast > 800 km.
- C8a: only pairs where SST is < 5°C.
- C8b: only pairs where SST is in the range [5, 15]°C.
- C8c: only pairs where SST is > 15°C.

- C9a: only pairs where SSS is < 33.
- C9b: only pairs where SSS is in the range [33, 37].
- C9c: only pairs where SSS is > 37.

Table 1: Statistics of ΔSSS (ISAS - TSG (NCEI-0170743))

Condition	#	Median	Mean	Std	RMS	IQR	r^2	Std*
all	589751	0.03	0.02	0.23	0.23	0.21	0.890	0.16
C1	108420	0.07	0.07	0.18	0.19	0.17	0.906	0.13
C2	292555	0.06	0.08	0.18	0.19	0.16	0.941	0.12
C3	123	0.07	0.08	0.03	0.09	0.01	1.000	0.01
C5	420918	0.05	0.07	0.17	0.18	0.15	0.943	0.11
C6	85459	-0.01	-0.01	0.32	0.32	0.45	0.792	0.34
C7a	205194	-0.01	-0.08	0.26	0.27	0.35	0.793	0.25
C7b	138113	0.07	0.09	0.21	0.23	0.22	0.932	0.16
C7c	246444	0.06	0.07	0.17	0.18	0.16	0.925	0.12
C8a	194461	0.00	-0.03	0.26	0.26	0.35	0.044	0.24
C8b	219434	0.06	0.08	0.15	0.17	0.13	0.919	0.09
C8c	124692	0.04	0.06	0.23	0.23	0.22	0.776	0.16
C9a	940	0.87	0.86	0.20	0.88	0.31	0.202	0.27
C9b	588811	0.03	0.02	0.22	0.22	0.21	0.892	0.15
C9c	0	NaN	NaN	NaN	NaN	NaN	NaN	NaN

Table 1 numerical values can be downloaded as a csv file here.

3 Summary

In the following summary section, some of the plots presented in the previous sections corresponding to the time distribution [3.1], SSS distribution [3.2], temporal mean [3.3] and std [3.4], and spatial density [3.5], are combined to emphasize similarities/differences between each *in situ* datasets.

3.1 Number of SSS data as a function of time

Figures 100 show the time distribution of the different TSG *in situ* datasets.

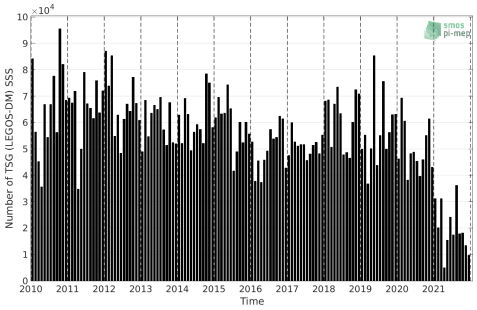

(a) TSG (LEGOS-DM)

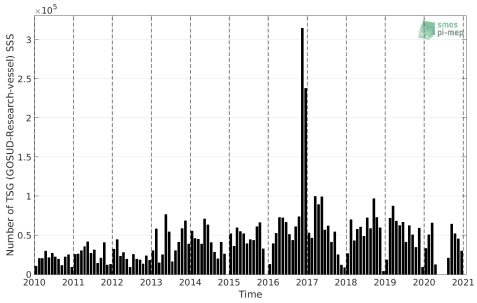

(b) TSG (GOSUD-Research-vessel)

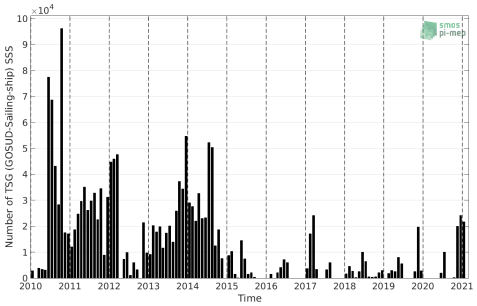

(c) TSG (GOSUD-Sailing-ship)

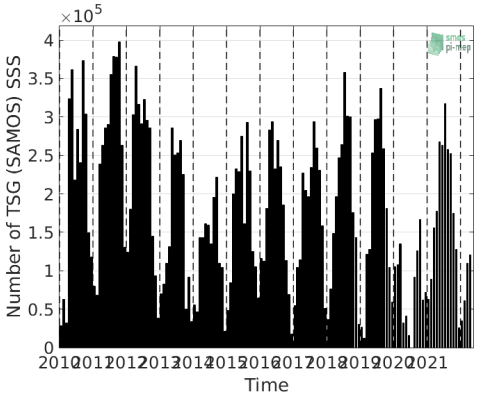

(d) TSG (SAMOS)

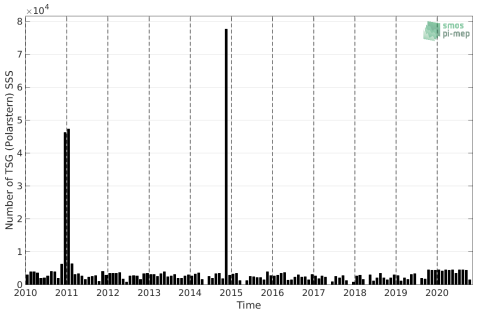

(e) TSG (Polarstern)

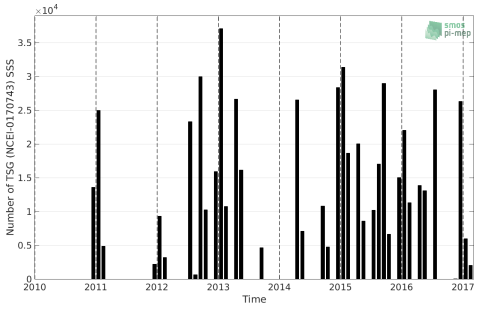

(f) TSG (NCEI-0170743)

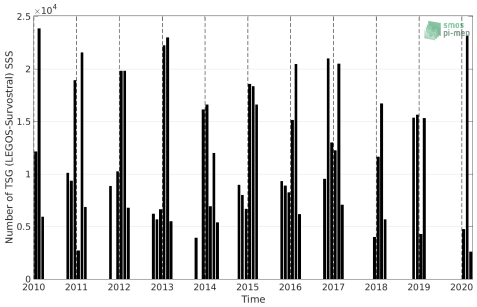

(g) TSG (LEGOS-Survostral)

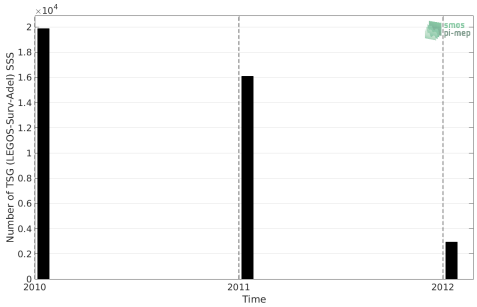

(h) TSG (LEGOS-Survostral-Adélie)

Figure 100: Number of SSS data as a function of time.

3.2 Histogram of SSS

Figures 101 show the SSS distribution of the different TSG *in situ* datasets.

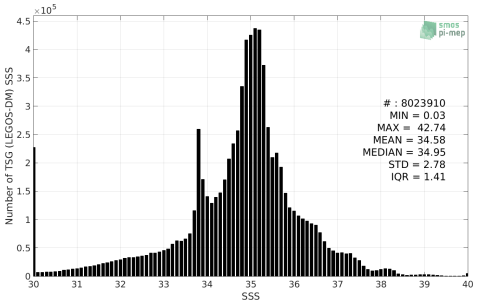

(a) TSG (LEGOS-DM)

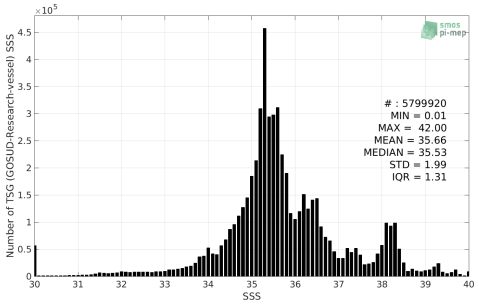

(b) TSG (GOSUD-Research-vessel)

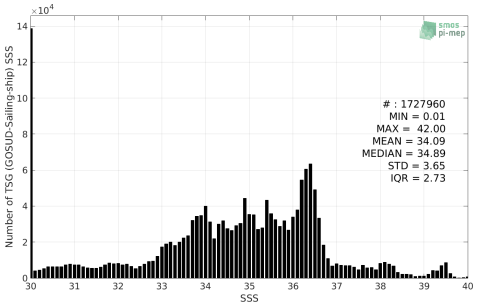

(c) TSG (GOSUD-Sailing-ship)

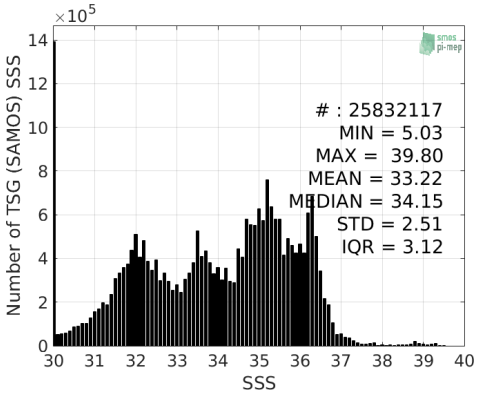

(d) TSG (SAMOS)

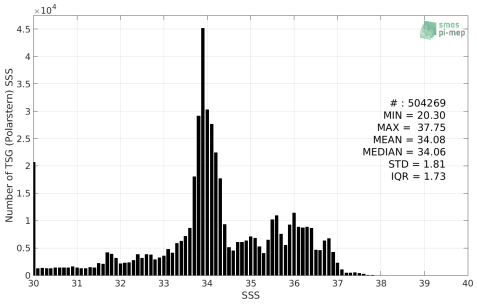

(e) TSG (Polarstern)

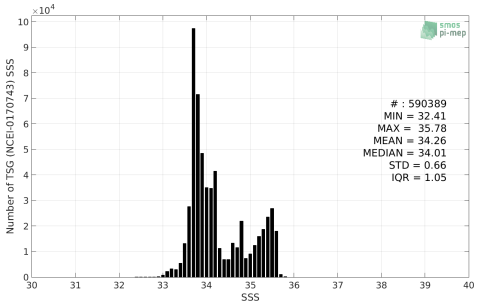

(f) TSG (NCEI-0170743)

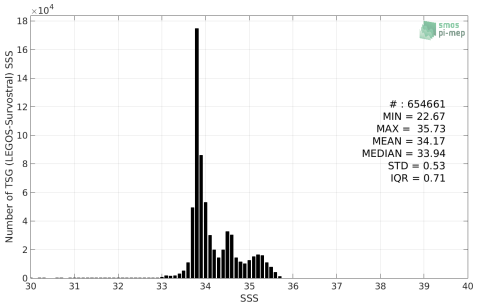

(g) TSG (LEGOS-Survostral)

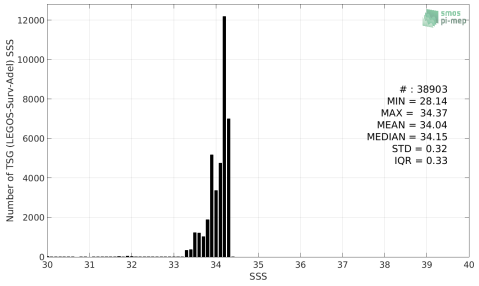

(h) TSG (LEGOS-Survostral-Adélie)

Figure 101: Distribution of SSS per bins of 0.1.

3.3 Temporal mean of SSS

Figures 102 show the temporal mean gridded over spatial boxes of size 1°x1° using the full period of each TSG *in situ* datasets.

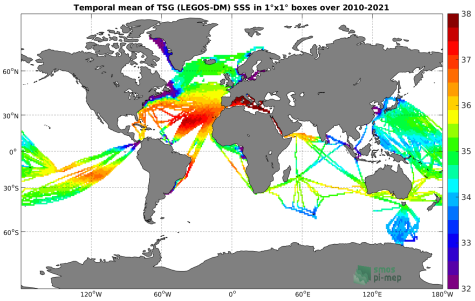

(a) TSG (LEGOS-DM)

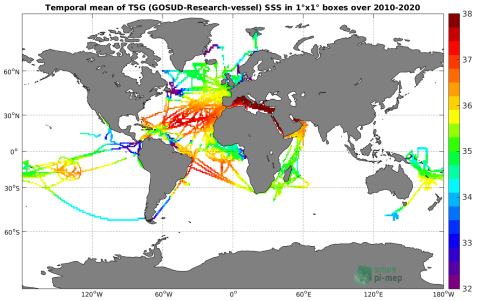

(b) TSG (GOSUD-Research-vessel)

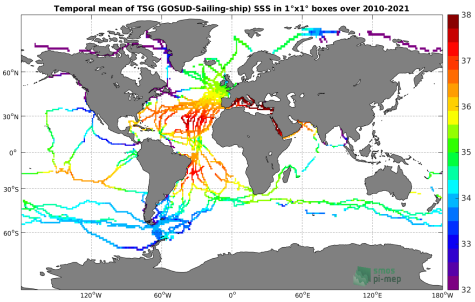

(c) TSG (GOSUD-Sailing-ship)

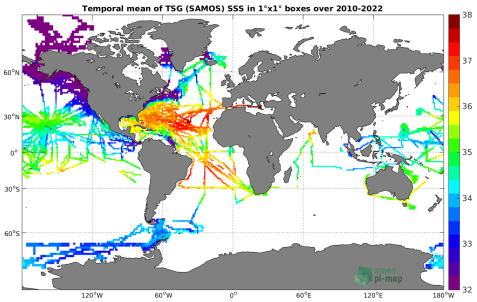

(d) TSG (SAMOS)

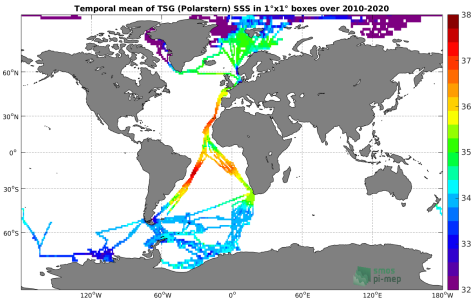

(e) TSG (Polarstern)

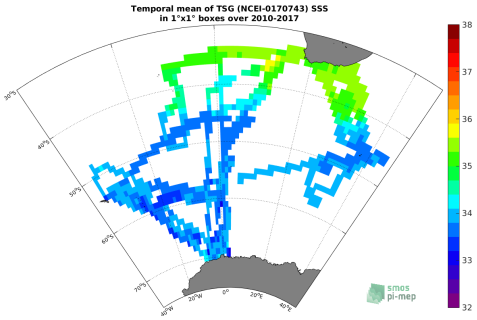

(f) TSG (NCEI-0170743)

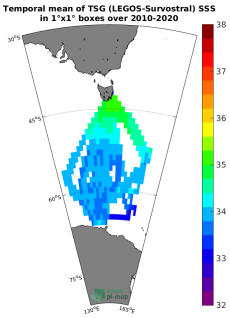

(g) TSG (LEGOS-Survostral)

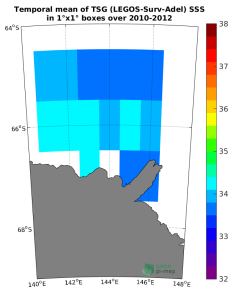

(h) TSG (LEGOS-Survostral-Adélie)

Figure 102: Temporal mean of SSS in 1°x1° boxes.

3.4 Temporal Std of SSS

Figures 103 show the temporal standard deviation (std) gridded over spatial boxes of size 1°x1° using the full period of each TSG *in situ* datasets.

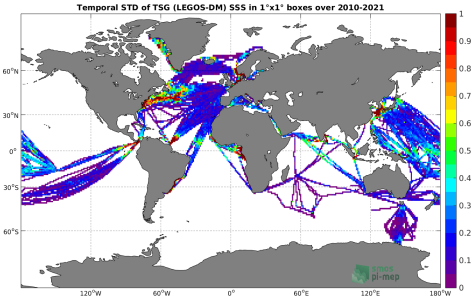

(a) TSG (LEGOS-DM)

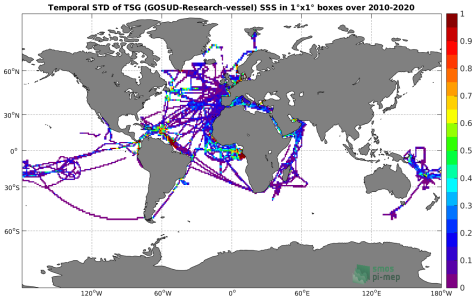

(b) TSG (GOSUD-Research-vessel)

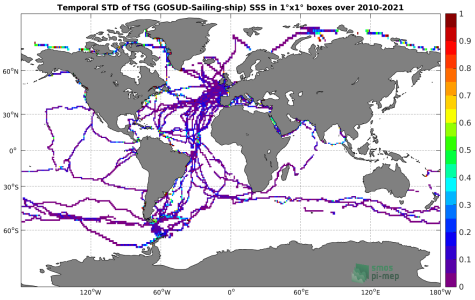

(c) TSG (GOSUD-Sailing-ship)

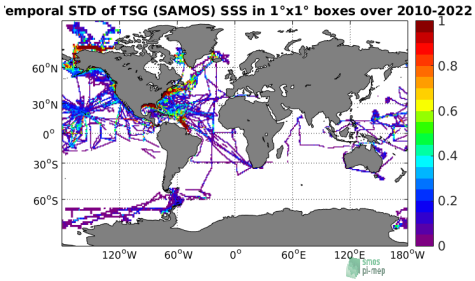

(d) TSG (SAMOS)

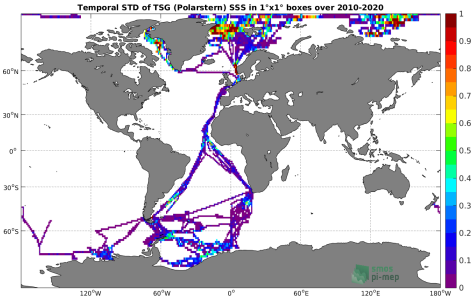

(e) TSG (Polarstern)

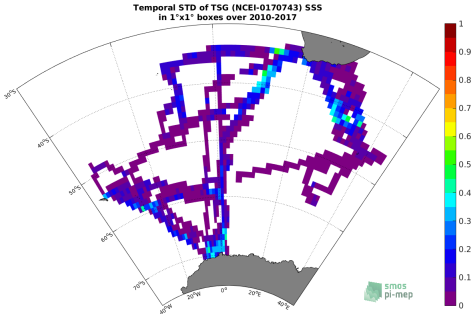

(f) TSG (NCEI-0170743)

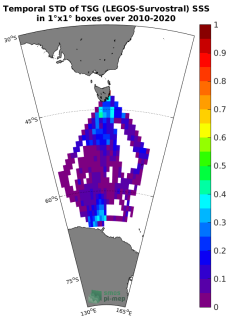

(g) TSG (LEGOS-Survostral)

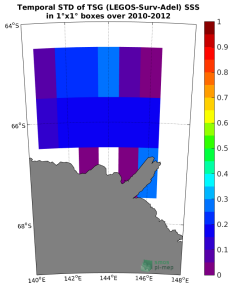

(h) TSG (LEGOS-Survostral-Adélie)

Figure 103: Temporal Std of SSS in 1°x1° boxes.

3.5 Spatial density of SSS

Figures 104 show the spatial distribution of SSS gridded over spatial boxes of size 1°x1° using the full period of each TSG *in situ* datasets.

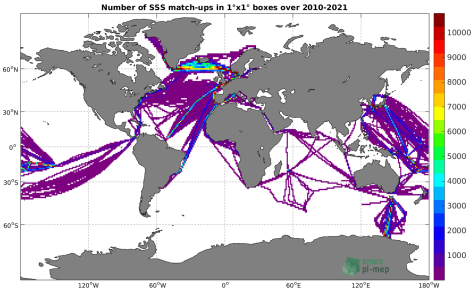

(a) TSG (LEGOS-DM)

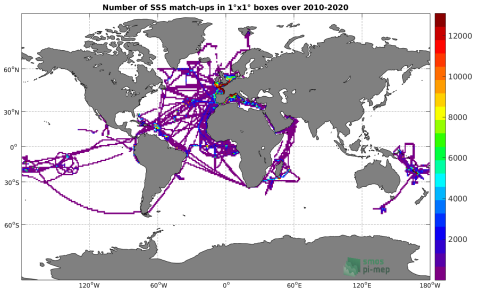

(b) TSG (GOSUD-Research-vessel)

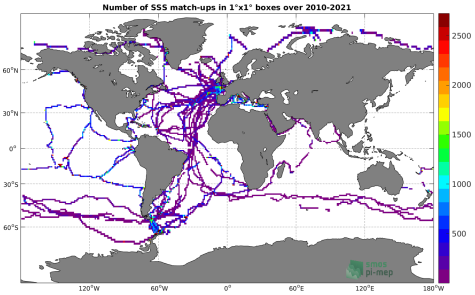

(c) TSG (GOSUD-Sailing-ship)

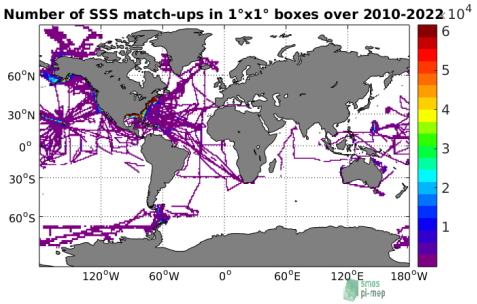

(d) TSG (SAMOS)

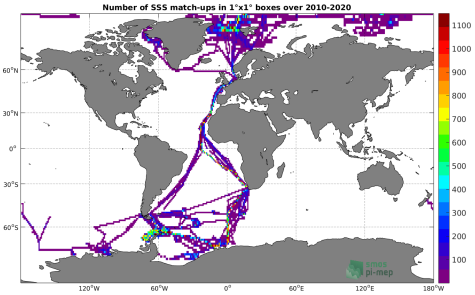

(e) TSG (Polarstern)

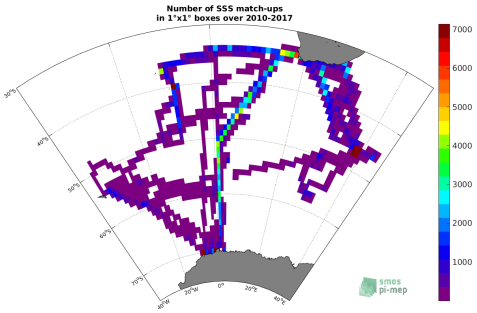

(f) TSG (NCEI-0170743)

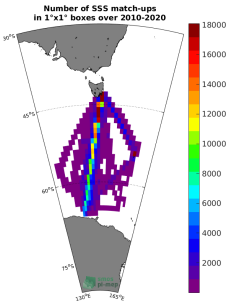

(g) TSG (LEGOS-Survostral)

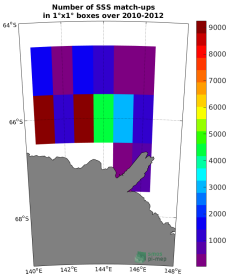

(h) TSG (LEGOS-Survostral-Adélie)

Figure 104: Number of SSS in 1°x1° boxes.

References

Gaël Alory, T. Delcroix, P. Téchiné, D. Diverrès, D. Varillon, S. Cravatte, Y. Gouriou, J. Grelet, S. Jacquin, E. Kestenare, and et al. The French contribution to the voluntary observing ships network of sea surface salinity. *Deep-Sea Res. Pt. I*, 105:1–18, November 2015. ISSN 0967-0637. doi: 10.1016/j.dsr.2015.08.005.

Giuseppe Aulicino, Yuri Cotroneo, Isabelle Ansorge, and Marcel Van Den Berg. Sea surface temperature and salinity collected aboard the S.A. AGULHAS II and S.A. AGULHAS in the South Atlantic Ocean and Southern Ocean from 2010-12-08 to 2017-02-02 (NCEI Accession 0170743), 2018. doi: 10.7289/v56m3545.

Abderrahim Bentamy and Denis Croize Fillon. Gridded surface wind fields from Metop/ASCAT measurements. *Int. J. Remote Sens.*, 33(6):1729–1754, March 2012. ISSN 1366-5901. doi: 10.1080/01431161.2011.600348.

Abderrahim Bentamy, Semyon A. Grodsky, James A. Carton, Denis Croizé-Fillon, and Bertrand Chapron. Matching ASCAT and QuikSCAT winds. *J. Geophys. Res.*, 117(C2), February 2012. ISSN 0148-0227. doi: 10.1029/2011JC007479.

Jaqueline Boutin, Y. Chao, W. E. Asher, T. Delcroix, R. Drucker, K. Drushka, N. Kolodziejczyk, T. Lee, N. Reul, G. Reverdin, J. Schanze, A. Soloviev, L. Yu, J. Anderson, L. Brucker, E. Dinnat, A. S. Garcia, W. L. Jones, C. Maes, T. Meissner, W. Tang, N. Vinogradova, and B. Ward. Satellite and In Situ Salinity: Understanding Near-Surface Stratification and Sub-footprint Variability. *Bull. Am. Meterol. Soc.*, 97(8):1391–1407, 2016. ISSN 1520-0477. doi: 10.1175/bams-d-15-00032.1.

Ralph R. Ferraro. SSM/I derived global rainfall estimates for climatological applications. *J. Geophys. Res.*, 102(D14):16715–16736, 07 1997. doi: 10.1029/97JD01210.

Ralph R. Ferraro, Fuzhong Weng, Norman C. Grody, and Limin Zhao. Precipitation characteristics over land from the NOAA-15 AMSU sensor. *Geophys. Res. Lett.*, 27(17):2669–2672, 2000. doi: 10.1029/2000GL011665.

Fabienne Gaillard, Thierry Reynaud, Virginie Thierry, Nicolas Kolodziejczyk, and Karina von Schuckmann. In Situ-Based Reanalysis of the Global Ocean Temperature and Salinity with ISAS: Variability of the Heat Content and Steric Height. *J. Clim.*, 29(4):1305–1323, February 2016. ISSN 1520-0442. doi: 10.1175/jcli-d-15-0028.1.

Robert J. Joyce, John E. Janowiak, Phillip A. Arkin, and Pingping Xie. CMORPH: A Method that Produces Global Precipitation Estimates from Passive Microwave and Infrared Data at High Spatial and Temporal Resolution. *J. Hydrometeorol.*, 5(3):487–503, June 2004. doi: 10.1175/1525-7541(2004)005⟨0487:camtpg⟩2.0.co;2.

Nicolas Kolodziejczyk, Gilles Reverdin, and Alban Lazar. Interannual Variability of the Mixed Layer Winter Convection and Spice Injection in the Eastern Subtropical North Atlantic. *J. Phys. Oceanogr.*, 45(2):504–525, Feb 2015. ISSN 1520-0485. doi: 10.1175/jpo-d-14-0042.1.

Nicolas Kolodziejczyk, Mathieu Hamon, Jacqueline Boutin, Jean-Luc Vergely, Gilles Reverdin, Alexandre Supply, and Nicolas Reul. Objective analysis of SMOS and SMAP sea surface salinity to reduce large-scale and time-dependent biases from low to high latitudes. *Journal of Atmospheric and Oceanic Technology*, 38(3):405–421, mar 2021. doi: 10.1175/jtech-d-20-0093.1.

Christian Kummerow, Y. Hong, W. S. Olson, S. Yang, R. F. Adler, J. McCollum, R. Ferraro, G. Petty, D-B. Shin, and T. T. Wilheit. The Evolution of the Goddard Profiling Algorithm (GPROF) for Rainfall Estimation from Passive Microwave Sensors. *J. Appl. Meteorol.*, 40(11): 1801–1820, 2001. doi: 10.1175/1520-0450(2001)040⟨1801:TEOTGP⟩2.0.CO;2.

Rosemary Morrow and Elodie Kestenare. Nineteen-year changes in surface salinity in the southern ocean south of australia. *J. Mar. Sys.*, 129:472–483, January 2014. doi: 10.1016/j.jmarsys.2013.09.011.

Thierry Reynaud, Nicolas Kolodziejczyk, Christophe Maes, Fabienne Gaillard, Gilles Reverdin, Floriane Desprez De Gesincourt, and Hervé Le Goff. Sea surface salinity from sailing ships : Delayed mode dataset, annual release, 2021. doi: https://doi.org/10.17882/39476.

Shawn R. Smith, Jeremy J. Rolph, Kristen Briggs, and Mark A. Bourassa. Quality-Controlled Underway Oceanographic and Meteorological Data from the Center for Ocean-Atmospheric Predictions Center (COAPS) - Shipboard Automated Meteorological and Oceanographic System (SAMOS), 2009. doi: 10.7289/v5qj7f8r.